Lunds Universitets Naturgeografiska Institution

Seminarieuppsatser Nr. 87

Coastal parallel sediment transport on the SE Australian inner shelf

A study of barrier morphodynamics

In collaboration with
the Coastal Studies Unit
Sydney University

Håkan Arvidsson

2002

Department of Physical
Geography,
Lund University
Sölvegatan 13, S-221 00
Lund, Sweden

Abstract

In SE Australia, sediments are moved northwards by longshore currents and deposited as barriers, dunes, and estuarine or inner shelf deposits. According to Roy & Thom (1981), the magnitude and complexity of the deposition morphology increase from south to north. Modelling by Cowell, Roy, and Jones (1995) shows that the steepness of the regional substrate is the primary influence on coastal morphodynamics. It is even more important than slow sea level changes. More sediment is available for transport where the shoreface slope is gentle (a larger volume of sand between any two depths), simply because waves will entrain more sand across a greater distance of the inner continental shelf. Correlation between the size of coastal sediment deposits and the inclination of the inner continental shelf (between 20 and 60 metres depth) for the coastline between Fraser Island (Lat. 25º S) and Cape Howe (Lat. 37.5º S) suggests that the direction of long-term residual sediment transport on the inner continental shelf is along, i.e. northward, and towards the coast during stable to semi-stable relative sea level.

The dataset consists of 698 two kilometre wide (north-south) segments of coast. The size of the sand deposits and the local substrate inclination for each segment are extracted from a GIS, created through the interpretation and digitisation of geologic, topographic, and bathymetric maps. A simple linear correlation shows that the size of a barrier is partly controlled by the size of the potential sediment supply directly offshore. Added lag shows that much more can be explained by littoral transport. The correlation improves when the size of a deposit is explained by the steepness of the substrate south of its location.

To see if the result can be reproduced on parts of the data, the coast is divided into four geologically separable sections. They are Fraser Island - Byron Bay, Byron Bay - Port Stephens, Port Stephens - Beecroft Head, skipping Jervis Bay, and St. Georges Head - Cape Howe. These four sections are in turn divided, yielding nine new zones that are analysed also.

There are variations in the strength of the correlation that seem to reflect the different sizes of the coastal cells. This can be seen when the correlation is plotted on one axis and the lag on the other. More importantly, each section has a different “lag correlation pattern”, which seems to give insight into the many different scales involved, i.e. we can see that the sand is transported from one embayment to the next, that the sand is transported passed the next major headland, and so on.

Roy, P.S. and Thom, B.G. (1981) Late Quaternary marine deposition in New South Wales and southern Queensland – an evolutionary model. *Journal of Geological Society of Australia*, **28**, 471-489.

Cowell, P.J., Roy, P.S. and Jones, R.A. (1995) Simulation of large-scale coastal change using a morphological behaviour model. *Marine Geology, Special Issue on Large Scale Coastal Behaviour*, **126**, 45-61.

Thesis submitted in fulfillment of the requirements for the degree of Masters of Science in Physical Geography, Lund University, 2002.

Sammanfattning

I Australien är intresset stort för kustprocesser, och en sådan process är masstransport av sand i kustnära områden. Utmed östra Australiens kust finns stora områden med sanddyner och de flesta stränder är sandstränder. I Queensland finns till och med mycket stora öar som består av sand. Den största av dessa öar heter Fraser Island.

Många forskare tror att sand transporteras av kustparallella strömmar längs med kusten söderifrån, och att sanden då ackumuleras i de norra delarna. Norr om Fraser Island finns stora havsdjup som slukar den sand som når så långt. Teoretiskt sett kan sanden på Fraser Island komma så långt ifrån som Cape Howe i söder.

Genom att mäta storleken på sandområden på land och korrellera dessa med sluttningsgraden på havsbottnen mellan tjugo och sextio meters djup är det möjligt att bestämma hur ett samband mellan dessa kan se ut. I studien i fråga delades kuststräckan mellan Cape Howe och Fraser Island upp i mindre områden för att underlätta undersökningen. Det visade sig svårt att bestämma huruvida ett samband existerar eller inte.

Med syfte att undersöka om man på något vis kan få visshet om sandens rörelseriktning i olika områden, förskjöts variablerna i förhållande till varann. En viss del av kusten korrelleras då med en del av havet som ligger antingen på ett bestämt avstånd norrut eller söderut ifrån den kustbiten. Det är då möjligt att genom jämnförelse av många kombinationers resultat få en bild av hur sanden möjligen rör sig.

Det är viktigt att man har klart för sig att sanden inte egentligen rör sig på det här sättet. Vad som beräknas är residualtransportriktningen, d v s den transportriktning som är övervägande. I själva verket rör sig sanden naturligtvis i tre dimensioner, eller i fyra om man räknar med tiden, men den här studien fokuserade alltså på en dimension.

Ett försök att utveckla studien så att fler dimensioner tas med i beräkningen gjordes i form av en datormodell som beräknar mängden sand som är i suspension under ett år. För att beräkna detta behöver modellen sandstorlek, vågdata och havsdjup. På grund av få sandstorleksprov i vissa områden, otillräckliga vågdata och nödvändiga generaliseringar i havsbottnens utseende producerade inte modellen fullgoda värden, men viss betydelse för undersökningen av residualtransportriktningen fick modellen trots allt.

Studiens slutsats är att sand mycket riktigt förs norrut längs östra Australiens kust, men det finns områden där mycket komplicerade processer styr hur sanden rör sig. Studiens slutsats baserar sig ingalunda på entydiga bevis, utan snarare på en överväldigande mängd indicier. Studien skulle kunna förbättras genom att räkna på volym, istället för på area, men det kräver ett omfattande fältarbete, som skulle ta flera år.

Framsteg inom oceanografin bäddar för bättre möjligheter att förstå de här processerna. Än så länge är det mesta som föregår under vattenytan tämligen lite undersökt. Nya sensorer och avancerad radarutrustning kan förhoppningsvis hjälpa oss i vår förståelse av processer av det här slaget i framtiden.

Acknowledgements

My thanks go to Dr. Peter Cowell for inviting me to do research at The Coastal Studies Unit, and for providing me with a great study, the computer model, excellent lectures, and tons of inspiration.

I thank the Dept. of Geography for their cooperation and all-around goodwill, and Sydney University for giving me the opportunity to experience everything that is Sydney Uni.

I would like to thank Prof. Andrew Short for letting me sit in on his lectures, and for the excursions that provided a better understanding of the coastal landscapes and their morphology. In addition, I thank Andrew Short for contributing the sand grain size data, and making the wave data from the Maritime Services Board available.

The barriers were mapped out by Dr. Peter Roy on maps from the National Topographic Map Series. I could not have done this study without Peter Roy's expertise in coastal geology. Peter Roy also took active part in the preparation of data prior to the statistical analysis.

The Geography Map Library was very helpful, and provided me with all the maps I needed, including the National Topographic Map Series and the National Bathymetric Map Series. Especially, I thank Mr. Peter R. Johnson for his impeccable services.

For test-running the computer model and for providing some invaluable input, I thank Dr. Chris Jenkins.

I would also like to thank Aaron Coutts-Smith and Arthur Trembanis for their comradeship and assistance. I extend my thanks to Riko Hashimoto, Werner Hennecke, and Catharina Greve, who all made my stay more enjoyable.

My thoughts go to all other students and staff that I had the pleasure of associating with during my stay in Sydney in 1999/2000. Especially, I think of the soccer teams I had the opportunity to coach and my very good friends Vanessa Bosnjak and Aaron Coutts-Smith.

Finally, I would like to thank Dr. P. J. Cowell, Dr. P. S. Roy, and Dr. Jonas Åkerman for supervising this thesis.

I dedicate this thesis to Hazel Easthope

My Star

My Love

My Southern Cross

Contents

1 Introduction 1

2 Method 2
2.1 The database 2
2.2 Statistical Analysis 3

3 Physical Setting 4
3.1 The morphology of the SE Australian coast 4
3.1.1 The Continental Shelf 4
3.1.2 Sand Barriers 5
3.2 Wave Climate 5
3.2.1 Climate 5
3.2.2 Oceanography 5

4 Barrier Morphodynamics 7
4.1 Barrier type and evolution 7
4.1.1 Substrate gradient 7
4.1.2 Sediment supply 7
4.1.3 Waves 8
4.1.4 Tides 8
4.1.5 Wind 8
4.1.6 Sea level 9
4.1.7 Geology 9
4.1.8 Tectonism 9
4.2 Barrier genesis in SE Australia 10

5 Scale Issues 11
5.1 The Coastal Tract 11
5.2 The Coastal Cell 11

6 Sediment transport 12
6.1 Wave Parameters 12
6.2 Seabed parameters 13
6.2.1 Boundary Layers 13
6.2.2 Bed Roughness 14
6.2.3 Bed Friction 15
6.3 Sediment entrainment by waves 15
6.4 Waves and Currents 17

7 Results 19
7.1 The whole data set without exceptions 20
7.2 The whole data set, Jervis Bay excepted. 22
7.3 The four zones 24
7.3.1 Fraser Island to Byron Bay (Boxes 1-204) 24
7.3.2 Byron Bay to Port Stephens (Boxes 202-433) 26
7.3.3 Port Stephens to Beecroft Head (Boxes 429-558) 28
7.3.4 St. Georges Head to Cape Howe (Boxes 566-698) 30
7.4 The nine zones 32
7.4.1 Fraser Island to Caloundra Head (Boxes 1-109) 32
7.4.2 Caloundra Head to Byron Bay (Boxes 101-204) 34
7.4.3 Byron Bay to Smoky Cape (Boxes 202-329) 36
7.4.4 Smoky Cape to Sugarloaf Point (Boxes 330-414) 38
7.4.5 Sugarloaf Point to Port Stephens (Boxes 412-433) 41
7.4.6 Port Stephens to Botany Bay (Boxes 429-499) 42
7.4.7 Botany Bay to Beecroft Head (Boxes 500-558) 44
7.4.8 St. Georges Head to Burrewarra Point (Boxes 566-604) 46
7.4.9 Burrewarra Point to Cape Howe (Boxes 605-698) 48

8 Discussion 50

9 Conclusion 53

References 54

Appendices 56
Appendix I Digitised Maps 56
Bathymetric Maps 56
Topographic Maps 57
Appendix II Mapinfo Map 58
Fraser Island to Caloundra Head (Boxes 1-109) 59
Caloundra Head to Byron Bay (Boxes 101-204) 60
Byron Bay to Smoky Cape (Boxes 202-329) 61
Smoky Cape to Sugarloaf Point (Boxes 330-414) 62
Sugarloaf Point to Port Stephens (Boxes 412-433) 63
Port Stephens to Botany Bay (Boxes 429-499) 63
Botany Bay to Beecroft Head (Boxes 500-558) 64
St. Georges Head to Burrewarra Point (Boxes 566-604) 64
Burrewarra Point to Cape Howe (Boxes 605-698) 65
Appendix III Diagrams 67
Fraser Island to Byron Bay (Boxes 1-204) 68
Byron Bay to Port Stephens (Boxes 202-433) 68
Port Stephens to Beecroft Head (Boxes 429-558) 69
St. Georges Head to Cape Howe (Boxes 566-698) 69
Appendix IV Visual Basic code 70
Variables and outputs 70
Visual Basic code for calculating sediment suspension 71

1 Introduction

In SE Australia, the sediments are moved northwards by longshore currents and deposited as barriers, dunes, and estuarine or inner shelf deposits. According to Roy & Thom (1981) the magnitude and complexity of the deposition morphology increase from south to north. Modelling by Cowell, Roy, and Jones (1995) shows that the steepness of the regional substrate is the primary influence on coastal morphodynamics. It is even more important than slow sea level changes. More sediment is available for transport where the shoreface slope is gentle (a larger volume of sand between any two depths), simply because waves will entrain more sand across a greater distance of the inner continental shelf.

Although the circumstantial evidence and common sense supports the idea of northward transport of sand along the coast, it has yet to be proven. The main hypothesis for this thesis is that sand is moving northward. This hypothesis is tested in various ways by using a dataset consisting of samples of sand barrier areas and shelf areas extracted from 698 two kilometre wide (north-south) segments of coast spanning from Fraser Island (Lat. 25º S) to Cape Howe (Lat. 37.5º S).

The size of the sand deposits and the local shelf areas between 20 and 60 metres depth are extracted from a GIS, created through the interpretation and digitisation of geologic, topographic, and bathymetric maps. The coast is divided into four geologically separable sections. They are Fraser Island - Byron Bay, Byron Bay - Port Stephens, Port Stephens - Beecroft Head, skipping Jervis Bay, and St. Georges Head - Cape Howe. These four sections are in turn divided, yielding nine new zones that are analysed also.

In order to see if suspension rates can be correlated with the size of sand barriers, yearly sediment suspension estimates are generated with a computer model. The model uses sand grain sizes and wave data, and builds on complex theoretical and empirical relationships of sediment entrainment at the seabed under wave action. The principles of sediment transport is presented in chapter 6.

Further theoretical background for this thesis can be found in chapter 4, which is an introduction to barrier morphodynamics, and chapter 5, which deals with scale issues. A general overview of the sediments, morphology, and the wind and wave climate of the coast and shelf in SE Australia is presented in chapter 3. The method is discussed in chapter 2.

In the Appendices, the dataset is displayed as extracted maps from Mapinfo, and as processed data in diagrams. These pages may be helpful to glance at occasionally, especially when reading the results and discussion. The Appendices also include information on the digitised maps and the core code for the sediment entrainment model.

2 Method

2.1 The database

Using the National Bathymetric Map Series and Naval Chart 806 (see Appendix I for a complete listing of the maps used), the isobaths for 20 m and 60 m where digitised with Mapinfo and converted into polygons with a maximum size of 840 km^2. This restriction of polygon size was made in order to facilitate more exact calculations of union operations. The sand barriers were mapped out by Peter S. Roy on maps from the National Topographic Map Series. The areas were thereafter digitised as lines and converted into polygons.

The coast needed to be divided into sections of small enough size to make an acceptable model of the large-scale coastal morphology. It was decided that 2 km wide segments would be adequate, and rectangular polygons with a longitude parallel (roughly coastal parallel) 2 km wide side and a latitude parallel 80 km long side were constructed in Mapinfo. As an effect of the most northerly rectangle being created first and then copied and pasted south of it, a minor size difference exists; with smaller rectangles to the south as a consequence of projection (Transverse Mercator Projection: Australian Map Grid 1966 (Zone 56 & 55)). This result in 698 segments, spanning from Lat. 25° S (north tip of Fraser Island) to Lat. 37° S (Cape Howe). See Appendix II for a complete visual overview of the digitised Mapinfo map.

In order to calculate the size of areas of sand barriers and areas of shelf between 20 and 60 metres of depth within the segments, the unions of each rectangular polygon and its overlapping sand and shelf polygons were calculated in Mapinfo. The needed areas can then be calculated as rectangular polygon minus union polygon plus sand/shelf polygon. These calculations took place in Excel after extracting tabular data from Mapinfo.

It was found that Mapinfo sometimes makes mistakes when performing union operations. After carefully eliminating any miscalculations brought on by human mistakes, all areas were recalculated so that their sum is equal to the original polygon areas. To remove any effects of projection a recalculation of all areas was made using the size of the rectangular polygons.

After a satisfying statistical overview of the data and extensive experimental analysis in Minitab, the following variables were constructed: Cumulative areas, Mean areas of merged segments ranging from 4 km to 10 km, a column where segments without barriers are skipped, and lagged shelf areas ranging from 20 km north to 100 km south, transect length, slope length, and slope mean angle. The dataset was also divided into five parts based on differences in geology and morphology.

The results of the ensuing analysis were discussed with Peter Roy and Peter Cowell, after which some new barrier areas were added to the GIS, the area of Jervis Bay was excluded from the analysis, and a new division of the dataset was made. The dataset is broken up into nine sub areas. These sub areas are then combined to form four larger areas. The data is analysed both as a whole and as thirteen zones. A graphic representation of the coastal areas and the corresponding shelf sand areas is found in Appendix III.

Utilising offshore wind data and sand grain size data from beaches, an estimate of the amount of sand in suspension over a year was calculated using a model written for Tektronix 4051/4052A series mini-computers by Peter Cowell, and recoded in Visual Basic by author for use in Excel (the core code can be reviewed in Appendix IV). Predicted suspension rely on the assumptions that the waves determine when and how much sand can be transported, that the synoptic information on the regional wave and current regime is uniformly representative over the entire duration of the Holocene post-stillstand period, and also more

or less representative for the whole study area, and that there is strong homogeneity of near-bed wave motions along each isobath throughout the region.

The assumption that wave motions dominate in agitating sediments and thereby control the concentration of sand potentially available for transport, whereas currents are responsible for net sediment advection, is based on the relationship between suspended sand concentrations and waves, which in turn is based on empirical data in which scatter is considerable (Cowell and Nielsen, 1984). The presence of wave rippled beds in sidescan sonar images supports this assumption. The climatic assumption is supported by climatic reconstructions that show no sign of any major trends through the Holocene for southeast Australia, but only fluctuations in the degree of storminess (Thom, 1978; Bowler, 1983). The last assumption requires a constant offshore decrease in downwelling currents, which is generally expected (Swift et al., 1983). Although little is known about the spatial characteristics of the near-bed flow over the inner shelf, the assumed isobathic homogeneity probably describes the conditions in the study area well enough for the purpose of this study.

In order to limit the computer hours needed to run the model, the two variables had to be converted into discreet classes. Based on 8298 observations during the years 1977-1999, the wave climate is described as occurrences of wave height and wave period over a year. Replacing the sand grain size classes with their respective modelled annual suspension concentration (m^3/km^2) averaged for the water depths between 20 and 60 metres, the amount of sand suspended over a year in each segment of shelf was calculated. In addition, the cumulative concentration, the mean concentration for merged segments ranging from 4 km to 10 km and the lagged concentrations for shelf areas ranging from 20 km north to 100 km south was added to the dataset.

2.2 Statistical Analysis

Statistical analysis was performed in Minitab, using Excel for calculations, formatting, and storage of data. An initial general overview of the fifteen datasets (the dataset including Jervis Bay was also analysed) showed nothing that would impair any planned methods of analysing the data. However, in some cases the values available for analysis are quite few, and therefore the results in those cases are highly unreliable. This problem occurs in some of the smaller sections and especially in the lagged data for those sections.

In order to understand what happens spatially, different ways of showing the dataset graphically where experimented with in both Minitab and in Excel. Straightforward correlation analysis and plotting of the correlations for lagged data are the two major methods used to extract information from the data. Correlation analysis proved quite useful, especially when dealing with the lagged data.

3 Physical Setting

3.1 The morphology of the SE Australian coast

The coast can be divided into three general morphological categories. The first coastal type predominates south of Coffs Harbour, where prominent headlands separate the small bay barriers occupying them. The steep offshore gradients combined with the restricted size of coastal embayments have resulted in limited sedimentation (Roy, 1998).

South of Jervis Bay, the coastline is rocky with minor Quaternary deposits. The coastline is characterized by high relief near the coast and steep offshore gradients. Between Wollongong and Newcastle, the coastal rocks are Mesozoic sandstone, which have been eroded by marine processes to form the vertical coastal cliffs and sand filled embayments that characterize the region. In the Sydney region, and a few other places, are extensive estuarine systems, where fluvial sediments are trapped, hindering sand sized particles from reaching the coast. From Port Stephens to Smokey Cape, the combination of valleys and ridges has created large sediment traps for marine and fluvio-estuarine sediments. Between Nambucca Heads and Coffs Harbour, the coast is characterized by marine eroded cliffs and small coastal rivers (Chapman et al., 1982).

The second coastal type extends from Coffs Harbour to Southport in southern Queensland, with its larger river systems, low coastal relief with small headlands, broad embayments, and bay barriers. The third coastal type is found north of Southport, where a barrier island coast with large dune islands dominate the morphology (Roy, 1998).

3.1.1 The Continental Shelf

The continental shelf is narrow, generally being less than fifty kilometres wide. The near shore zone extends from the shoreline out into 20 to 30 metres depth, and is dominated by mid to high energy waves. Further out is the steep and narrow inner shelf, while the more gently sloping mid shelf starts at a depth of between 50 and 80 metres. The mid shelf change seaward into the nearly horizontal outer shelf plain. The shelf ends rather abruptly at depths of 140 to 150 metres south of Lat. 33° S, and at 70 to 130 metres depth to the north of Lat. 33° S. Shore normal profiles across the shelf from Fraser Island to Cape Howe show that the shelf deepens, steepens and narrows to the south (Chapman et al., 1982).

Inner shelf deposits primarily occupy a zone between 20 and 70 metres depth on the inner part of the continental shelf. The two discrete stratigraphic units that can be recognised are regressive shelf barriers on gently sloping parts of the shelf and headland-attached shelf sand bodies on steeply sloping substrate. Both units lie seaward of modern shorefaces, and they are composed of relatively clean marine (shelf-derived) sand (Roy, 1998).

The regressive shelf barriers are 10 to 20 metres thick with gently seaward dipping, concave-up surfaces. Simulation modelling shows that when sea level is falling on a sand-rich shelf, erosion occurs in inner shelf water depths, and sand moves onshore to prograde the barrier shoreface (Cowell, Roy & Jones, 1995). As sea level continue to fall, the regressive barrier builds seaward into the newly excavated zone, with the result that the former sea bed morphology is reconstructed, and sand starts moving onshore (Roy, Cowell et al., 1995).

The shelf sand bodies are large, coast-parallel, lens shaped accumulations with convex upper surfaces. Initial deposits were transgressive sand sheets, and their thicknesses depend on the slope of the pre-existing land surface. When sea level stabilised, regressive deposits

began building upwards and seawards, which account for the convexity of the shelf sand bodies (Roy, 1998).

3.1.2 Sand Barriers

Coastal sand barriers extend from inland to between 1.0 km and 1.5 km offshore, in water depths of about 20-25 m, and range in length from a few kilometres to more than 100 km. The beaches and dunes make up a small part of the total sand mass. The barriers have both transgressive and regressive parts, and have mostly been formed during the last 6500 years. There is a general trend for the sand deposits to increase in age, extent, and morphological as well as stratigraphic complexity from Cape Howe to southern Queensland (Roy & Thom, 1981).

In New South Wales, two bay barrier systems can be identified: inner barriers of late Pleistocene age and outer barriers of Holocene age (Thom, 1965; Thom, Shepherd et al., 1992). The Holocene barriers are found all along the coast, while the Pleistocene barriers occur only north of Newcastle (Thom, 1984).

3.2 Wave Climate

3.2.1 Climate

The climate of the SE Australian coast ranges from subtropical in the north to cool temperate in the south. Summer temperatures are warm to hot, while winter temperatures are mild. Annual rainfall measures 750 to 1500 mm, and is evenly distributed throughout the year. Intense local storms do occur erratically, and there are major fluctuations in flood frequency on a decade-scale (Pittock, 1975). The storms and floods are major factors in the shaping of the morphologies of coastal river channels and their floodplains (Erskine & Nanson, 1988; Warner, 1991; Warner, 1994), and causes major shifts in beach face positions (Thom & Roy, 1985). In spite of the moderate to heavy rainfall, the supply of sand from rivers to the present coast is limited, and the coastal sand barriers receive their sand mainly form the shelf.

3.2.2 Oceanography

The chief elements controlling the hydrodynamic regime of the SE Australian shelf are storm waves, swell waves, and currents. The area is micro tidal, with a maximum spring tide range of two metres. Tides are semi-diurnal and, except in tidal inlets at the present coast, tides only generate weak shelf currents. Tidal flows are generally too weak to transport sand (Roy, 1998).

The ocean wave climate on the shelf is dominated by eastward-tracking mid-latitude cyclones, which cross the southern half of the Australian continent, and generate southerly storm waves and long-period swell in the south Tasman Sea. Average wave heights are in the order of 1.5 to 2.0 metres, with periods of 7 to 12 seconds. Storm waves, capable of stirring bottom sediments in mid-shelf water depths, frequently reach heights of five metres and may exceed ten metres (Short & Trenaman, 1992). The persistent, long-period swell has the ability to excite sand from water depths of as much as 45 metres, while storm waves, generated by tropical cyclones, may set sand into motion at even greater depths. These storm waves mainly impact on the coast of northern New South Wales and southern Queensland.

The orientation of the continental margin suggests that southerly storms may induce a northward littoral drift of sediments. Transport rates are influenced locally by the size of

headlands and the degree of coastal embayment. North of Coffs Harbour, transport rates are estimated to increase northward to half a million cubic metres per year at the New South Wales - Queensland border, and to reach a maximum of about one million cubic metres per year at Fraser Island in Queensland (Roy, 1998).

The East Australian Current is a western boundary current, flowing southwards on the outer shelf and upper slope at speeds of up to two metres per second. It diverges seawards around latitude 32.5° S, forming large counter-clockwise gyres that slowly migrate southwards beyond the shelf edge. This current may indirectly influence shelf water movements (Godfrey, Cresswell et al., 1980). On the central and southern shelf, currents fluctuate in intensity, and normally reach velocities of 1.0 to 1.5 m/s. Direction reversals at intervals of five to ten days may be related to coastal-trapped waves moving northwards along the southern coast (Church, Freeland & Smith, 1986). Current velocity tends to diminish with depth and towards the north. However, constriction caused by headlands or islands accelerate currents locally (Griffin & Middleton, 1991).

The mid-latitude cyclones produce winds in excess of 35 metres per second over large distances for periods longer than seven days. These winds initiate long-period storm waves as they move out into the south Tasman Sea. The swell waves created by the storms in the Tasman Sea excites sediments on the shelf and speeds up currents. Local coastal storms are usually associated with the same weather systems, which means that the sediment suspension potential is unusually high during these storms. This provides the rare conditions for massive sediment transport events in relatively deep water (Roy, 1998).

The strong northward flowing currents with a downwelling element, which are generated by mid latitude cyclonic storms, dominate near bottom flows on the inner shelf (Field and Roy, 1984). The water motions on the shelf are completely dominated by friction under these conditions, and it is the friction dominated flows that control sedimentation processes on the inner shelf (Cowell and Nielsen, 1984).

4 Barrier Morphodynamics

4.1 Barrier type and evolution

A barrier is a shore parallel accumulation of sediment formed by waves, tides, and aeolian processes, which separates older coastal landforms and the sea. There are many different types of barriers, and they differ in size, stability, and arrangement. The determining factors are: substrate gradient, sediment supply, waves, tides, wind, sea level, geology, and tectonism (Hesp and Short, in press).

4.1.1 Substrate gradient

According to Roy et al. (1995), beach deposits will only form when the substrate gradient is between 0.05° and 0.8°, with an optimum at 0.1°. Where the inclination is less than 0.05°, frictional wave shoaling decreases wave energy, resulting in subaqueous shoals and tidal deposits. Extremely steep gradients will force sediment to move offshore, where it accumulates as inner shelf sand deposits.

Substrate gradient predetermine what waves and tides can do with available sediments. Over time, waves and tides can change the substrate gradient, but radical transformations are mainly due to tectonism and changes in sea level. Gentle inclinations favour the development of barrier islands, while steeper gradients produce mainland beaches and attached barriers. The arrangement, i.e. the positioning of the barrier, is a function of the difference between the inclination of the substrate and the barrier sand body gradient (ibid.).

4.1.2 Sediment supply

The grain size most commonly found in barriers is sand, but barrier sediments can range from mud to boulders. The size, mineralogy, and quantity depend on local to regional geological and climatic factors, while the rate of supply is determined by waves, tides, currents, and aeolian processes. Many barriers consist of reworked shelf deposits, but sediments can also originate from erosion of adjacent headlands and drumlins, and they can be river sediments, or even resulting from in situ carbonate production (Hesp and Short, in press).

A continuous supply of sediment is in many cases necessary to sustain and stabilise a barrier (Roy et al., 1995). When the sea level is stable, barrier stability is largely dependent on the sediment budget. A positive beach budget leads to shoreline progradation, a negative budget to retrogradation, while a balanced budget may tend towards shoreline stability.

Sediment rich shelves are more likely to have major barrier systems. However, if the steepness of the substrate locally does not support the creation of barriers, sediment will be transported, and perhaps result in barriers systems being developed in areas where the local sediment supply is actually quite small.

4.1.3 Waves

Waves are essential for barrier formation, as they initiate sediment transport, and thereby influence the grain size and quantity of sediment, and indirectly affect the supply rate and barrier type. In addition, the waves continually rework the sediments, and induce and enhance sediment-transporting currents. The rate of sediment transport is directly related to the level of wave energy. Storm waves and long-period swell waves are largely responsible for initiating sediment transport, and consequently instrumental in creating barrier systems. Waves exact further control on barriers by shaping and reshaping the ever-changing extremities, such as spits, sand bars, bed ripples, and swash zone features.

4.1.4 Tides

Tides are not necessary for barrier development, but all ocean barriers are influenced by tides and tidal currents. A modest tidal range has little effect on sediment transport. However, on a gently sloping substrate, where barrier islands have developed, tides have the effect of limiting the length of the islands. The greater the tidal range, the shorter are the islands. This is simply because more inlets are needed to accommodate the more substantial exchange of water with the ocean at ebb and flood. Over time, these inlets produce deltas that contain an increasing percentage of the barrier sediments, especially of finer sediment fractions. In addition, waves and tides rework the inlets, affecting the shape of the inlet, but also the morphology of the barrier and the delta (Hesp and Short, in press).

4.1.5 Wind

Coastal dunes are an integral part of many barrier systems. Subaerial barrier sediments constitute the sediment supply, while the wind conditions determine the supply rate of aeolian sediment to the backshore. Aeolian processes have major impacts on the nature and extent of many barrier systems. The forming of sand dunes allows for larger amounts of sand to accumulate on land.

Dunes come in many different shapes and sizes, depending on the nature of the sediment, wind direction, velocity, and frequency, the morphology of the barrier and coastal landscape, vegetation, and climate. Dunes may be stabilised by vegetation, and consequently become more constant parts of the coastal landscape, or they may migrate and/or scatter over large areas. Then again, aeolian processes may partially, or fully, disperse the dunes, transporting the sediments back to the ocean or even further inland.

4.1.6 Sea level

Where sea level is rising, receding barriers and eroding cliffs dominate, while areas of falling sea level may demonstrate a sequence of beach ridge plains and foredune plains. In Australia, sea level has been relatively stable for the past 6,500 years. Stable sea level promotes a wide range of coastal barriers and landform types.

Roy et al. (1995) claim that rising sea level produces retrogradational (transgressive) barrier islands and bay barriers on coastal plains and embayed coasts, and offshore transport to shelf sand bodies on steeper coasts. Falling sea level produces progradational (regressive) barrier strandplains. Beaches, beach ridges, and foredunes are developed on coastal plains and embayed coasts, while shelf deposits are reworked where the substrate is steep. At stable sea level, barrier islands, spit barriers, and inner shelf sand bodies occur on embayed coasts, while steeper, cliffed coasts, display mainland beaches and shelf sand bodies.

4.1.7 Geology

Barrier development is influenced by coastal bedrock composition and topography. Where a transgression has taken place, or is under way, the coastal bedrock becomes the substrate, and its inclination determines the direction of sediment transport. In areas where the whole coast consists of easily erodible rock, and the sea level is stable or rising, a straight or slightly curved coastline with low relief will be developed. During stable se level, the coastal bedrock may develop into a headland and bay topography, where more resistant rocks develop into headlands, and more easily eroded rocks crumble and form bays. The SE Australian coast is mainly of this type (Thom et al., 1992).

Relict barrier forms at, or near, present sea level, occupy potential accommodation space, and impact on the evolution and form of subsequent Holocene barrier deposits (Roy et al., 1995) In addition, cementation of former barriers may be a factor. Cemented barriers can remain as reefs, rocks and cliffs, as well as occupying potential accommodation space (Hesp and Short, in press).

4.1.8 Tectonism

Coasts may be forever adjusting to new base levels as the land rises or falls due to tectonics. Uplift changes everything. The sediment supply may increase or decrease, but the main determining factor is the rate at which uplift occurs. Continuous uplift may result in the formation of a staircase of marine terraces, where, depending on the frequency, either relict barrier systems may be found, or no evidence of coastal processes may be observed (ibid.). A very slow uplift rate may hardly be detectable, as erosion often works faster, and levels the land as it rises.

Coasts that experience rising sea level because of tectonics are usually even less conspicuous. The receding barriers and eroding cliffs of these coasts are morphologically not distinguishable from the same coast during stable conditions. This is because rising sea level, no matter why the sea level rises, has similar effect as erosion during stable sea level. On the other hand, in areas with low relief, the consequences can be quite catastrophical, as large coastal areas are suddenly submerged.

4.2 Barrier genesis in SE Australia

In SE Australia, large transgressive dune field barriers, barrier islands, and prograded barriers are found mainly in the north, while smaller stationary barriers (formed during stable sea level), receded barriers, and mainland beaches occur in the south (Langford-Smith & Thom, 1969; Roy & Thom, 1981). As shown by Cowell, Roy and Jones (1992) and Roy, Cowell et al. (1995), shore-normal sand movements are largely independent of sea level fluctuations. However, sand transport is strongly influenced by subtle changes in shelf gradient. On steep shelves (> 0.8°), e.g. in southern New South Wales, sand tends to move seaward, while on flatter slopes, for example in southern Queensland, sand moves landward. This process has lead to the accumulation of sand on the SE Australian coast and shelf, while the southern sediment supply has become depleted (Roy & Thom, 1981; Roy, Cowell et al., 1995).

Regional variations in the genesis of Pleistocene and Holocene barriers on this coast can be explained in terms of accommodation space, preservation potential, and shoreface equilibrium under stable sea level conditions (Roy & Thom, 1981). The northern shelf has successfully trapped and preserved barriers since late Pleistocene, which has hindered the development of late Holocene barriers. The barrier islands in southern Queensland exhibit the greatest stratigraphic complexity of barriers anywhere on this coast (Ward, 1977; Ward, 1978). The massive sand barrier islands and the large prograded barriers in this region suggest that the sand supply rate has been high throughout Holocene, and well into Pleistocene. In southern New South Wales, Pleistocene barriers have been eroded by rivers during lower sea level. The steepness of the inner shelf limits the sediment supply, and the compartmentalised coast restricts the alongshore size of barriers. Receded barriers and mainland beaches suggest that sand loss have been a continuous process throughout Holocene (Roy, Thom & Wright, 1980).

5 Scale Issues

It is a widely accepted fact that large time scales allow for the description of processes of low order, and the morphologies associated with low-order processes. However, in barrier morphodynamics, a large time scale actually increases the order of the features and processes that can be resolved. A single storm may have a tremendous impact on a beach, but when trying to understand what happens to the beach over decades to millennia that single storm is just part of the data making up a statistical climatology, and the long term sediment transport is the result of residual displacements with quite small net changes. Geological and climatic data is more important than observations of contemporary changes in morphology.

It is necessary to consider changes to large-scale coastal systems as a function of the residual results of long-term processes. Studying low-order morphologies, it is necessary to generalise parameters such as waves, and currents, while disregarding along-shore fluctuations in high-order morphology, which can be considered as noise.

5.1 The Coastal Tract

One way of generalising is to convert the coastal cell, a two dimensional representation of a part of the coast, into a shore-normal one-dimensional line. Such a generalisation is the construct of the coastal tract (de Vriend, ed., in review). The coastal tract assumes along-shore homogeneity, relying upon the absence of systematic variation in time-averaged morphology and coast parallel transport processes within the coastal cell. The coastal tract represents the lowest order, while higher-order processes form a cascade, in which coastal behaviour at any intermediate level results from the residual effects of higher-order processes, while constrained by the effects of lower-order systems in the cascade. These constraints constitute internal boundary conditions that operate in addition to the external boundary conditions.

5.2 The Coastal Cell

This study makes use of 698 shore-normal one-dimensional lines, which are only described by two variables, i.e. substrate gradient (shelf area) and barrier area. Each of these lines is similar to a coastal tract, with one important difference. These lines, or segments, do not correspond to 698 coastal cells. The coastal cell is a part of the coast that can be considered as a self-contained unit. A coastal cell can be as small as a bay, or a system of bays, or an area between two major headlands, as long as the along-shore homogeneity can be assumed.

Homogeneity cannot exist perpendicular to the shore because of systematic shore-normal variation in water depth and morphology. However, in this study the substrate gradient is generalised as the vertical angle between two water depths on the shelf, while the morphological shore-normal variation is ignored. While the coastal tract describes how sediment may be transported in a shore-normal direction, this study attempts to describe how sediment is transported along the shelf. The size of coastal cells along the coast may be inferred from the correlation of lagged data, which shows variation that can be interpreted as a result of the existence of the coastal cell, its different sizes, and different scales.

6 Sediment transport

6.1 Wave Parameters

The entrainment of sediment under the influence of waves is related to the wave height (H), wave period (T), and the water depth (h). The wave height used in the model is significant wave height, i.e. the mean of the highest 1/3 of the waves recorded during a sampling period. The wavelength for deep-water waves is given by:

$$L = gT^2 / 2\pi \tag{6.1}$$

In deep water, defined as water depths larger than 1/4 given by the ratio h/L, where h is water depth, the water particles orbital path is elliptical. The orbital diameter is calculated as:

$$d_0 = H^{k_0 z} \tag{6.2}$$

where z is the depth to the centre of the orbit, and k_o is the deep-water wave number:

$$k_0 = 4\pi^2 / gT^2 \tag{6.3}$$

The relevant flow parameters under waves are the near-bed semi excursion (a) and the near-bed velocity (aω). In shallow water, the orbital motion becomes increasingly elliptical, the near-bed velocity increases, and so does the near-bed semi excursion. The near-bed semi excursion is given by:

$$a = H / 2k\sinh \tag{6.4}$$

the wave number (k) used here is calculated using Nielsen's (1983) approximations:

for $k_0h < 1.26$

$$k = (k_0h)^{0.5} \times (1 + k_0h / 6 + 11 / 360 + (k_0h)^2) \tag{6.5a}$$

and for $k_0h > 1.26$

$$k = k_0h \times (1 + 2e^{-2k_0 h}) \tag{6.5b}$$

The near-bed velocity ($a\omega$) is given by:

$$a\omega = H / T\sinh \tag{6.6}$$

where ω is the angular velocity:

$$\omega = 2\pi / T \tag{6.7}$$

6.2 Seabed parameters

6.2.1 Boundary Layers

The seabed boundary layer is the layer close to the seabed, where fluid motion is affected by the seabed (Cowell and Nielsen, 1984). Within the boundary layer, the velocity distribution $u(z)$ is a result of the free flow conditions (above the boundary layer) and the bed roughness and geometry. Friction between the boundary and the fluid results in shear stress within the fluid. The shear stress (τ) at a distance (z) from the bottom of the boundary layer is proportional to the velocity gradient du/dz:

$$\tau = pv_t \times du / dz \tag{6.8}$$

where p is the fluid density and v_t is the eddy viscosity (ibid.).

If the direction of fluid flow reverses periodically, the thickness of the boundary layer (δ) is proportional to the square root of the wave period (T):

$$\delta = (Tv_t)^{0.5} \tag{6.9}$$

Waves with relatively short period, e.g. 10 seconds, have thin boundary layers, while longer period motions, generated by for example surf waves and tidal currents, produce much thicker boundary layers. Seabed ripples produce strong rhythmic vortices, extending the boundary layer about four or five times the ripple height. Increases in the thickness of the boundary layer results in larger shear stresses at the seabed, which enhance sediment entrainment potential (ibid.).

6.2.2 Bed Roughness

The bed roughness (r) depends upon the bed-form geometry, sand grain size (d), and the motion of the sand grains near the seabed (Cowell and Nielsen, 1984). For relatively flat seabeds, bed roughness can be estimated by:

$$r = 2.5d \tag{6.10}$$

The bed roughness for a bed covered with ripples can be estimated using Cowell and Nielsen's (1984) formula:

$$r = 8\eta^2 / \lambda + 190 \times (\theta - 0.05d)^{0.5} \tag{6.11}$$

where the ripple length (λ) and ripple height (η) can be estimated using the mobility number (ψ) and Nielsen's (1981) equations:

$$\lambda / a = \exp((693 - 0.37\ln\psi^8) / (1000 + 0.75\ln\psi^7)) \tag{6.12}$$

and (for $\psi \geq 10$)

$$\eta / a = 21\psi^{1.85} \tag{6.13a}$$

else

$$\eta / a = 0.275 - 0.022 \times \sqrt{\psi} \tag{6.13b}$$

where

$$\psi = (a\omega)^2 / ((s - 1) \times gd) \tag{6.14}$$

6.2.3 Bed Friction

The wave friction factor (f_w) and the energy dissipation factor (f_e) are theoretically different, and under some conditions have slightly different values. However, for the purpose of the sediment suspension model it is not necessary to distinguish between them.

An estimate of f_e is given by the following equations:

for $r/a < 0.63$

$$f_e = \exp(5.213 \times (r / a)^{0.194} - 5.977 \quad (6.15a)$$

and for $r/a \geq 0.63$

$$f_e = 0.3 \quad (6.15b)$$

where r is the bed roughness, and a is the near-bed semi excursion.

6.3 Sediment entrainment by waves

Sediment entrainment by waves is controlled by the peak near-bed orbital velocity, the bed roughness, and the sediment characteristics. The significant sediment characteristics are the relative sediment density (s), which is 2.65 kg/m^3 for quartz sand, and the grain diameter (d). The most salient parameter for sediment mobility under waves is Shields parameter (θ), which expresses the ratio between the moving shear force near the bed (τd^2) and the stabilizing gravity force ($pg(s-1)d^3$) (where p is pressure). Shield's parameter values less than 1.0 means that ripples can exist on the seabed, while higher values indicate that all bed forms are flattened by high shear stress. The Shield's parameter can be estimated using:

$$\theta = 0.5 f_w \times ((a\omega)^2 / ((s - 1) \text{ x } gd) \quad (6.16)$$

where f_w equals f_e, which can be calculated using equations 6.15a and 6.15b.

Grain motion is initiated in laminar boundary layers ($d \leq 0.55 \times 10^{-3}$ m) when

$$\theta = 0.21 \times 2a^{2/3} / d \tag{6.17a}$$

and for turbulent boundary layers ($d > 0.55 \times 10^{-3}$ m) when

$$\theta = 0.46\pi \times 2a^{2/3} / d \tag{6.17b}$$

The total amount of suspended material is calculated as:

$$\int_0^\infty cdz = c(0)\iota_s \tag{6.18}$$

where (c) is the sediment concentration, (z) is a vertical coordinate, and (ι_s) is the vertical length scale of the exponential concentration profile, i.e. the boundary layer diffusion length, which can be estimated using Cowell and Nielsen (1984) equations:

for $(a\omega / w) \leq 17.4$

$$\iota_s / \eta = 0.050 \times (a\omega / w)^{1.25} \tag{6.19a}$$

and for $(a\omega / w) > 17.4$

$$\iota_s / \eta = 3.32 \times (a\omega / w)^{-0.22} \tag{6.19b}$$

where w is the sediment fall velocity.

The sediment fall velocity is approximated by Raudkivi (1976) as:

for $d \leq 1.5 \times 10^{-4}$

$$w \approx 663d^2 \quad (6.20a)$$

and for $d \geq 1.5 \times 10^{-3}$

$$w \approx 134.5 \times \sqrt{d} \quad (6.20b)$$

and for $1.5 \times 10^{-4} < d < 1.5 \times 10^{-3}$

$$w \approx 109.9d \quad (6.20c)$$

6.4 Waves and Currents

Waves are effective in initiating sediment movement, especially in the presence of bed forms such as wave ripples. However, waves are inefficient in transporting sediment. The theory that waves entrain sediment, while currents are responsible for the actual transport, is a simplification of the actual processes involved. At this stage, little is known about the flow structure of turbulent boundary layers under the combined action of waves and currents.

Cowell and Nielsen's (1984) computer program for wave mobilisation of sand beds does not take currents into consideration, but does only calculate the sediment suspension potential as a result of wave action. It cannot be used to calculate which direction the sediment may be transported upon entrainment. Perhaps current parameters can be introduced into the model, making it possible to calculate plausible sediment transport directions as well. The next step would be to make this model run simulations in a GIS, where one could evaluate the model, and find ways of improving its accuracy.

7 Results

The results of the statistical analysis are numerous, and are here presented in fifteen sections. The fifteen sections present the findings for the fifteen different ways the data has been divided prior to analysis. Each section starts with a plot of coastal sand area against shelf sand area. Thereafter the results of the correlation analysis of sixteen defining variables and six dependent variables are presented and commented on. Diagrams of correlation of lagged data are also presented. The lagged variables are SumSea (same as lag0) and slag0 (Suspension multiplied by SumSea).

The correlations presented are at least significant at a one-tailed 0.10 significance level. In most cases, the significance is much higher, i.e. the level is lower (closing on zero). However, not including the correlations with low significance makes it easier to ignore the differences in significance level for the rest of the results. Naturally, it would be of interest to decide if a correlation is valid or not, but what is more interesting is the variation in correlation between the different variables. In addition, correlations with fewer samples than thirty are disregarded. Non-significant correlations are marked with an asterisk (*).

The dependent variables in the correlation tables are:

SumSand: Barrier sand area in square km (2 km samples).
Sandbypass: Same as SumSand, but samples without sand barriers are not included.
Sand4k: Two SumSand 2 km samples added up and averaged.
Sand6k: Three SumSand 2 km samples added up and averaged.
Sand8k: Four SumSand 2 km samples added up and averaged.
Sand10k: Five SumSand 2 km samples added up and averaged.

The defining variables in the correlation tables are:

SumSea: Shelf sand area in square km (2 km samples).
Sea4k: Two SumSea 2 km samples added up and averaged.
Sea6k: Three SumSea 2 km samples added up and averaged.
Sea8k: Four SumSea 2 km samples added up and averaged.
Sea10k: Five SumSea 2 km samples added up and averaged.
Slopeangle: Inclination of seabed in degrees (2 km samples).
Slope4k: Two Slopeangle 2 km samples added up and averaged.
Slope6k: Three Slopeangle 2 km samples added up and averaged.
Slope8k: Four Slopeangle 2 km samples added up and averaged.
Slope10k: Five Slopeangle 2 km samples added up and averaged.
Suspension: The total amount of sediment in suspension during a year.
Slag0: Suspension multiplied by SumSea.
Sus4k: Two Suspension samples added up and averaged.
Sus6k: Three Suspension samples added up and averaged.
Sus8k: Four Suspension samples added up and averaged.
Sus10k: Five Suspension samples added up and averaged.

7.1 The whole data set without exceptions

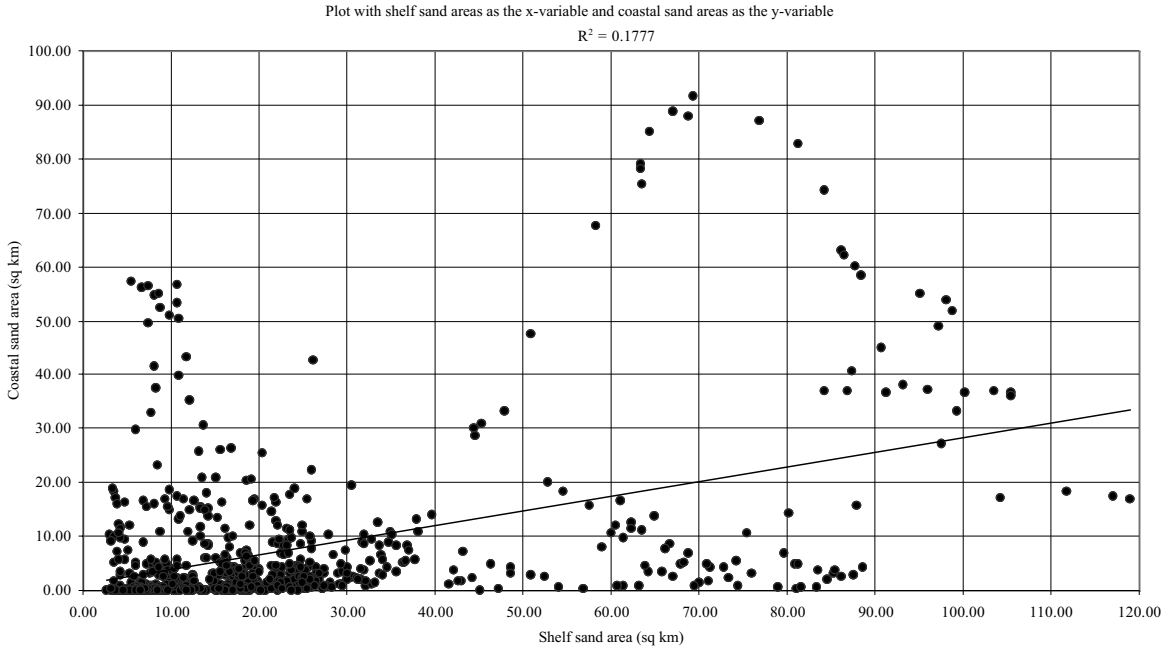

Plot 7.1. Correlation of SumSea and SumSand shows a lot of scatter.

Table 7.1. Significant correlations between computed variables.

	SumSand	Sandbypass	Sand4k	Sand6k	Sand8k	Sand10k
SumSea	0.422	0.403	0.415	0.406	0.397	0.392
Sea4k	0.437	0.419	0.426	0.408	0.409	0.397
Sea6k	0.449	0.434	0.431	0.432	0.392	0.514
Sea8k	0.47	0.457	0.453	0.411	0.437	0.493
Sea10k	0.463	0.45	0.478	0.5	0.493	0.441
Slopeangle	-0.179	-0.145	-0.178	-0.168	-0.174	-0.107
Slope4k	-0.199	-0.17	-0.189	-0.197	-0.182	*
Slope6k	-0.204	-0.18	-0.214	-0.191	-0.234	*
Slope8k	-0.236	-0.218	-0.224	-0.244	-0.205	-0.278
Slope10k	-0.233	-0.222	-0.248	-0.257	-0.285	-0.2
Suspension	0.158	0.161	0.181	*	*	*
slag0	*	*	*	*	*	*
Sus4k	*	*	*	*	*	*
Sus6k	*	*	*	*	*	*
Sus8k	*	*	*	*	*	*
Sus10k	*	*	*	0.472	*	*

The scatter in the plot is great, and this makes it easy to doubt that the correlation is an indication of an actual relationship, but it also makes it hard to disprove that such a relationship in fact exists. Correlation increases when sand barriers are correlated with averages of larger areas of seabed. However, using averages of larger sand barrier areas does not seem to have any clear tendency to affect the correlation. The correlations with seabed inclination are negative because more sand move onshore when the inclination of the seabed is gentle than when it is steep. The modelling of sand suspension did not give satisfactory results, and hence the correlations with sand suspension are largely insignificant.

Diagram 7.1. Lagged SumSea correlated with SumSand and Sandbypass.

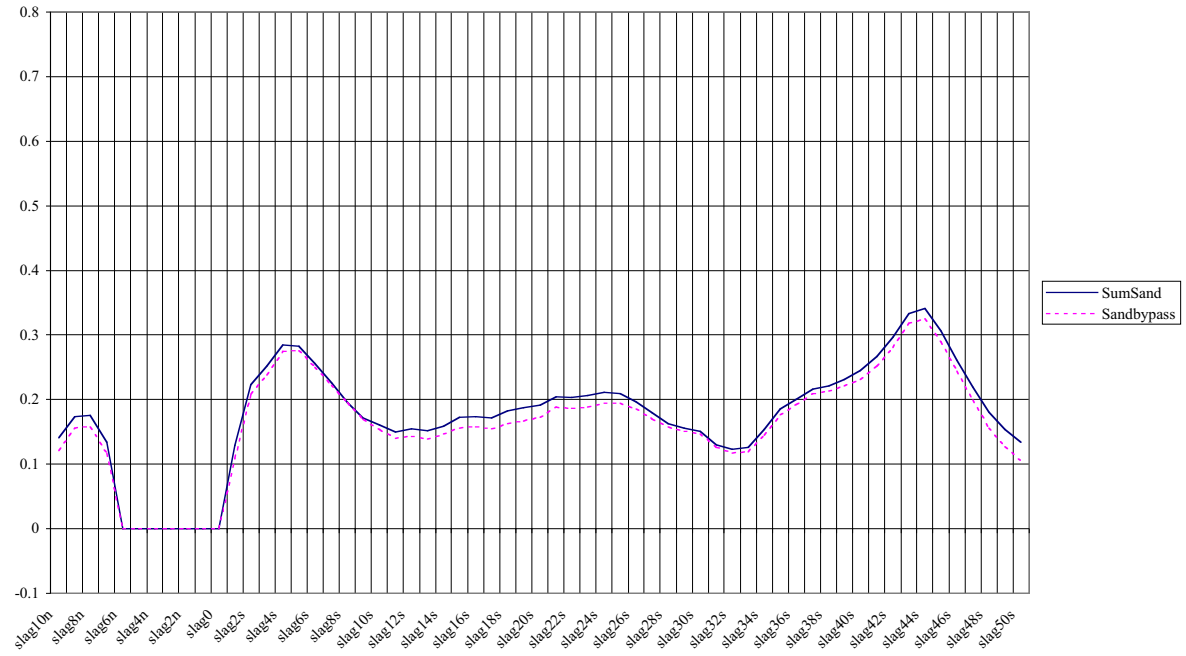

Diagram 7.2. Suspension multiplied with SumSea is here lagged and correlated with SumSand and Sandbypass.

The correlation of lagged SumSea and SumSand/Sandbypass in diagram 7.1 increases with increased lag, which might suggest a northward flow of sand. The dip in the curve is a re-occurring phenomenon, and will be discussed later. The other diagram's curve is more erratic, but does show the same tendency, and does have the same dip. The slope towards slag50s is probably a boundary effect. At some point, correlation must fail simply due to the two variables being too geographically distant from each other. It is evident that it is hard to say anything certain about the whole data set.

7.2 The whole data set, Jervis Bay excepted.

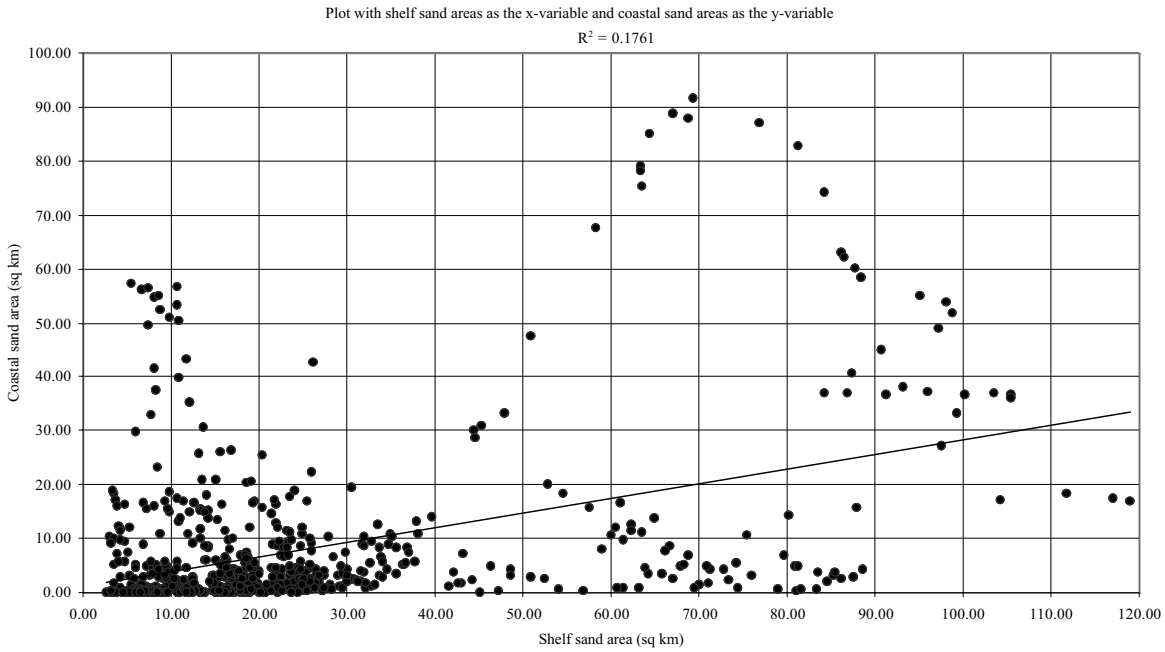

Plot 7.2. Correlation of SumSea and SumSand without Jervis Bay.

Table 7.2. Significant correlations between computed variables.

	SumSand	Sandbypass	Sand4k	Sand6k	Sand8k	Sand10k
SumSea	0.42	0.402	0.413	0.405	0.397	0.395
Sea4k	0.435	0.419	0.424	0.409	0.41	0.397
Sea6k	0.447	0.429	0.429	0.38	0.396	0.514
Sea8k	0.469	0.454	0.452	0.415	0.436	0.486
Sea10k	0.463	0.444	0.476	0.501	0.492	0.389
Slopeangle	-0.176	-0.145	-0.177	-0.168	-0.18	*
Slope4k	-0.195	-0.167	-0.185	-0.2	-0.188	*
Slope6k	-0.201	-0.173	-0.209	*	-0.254	*
Slope8k	-0.231	-0.21	-0.221	-0.253	-0.205	*
Slope10k	-0.233	-0.211	-0.243	-0.252	-0.266	*
Suspension	0.158	0.163	0.173	*	*	*
slag0	*	*	*	*	*	*
Sus4k	*	*	*	*	*	*
Sus6k	0.165	*	*	*	*	*
Sus8k	*	*	0.379	*	0.45	*
Sus10k	0.196	*	*	0.463	*	*

Removing the area of Jervis Bay from the analysis does not make much difference for the whole dataset. In comparison, the correlations are very similar, although in most cases the correlation is slightly lower when Jervis Bay is excluded. It may be a mistake to manipulate the data in this way. However, when analysing different zones within the data set it can be quite valuable to exclude areas that may otherwise skew the population unnecessarily. Jervis Bay is excluded because of the shape of the bay, which is cut off from the open sea by a major headland. It has no sand barrier, and the areas between twenty and sixty metres of depth are outside the headland.

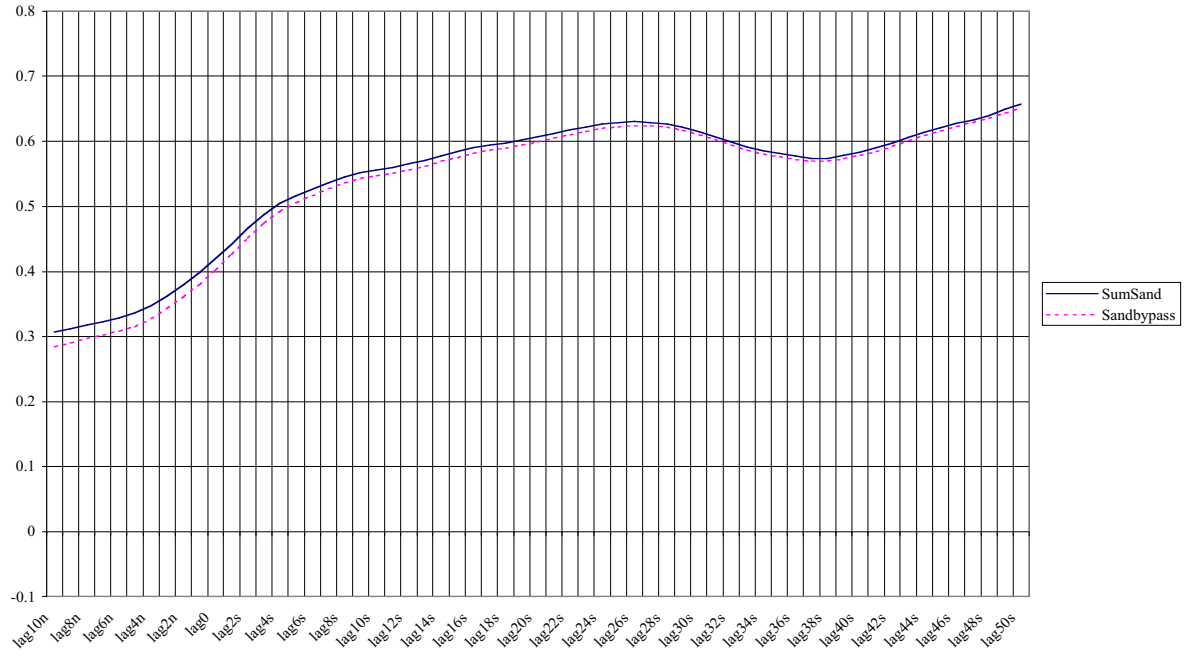

Diagram 7.3. Lagged SumSea correlated with SumSand and Sandbypass.

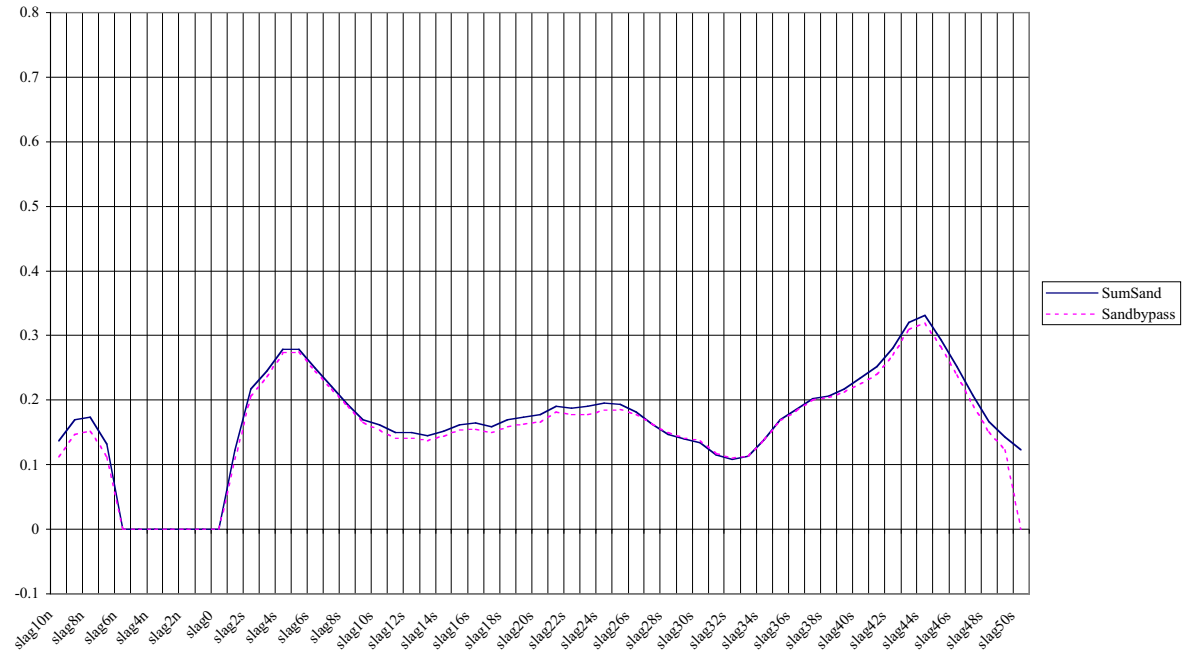

Diagram 7.4. Suspension multiplied with SumSea is here lagged and correlated with SumSand and Sandbypass.

As in the previous correlation analysis, these diagrams are very similar, although not identical to the diagrams for the whole data set (including Jervis Bay). One reason the correlations are so similar is simply because Jervis Bay is represented by a few samples in a large data set. It still has an effect, which can be explained by the large-scale processes that are at work. On a smaller scale, Jervis Bay has no effect, as the sand simply moves past the headland. This is why Jervis Bay easily can be excluded when analysing the smaller sections of the data set.

7.3 The four zones

7.3.1 Fraser Island to Byron Bay (Boxes 1-204)

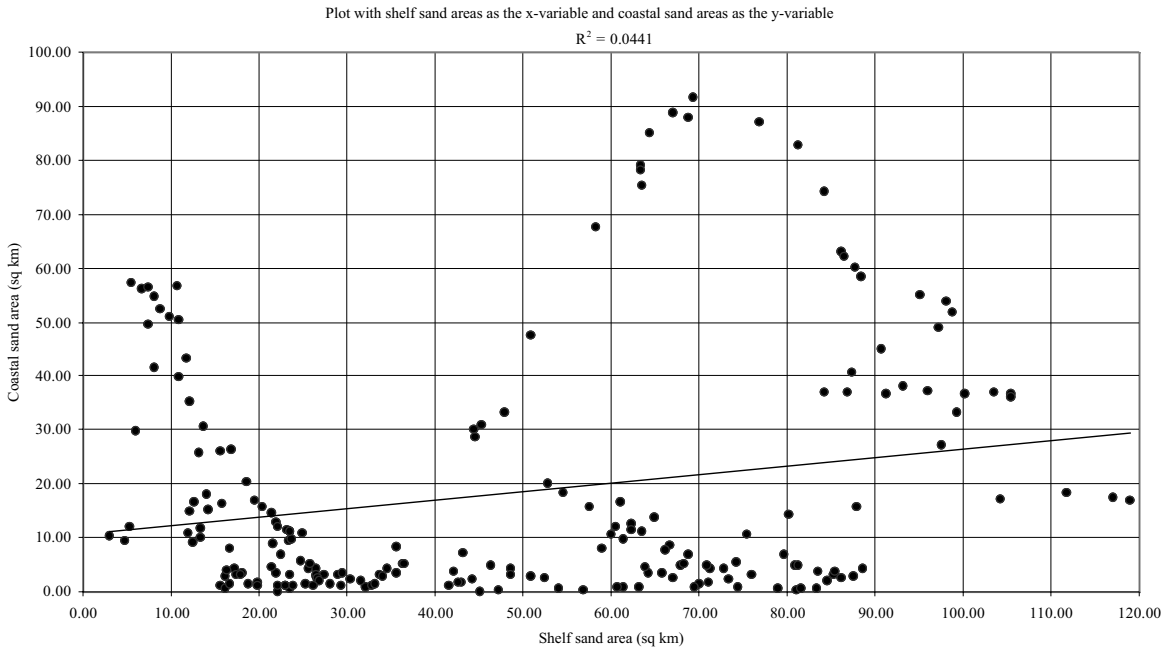

Plot 7.3. Correlation of SumSea and SumSand for Fraser Island to Byron Bay.

Table 7.3. Significant correlations between computed variables.

	SumSand	Sandbypass	Sand4k	Sand6k	Sand8k	Sand10k
SumSea	0.21	0.21	0.197	*	*	*
Sea4k	0.228	0.228	0.21	*	*	*
Sea6k	0.246	0.246	0.232	0.216	*	*
Sea8k	0.262	0.262	0.238	*	*	*
Sea10k	*	*	*	*	*	*
Slopeangle	*	*	*	*	*	*
Slope4k	*	*	*	*	*	*
Slope6k	*	*	*	*	*	*
Slope8k	*	*	*	*	*	*
Slope10k	*	*	*	*	*	*
Suspension	*	*	*	*	*	*
slag0	*	*	*	*	*	*
Sus4k	*	*	*	*	*	*
Sus6k	*	*	*	*	*	*
Sus8k	*	*	*	*	*	*
Sus10k	*	*	*	*	*	*

The scatter in the plot is extremely great, because of the massive sand barriers and the areas between these massive sand barriers, that in comparison has next to no sand at all. Correlation increases when sand barriers are correlated with averages of larger areas of seabed. There are no areas without sand, and therefore the Sandbypass correlation is identical to the SumSand correlation. No correlation was found with seabed inclination. This is a bit surprising, but the inclination in this area is very gentle, and the large sand barriers probably introduce large anomalies into the data set, which makes correlation impossible. There are no

sand grain size samples for most of this area (north of Tweed Heads, 1-176), and therefore the correlations with suspension variables are ignored.

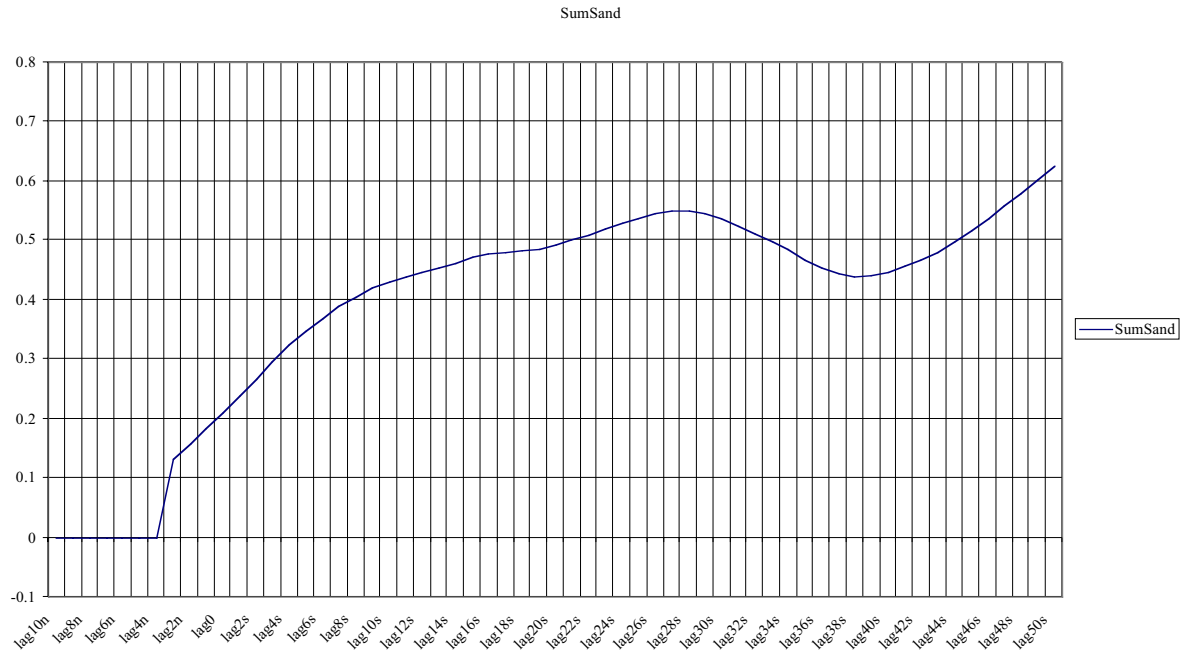

Diagram 7.5. Lagged SumSea correlated with SumSand.

The correlation of lagged SumSea and SumSand in diagram 7.5 increases with increased lag, which suggests a northward flow of sand. The variation in correlation is quite large, and so is the dip. This curve does not die off, which is a bit strange, but might be an indication that the sand in this area indeed comes from areas further to the south.

7.3.2 Byron Bay to Port Stephens (Boxes 202-433)

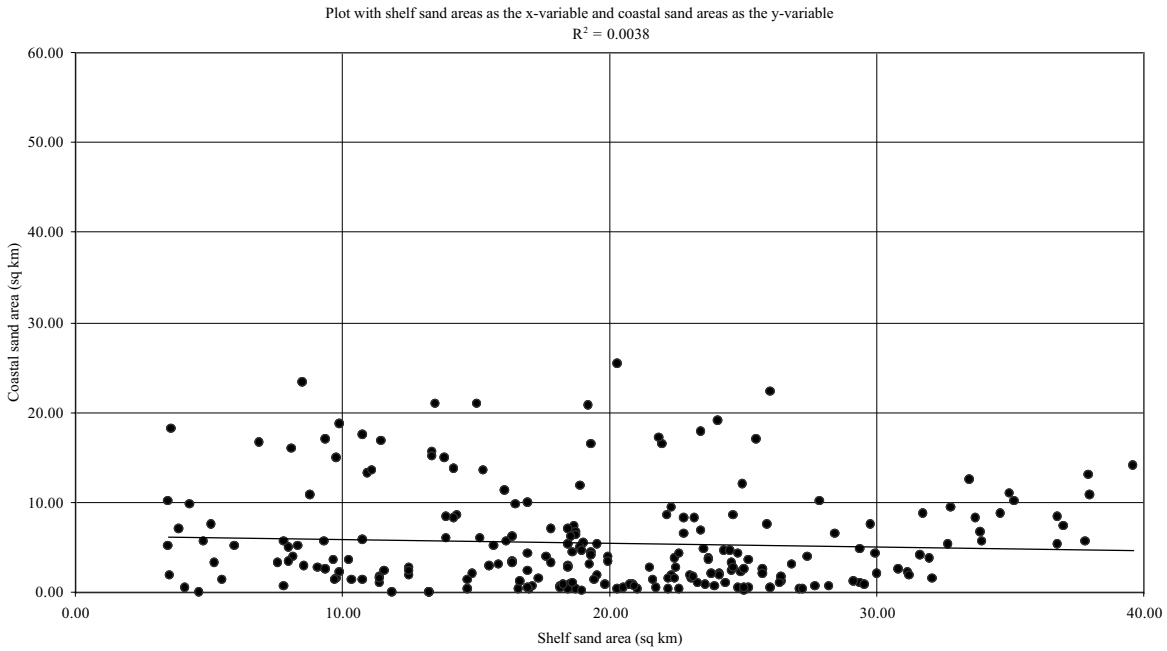

Plot 7.4. Correlation of SumSea and SumSand for Byron Bay to Port Stephens.

Table 7.4. Significant correlations between computed variables.

	SumSand	Sandbypass	Sand4k	Sand6k	Sand8k	Sand10k
SumSea	*	*	*	*	*	*
Sea4k	*	*	*	*	*	*
Sea6k	*	*	*	*	*	-0.468
Sea8k	*	*	*	0.538	*	*
Sea10k	*	*	*	-0.468	*	*
Slopeangle	*	*	*	*	*	*
Slope4k	*	*	*	*	*	*
Slope6k	*	*	*	*	*	*
Slope8k	*	*	*	*	*	*
Slope10k	*	*	*	*	*	*
Suspension	*	*	*	*	*	*
slag0	-0.23	-0.245	-0.301	-0.284	*	-0.491
Sus4k	*	*	*	*	*	*
Sus6k	*	*	*	*	*	*
Sus8k	*	*	*	-0.446	*	-0.55
Sus10k	*	*	*	*	*	*

This zone does not give many examples of significant correlation. The plot shows that there is no correlation between the size of sand barriers and the size of sand shelf areas. In addition, most of the significant correlations are negative, which indicates a southward flow of sand. The correlations of lagged data gives results that are even more interesting.

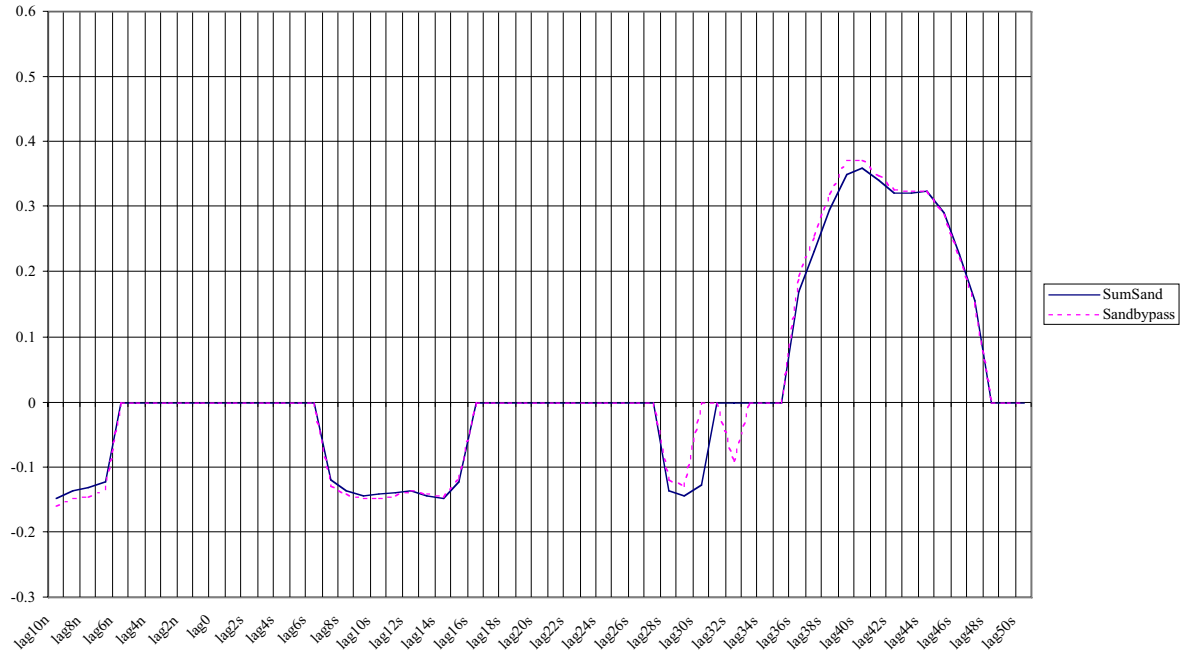

Diagram 7.6. Lagged SumSea correlated with SumSand and Sandbypass.

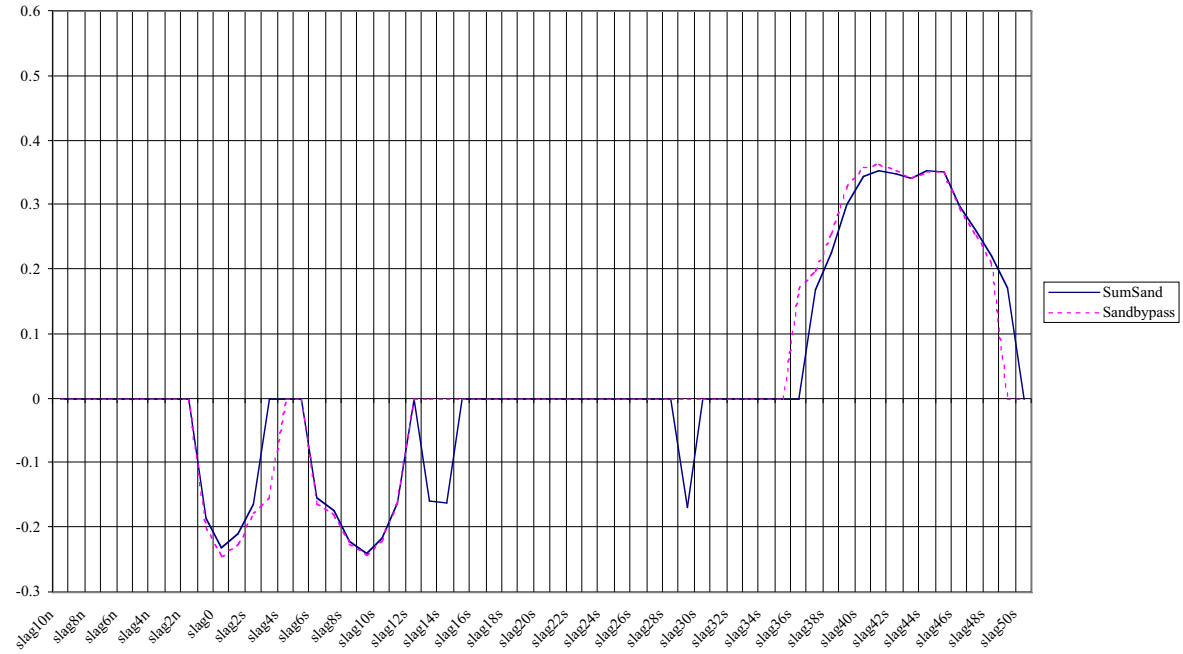

Diagram 7.7. Suspension multiplied with SumSea is here lagged and correlated with SumSand and Sandbypass.

Most of the correlations for lagged data where found to be insignificant. However, some returned significant correlations. These diagrams give complex information about this area. It seems that the transport locally might very well be southward, while the transport of sand on a larger scale is still northward. This area is clearly very complicated, and at present, no conclusive evidence supports a northward transport of sand throughout this area.

7.3.3 Port Stephens to Beecroft Head (Boxes 429-558)

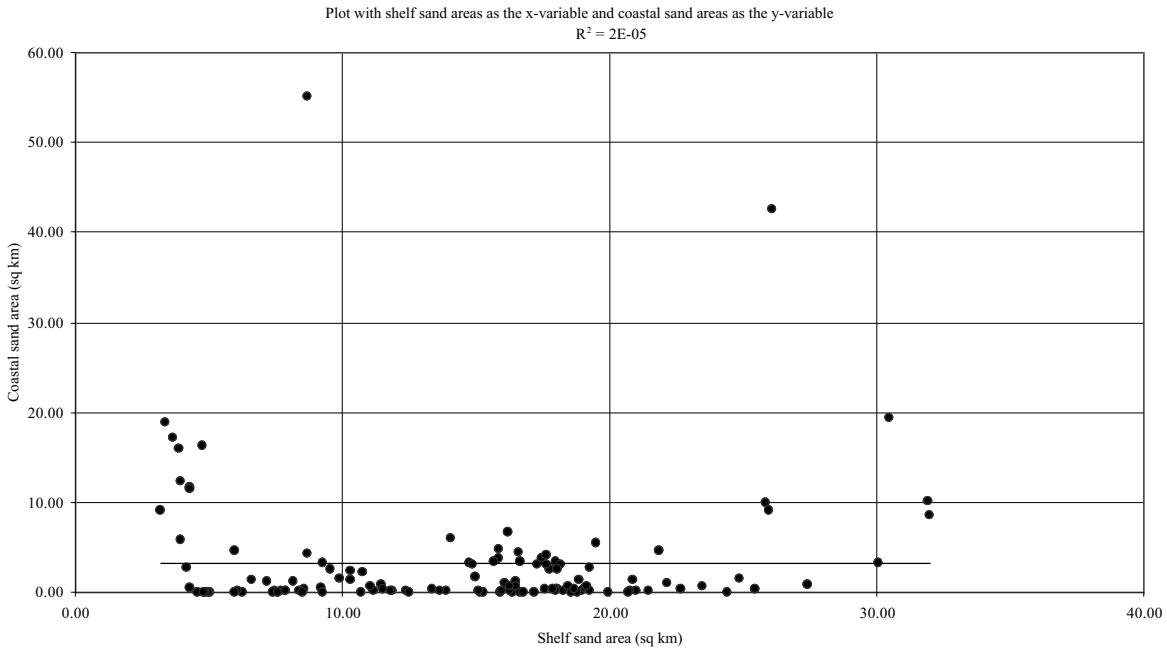

Plot 7.5. Correlation of SumSea and SumSand of Port Stephens to Beecroft Head.

Table 7.5. Significant correlations between computed variables.

	SumSand	**Sandbypass**	**Sand4k**	**Sand6k**	**Sand8k**	**Sand10k**
SumSea	*	*	*	*	*	*
Sea4k	*	*	*	*	*	*
Sea6k	*	*	*	*	*	*
Sea8k	*	*	*	*	*	*
Sea10k	*	*	0.535	0.601	0.551	*
Slopeangle	0.204	0.232	0.271	0.31	0.348	*
Slope4k	*	*	*	*	*	*
Slope6k	*	*	*	*	*	*
Slope8k	*	*	*	*	*	*
Slope10k	*	*	*	*	*	*
Suspension	0.345	0.359	0.317	*	0.443	*
slag0	*	*	*	*	*	*
Sus4k	*	*	*	*	0.349	0.591
Sus6k	0.353	0.352	0.505	0.303	0.74	0.729
Sus8k	-0.355	-0.405	*	*	*	*
Sus10k	*	*	*	*	*	*

Again, the plot shows no correlation. There is, however, significant correlation with the inclination of the seabed in this area, and this correlation increases when larger sand areas are used. The correlation is also better with Sandbypass than with SumSand.

The correlation with suspension variables gave many significant correlations as well. The best correlation is between Sand10k and Sus6k. This means that the collected sand samples in this area produced suspension rates that can be correlated with the size of the sand barriers.

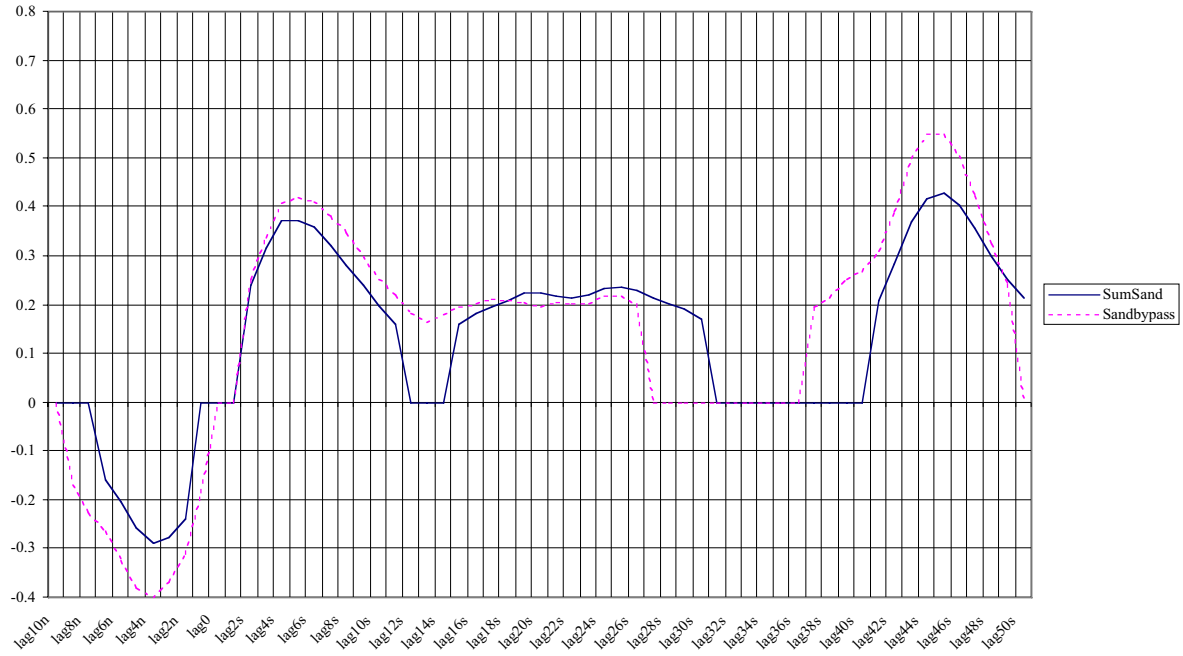

Diagram 7.8. Lagged SumSea correlated with SumSand and Sandbypass.

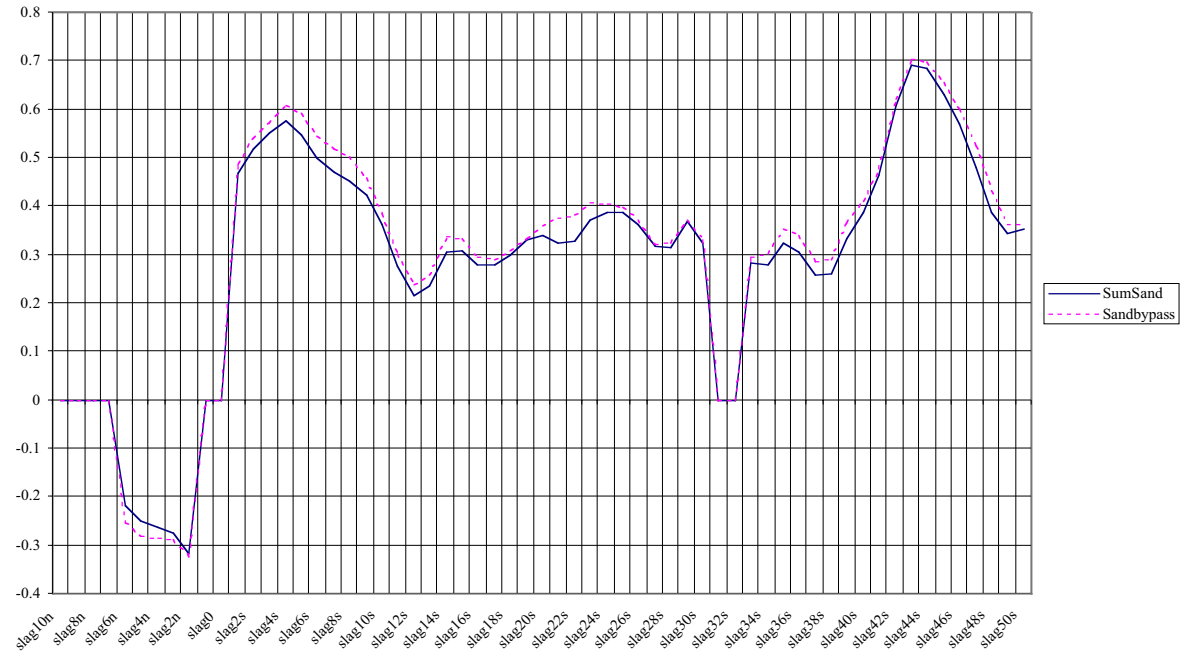

Diagram 7.9. Suspension multiplied with SumSea is here lagged and correlated with SumSand and Sandbypass.

The correlation of lagged SumSea and SumSand/Sandbypass increases with increased lag. These diagrams clearly show that the sand transport through this area is predominately northward. The variation in correlation is very large. It is interesting to note that Sandbypass gives higher correlation in most cases, and that the correlations for suspension lags are very high. The dip in the curve in diagram 7.9 is a very wide area with one dip down to zero. The many changes in the curve may be a result of the numerous beaches in this area, and the sand grain samples taken on these beaches.

7.3.4 St. Georges Head to Cape Howe (Boxes 566-698)

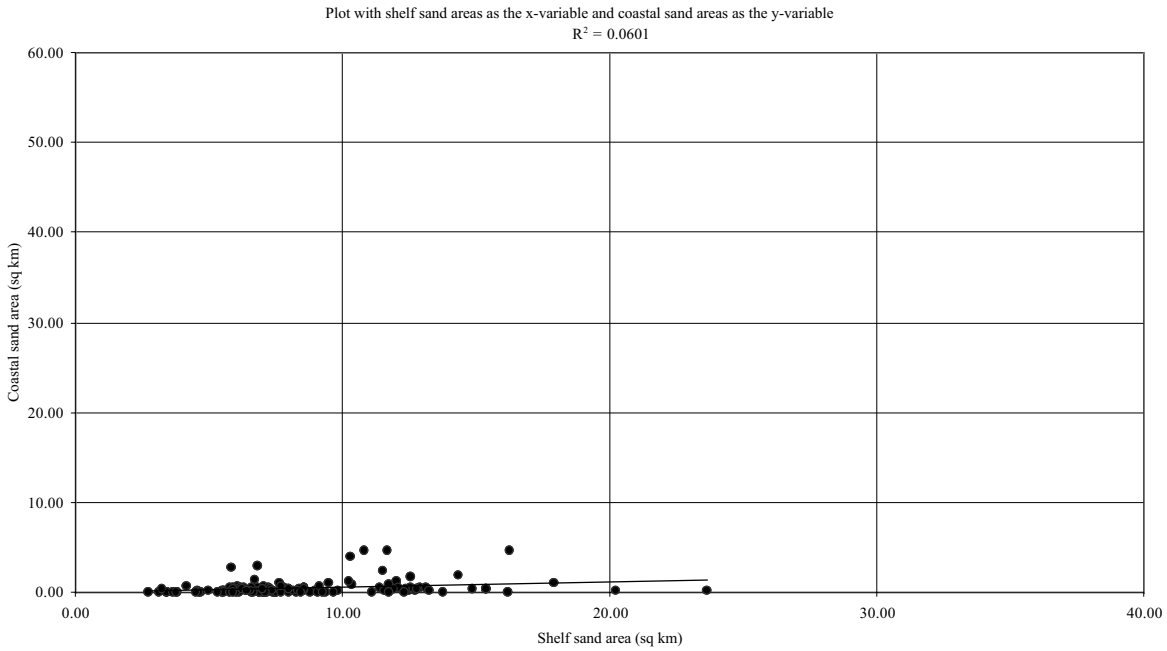

Plot 7.6. Correlation of SumSea and SumSand for St. Georges Head to Cape Howe.

Table 7.6. Significant correlations between computed variables.

	SumSand	Sandbypass	Sand4k	Sand6k	Sand8k	Sand10k
SumSea	0.245	0.171	*	*	*	*
Sea4k	0.228	*	0.231	*	*	*
Sea6k	0.319	*	*	0.312	*	*
Sea8k	*	*	*	*	*	0.778
Sea10k	*	*	*	*	*	*
Slopeangle	-0.25	-0.203	*	*	*	*
Slope4k	-0.257	*	-0.261	*	*	*
Slope6k	-0.323	-0.354	*	-0.317	*	*
Slope8k	-0.345	*	-0.303	*	*	-0.759
Slope10k	*	*	*	*	*	*
Suspension	*	*	*	*	*	*
slag0	0.339	0.349	*	*	*	*
Sus4k	*	*	*	*	*	*
Sus6k	0.332	*	0.491	*	*	*
Sus8k	*	*	0.379	0.755	*	-0.834
Sus10k	*	*	*	*	*	*

The size of the sand barriers is very small in this area, and thus the relationship between sand barrier size and shelf area size is not evident by looking at the data set. However, a significant correlation does exist. The correlation is lower for Sandbypass than for SumSand, which means that the areas without sand barriers are necessary for analysis.

It is hard to get a complete picture when so much of the correlation analysis gives non-significant results. The scattered results for this area seem to yield little information. The correlation with suspension shows some significant results, but it is much easier to get something out of the diagram with lagged SumSea multiplied with Suspension.

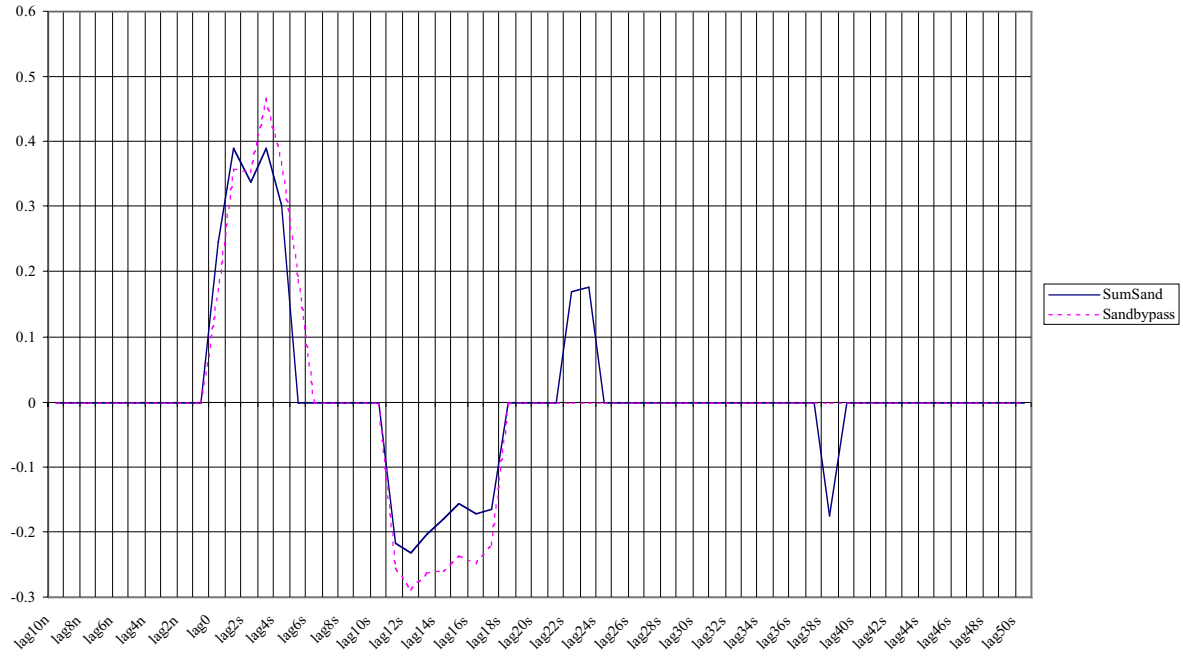

Diagram 7.10. Lagged SumSea correlated with SumSand and Sandbypass.

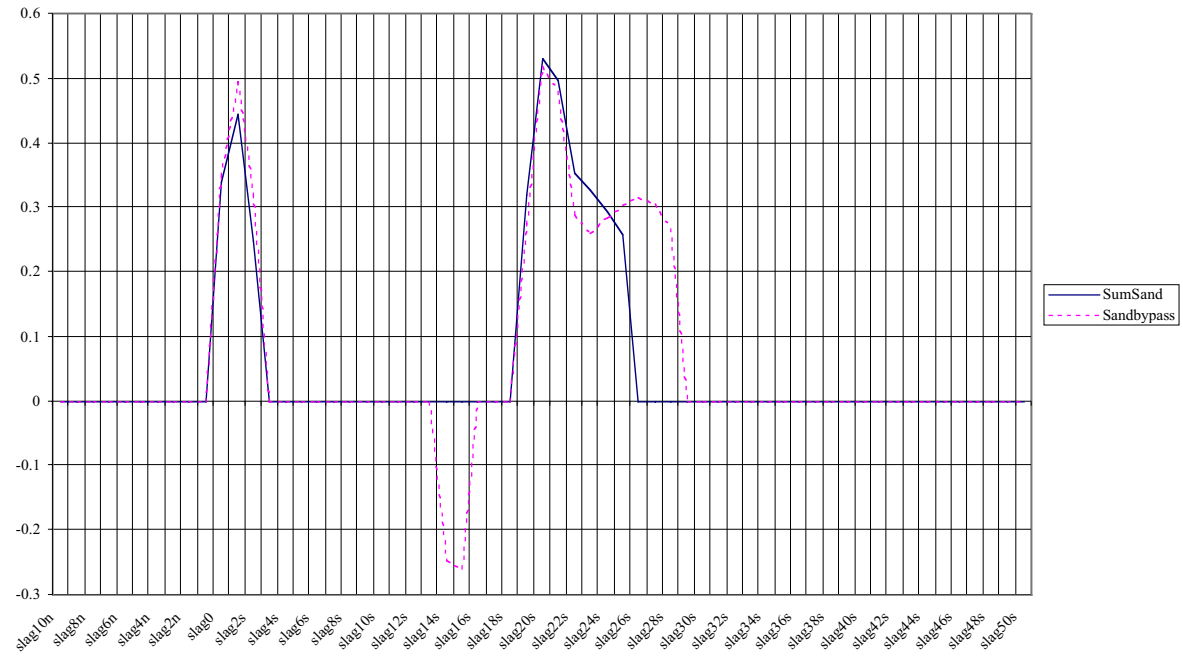

Diagram 7.11. Suspension multiplied with SumSea is here lagged and correlated with SumSand and Sandbypass.

The correlation of lagged SumSea and SumSand/Sandbypass in diagram 7.10 shows a high correlation for small lags. Further south it gets more uncertain and some negative correlation is present. The other diagram shows the same high correlation for small lags, but also has a large correlation for lags around 38-50 km south. Once again, the suspension rates enhance the analysis, and manage to strengthen correlation. The correlation for small lags indicate transport from bay to bay, while the correlation with areas further south supports the hypothesis of long way northward transport through this area.

7.4 The nine zones

7.4.1 Fraser Island to Caloundra Head (Boxes 1-109)

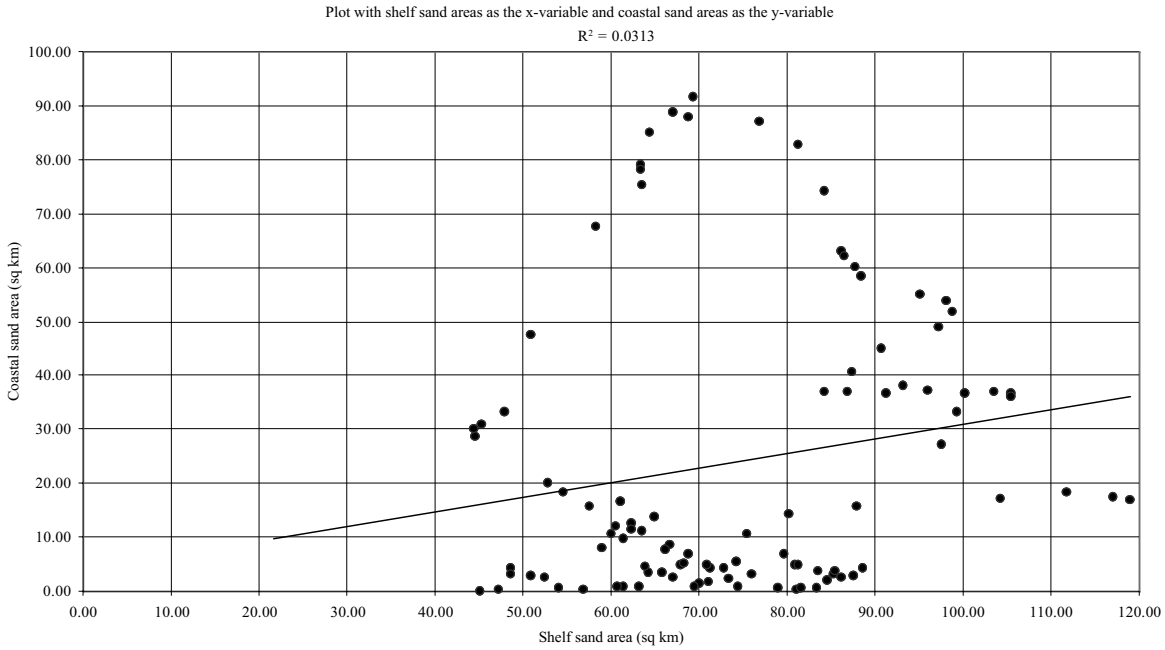

Plot 7.7. Correlation of SumSea and SumSand for Fraser Island to Caloundra Head.

Table 7.7. Significant correlations between computed variables.

	SumSand	Sandbypass	Sand4k	Sand6k	Sand8k	Sand10k
SumSea	0.177	0.177	*	*	*	*
Sea4k	*	*	*	*	*	*
Sea6k	*	*	*	*	*	*
Sea8k	*	*	*	*	*	*
Sea10k	*	*	*	*	*	*
Slopeangle	-0.171	-0.171	*	*	*	*
Slope4k	*	*	*	*	*	*
Slope6k	-0.29	-0.29	*	*	*	*
Slope8k	*	*	*	*	*	*
Slope10k	*	*	*	*	*	*

Plot 7.7 shows better correlation than plot 7.3, which can be explained by this area now not including areas further south that increase the scatter. The correlation is still low, and the scatter considerable. The correlation with lagged Sum Sea gives results that are more interesting.

There is no sand grain data for this zone, and therefore no computed suspension and other related variables.

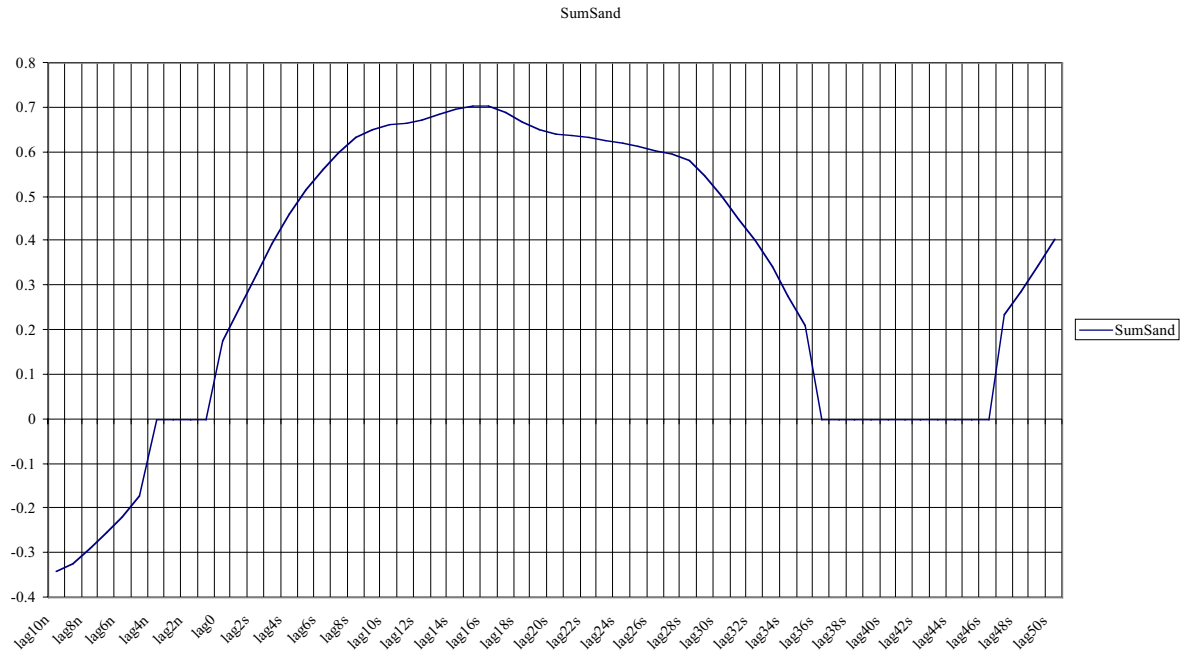

Diagram 7.12. Lagged SumSea correlated with SumSand.

The correlation of lagged SumSea and SumSand in diagram 7.12 produces a very nicely shaped curve with a maximum around 30 km south. The maximum indicates that the most common distance for a grain of sand to travel is 30 km north from any given location, settle, and then at some later stage be put into motion again and travel 30 km north, and so on. This is at least one way of interpreting the diagram.

At the far right, the curve goes up again, maybe indicating a second cycle, but this is very uncertain.

7.4.2 Caloundra Head to Byron Bay (Boxes 101-204)

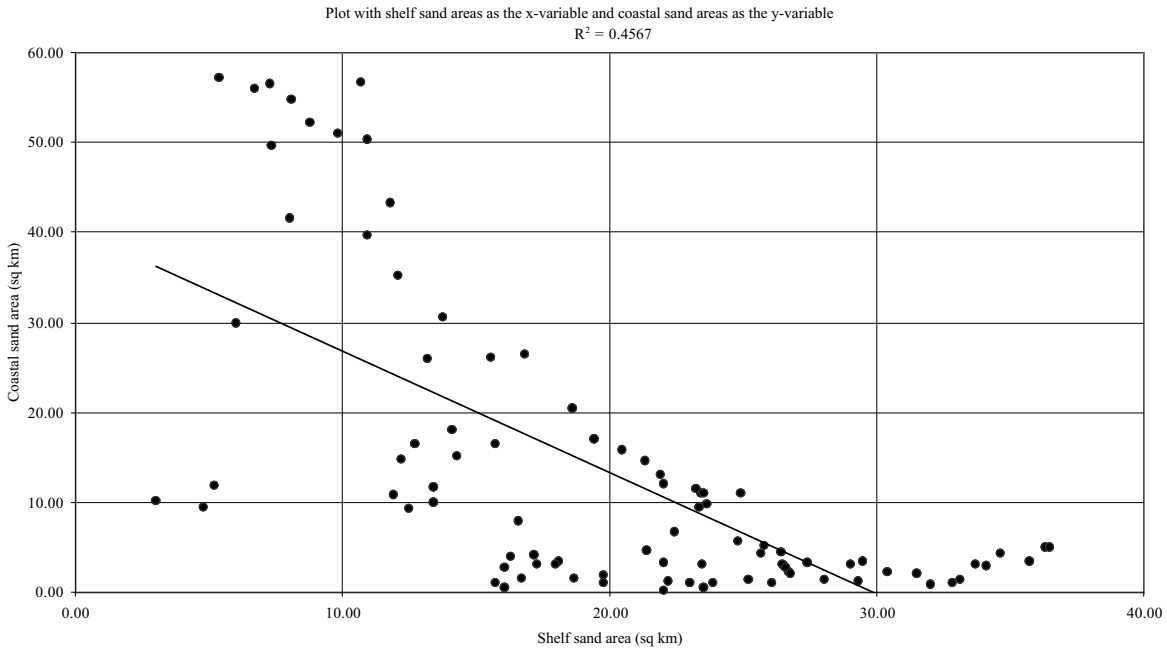

Plot 7.8. Correlation of SumSea and SumSand for Caloundra Head to Byron Bay.

Table 7.8. Significant correlations between computed variables.

	SumSand	Sandbypass	Sand4k	Sand6k	Sand8k	Sand10k
SumSea	-0.676	-0.676	-0.688	-0.687	-0.683	-0.751
Sea4k	-0.656	-0.656	-0.682	-0.612	-0.688	-0.714
Sea6k	-0.648	-0.648	-0.604	-0.692	-0.66	-0.769
Sea8k	-0.634	-0.634	-0.654	*	-0.697	-0.933
Sea10k	-0.631	-0.631	*	*	-0.895	-0.734
Slopeangle	0.542	0.542	0.653	0.643	0.651	0.714
Slope4k	0.519	0.519	0.558	*	0.527	*
Slope6k	0.474	0.474	*	0.561	0.361	0.812
Slope8k	0.487	0.487	0.511	*	0.59	0.875
Slope10k	0.431	0.431	*	*	*	0.632
Suspension	*	*	*	*	*	*
slag0	*	*	*	*	*	*
Sus4k	*	*	*	*	*	*
Sus6k	*	*	*	*	*	*
Sus8k	*	*	*	*	*	*
Sus10k	-0.926	-0.925	0.063	*	*	*

Oddly enough, this area shows negative correlation between SumSea and SumSand. This would suggest a southward transport of sand, which is unlikely, but quite possible locally. The correlation is definitely high enough to suggest such a relationship must exist. However, what is true locally might not hold true on a larger scale. An indication of this is that the correlation is smaller with larger sea areas.

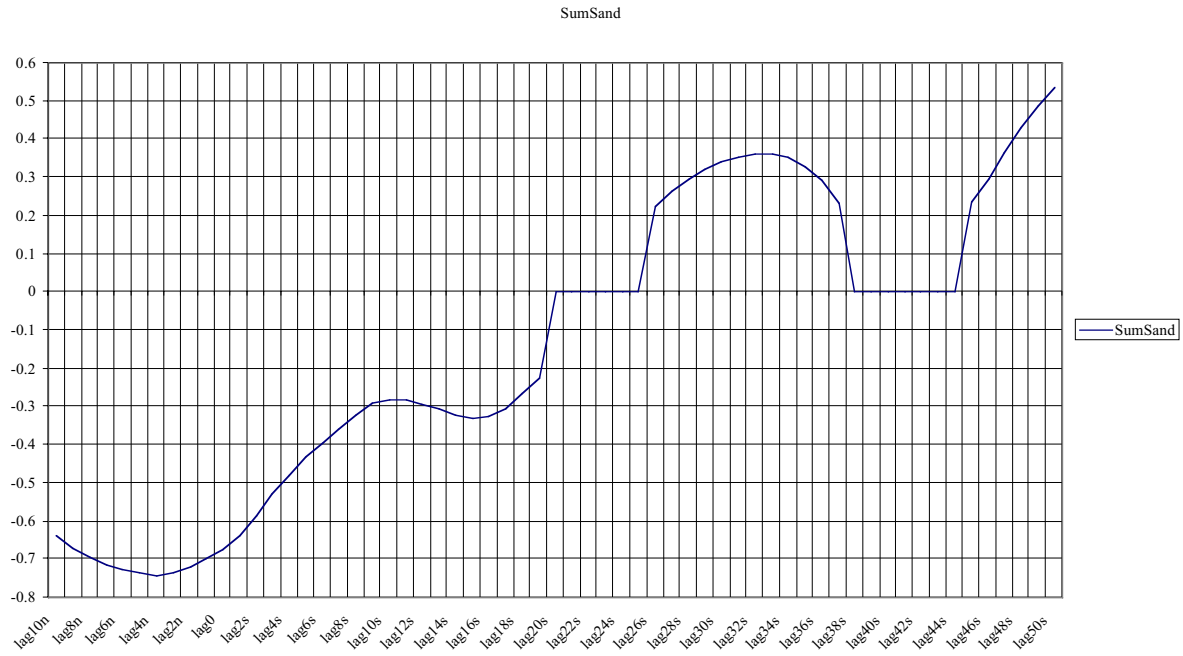

Diagram 7.13. Lagged SumSea correlated with SumSand and Sandbypass.

The shape of this curve suggests that sand is transported away from sand barriers in this area, in both a northerly and a southerly direction. Between 52 and 74 km south a positive correlation suggest northward transport on a larger scale through this region. This part of the curve looks like a small version of the curve in the previous section. The increasing correlation to the right in the diagram is also present.

There is unfortunately no significant correlation between suspended material multiplied with lagged shelf sand areas and SumSand for this zone.

7.4.3 Byron Bay to Smoky Cape (Boxes 202-329)

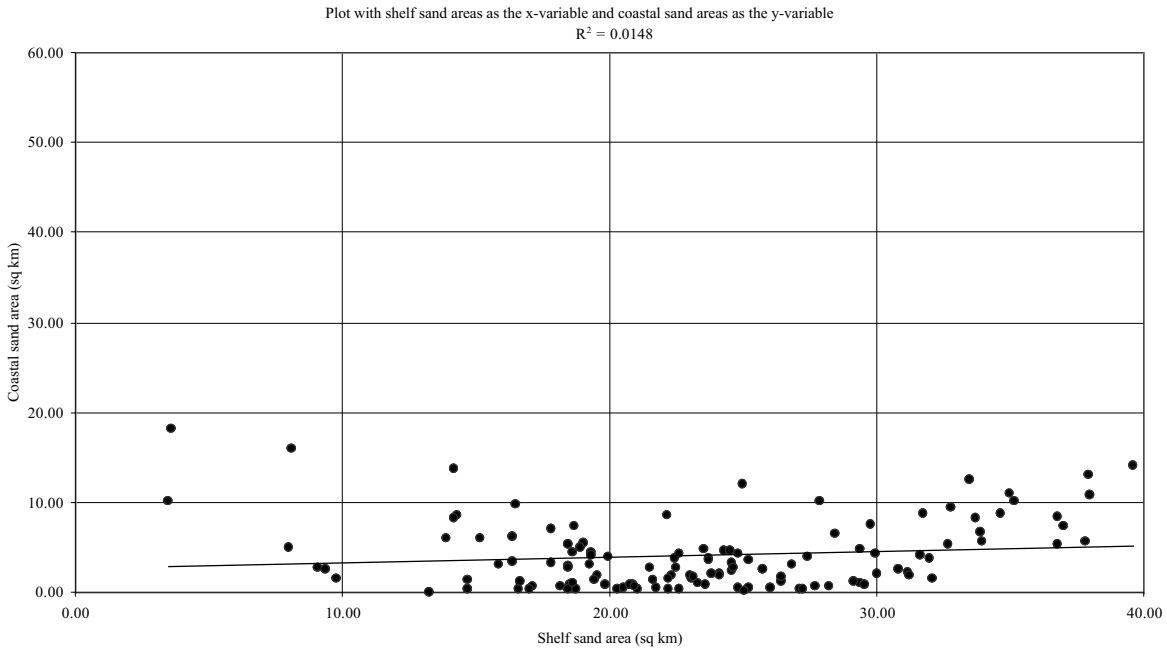

Plot 7.9. Correlation of SumSea and SumSand for Byron Bay to Smoky Cape.

Table 7.9. Significant correlations between computed variables.

	SumSand	Sandbypass	Sand4k	Sand6k	Sand8k	Sand10k
SumSea	*	*	*	0.325	*	*
Sea4k	*	*	*	0.472	*	*
Sea6k	0.295	0.295	0.564	0.315	0.649	*
Sea8k	*	*	*	0.752	*	*
Sea10k	0.723	0.709	0.658	*	*	0.448
Slopeangle	0.27	0.278	0.259	*	*	*
Slope4k	0.368	0.368	0.295	*	*	*
Slope6k	*	*	*	*	*	*
Slope8k	*	*	0.372	*	0.393	*
Slope10k	-0.578	-0.553	-0.514	*	*	*
Suspension	0.21	0.205	*	*	*	*
slag0	*	*	*	*	*	*
Sus4k	*	*	*	*	*	*
Sus6k	0.323	0.323	*	*	*	*
Sus8k	0.683	0.683	0.6	*	*	*
Sus10k	0.544	0.544	0.769	0.641	*	*

The correlation in the plot above is not significant. The correlation with Sea10k is very high, and it is interesting to note that there seems to be some kind of pattern, where six km averages seem to generate significant correlations. The highest correlation is found for Sand6k/Sea8k. That the significant correlations are found with the area averages can perhaps be explained by the length of the beaches in this area. This is pure speculation though.

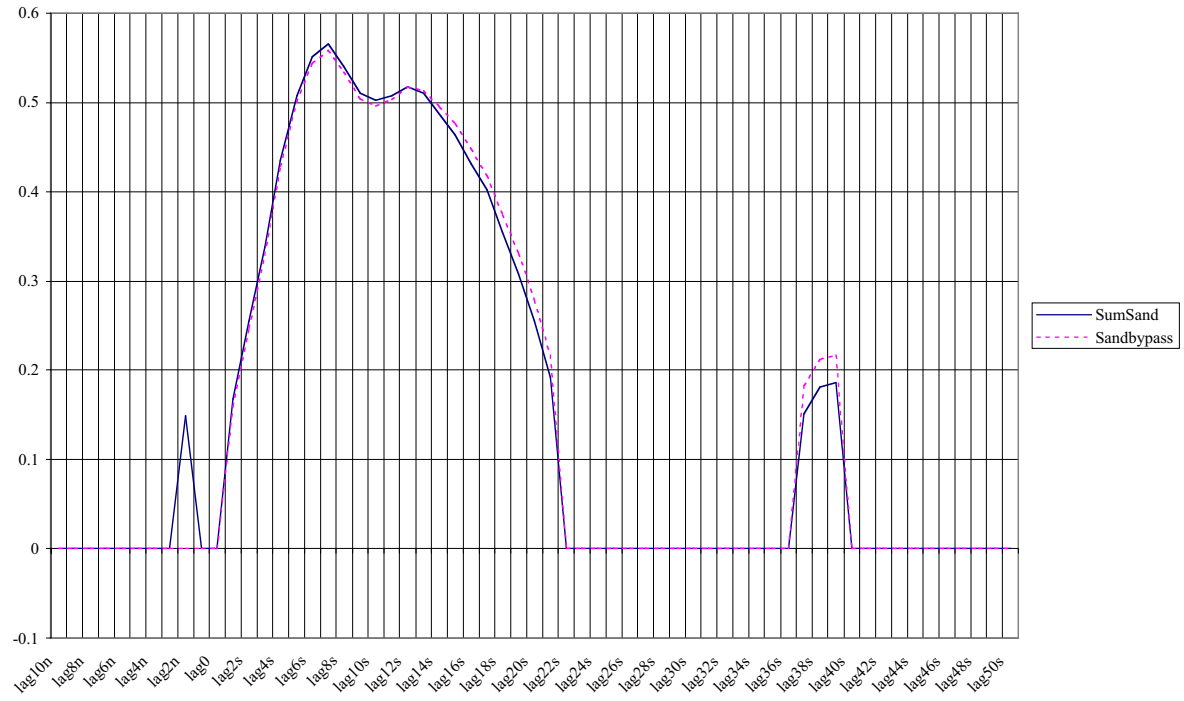

Diagram 7.14. Lagged SumSea correlated with SumSand and Sandbypass.

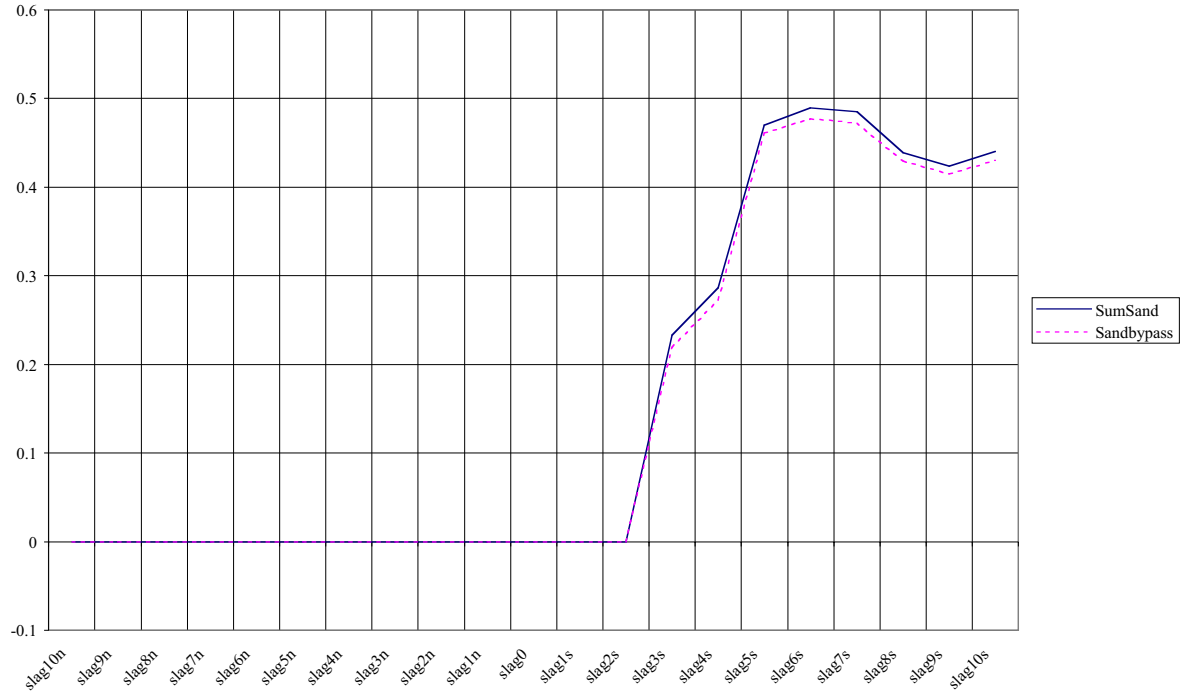

Diagram 7.15. Suspension multiplied with SumSea is here lagged and correlated with SumSand and Sandbypass.

The maximum correlation in diagram 7.14 is found between 12 and 14 km south, which is roughly twice the distance of the significant correlations for the area averages. There is also an area 74-78 km south, which has a significant correlation. Again, this all points to there being two distinct scales to consider. There is certainly evidence for a northward transport of sand in this area. Diagram 7.15 also supports the hypothesis.

7.4.4 Smoky Cape to Sugarloaf Point (Boxes 330-414)

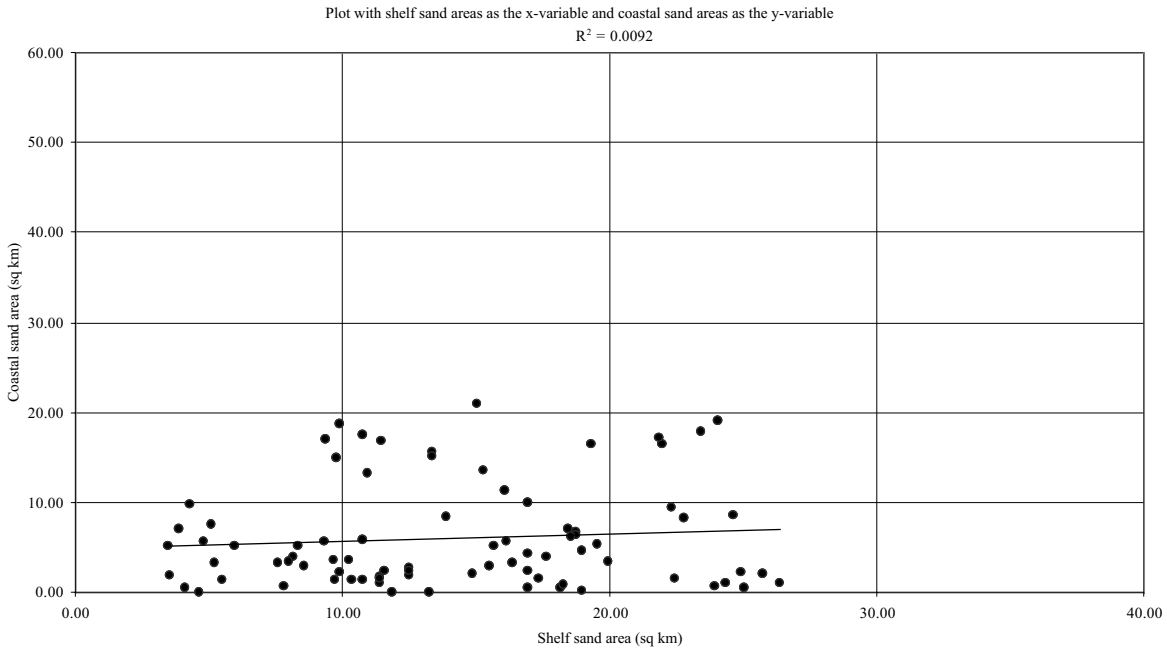

Plot 7.10. Correlation of SumSea and SumSand for Smoky Cape to Sugarloaf Point.

The correlation in the plot is not significant and there are no other significant correlations to show in a table here. The sand barriers in this area are saturated on sand. Therefore, northward sand transport probably simply moves past this area. The correlation of the lagged variables provides more information.

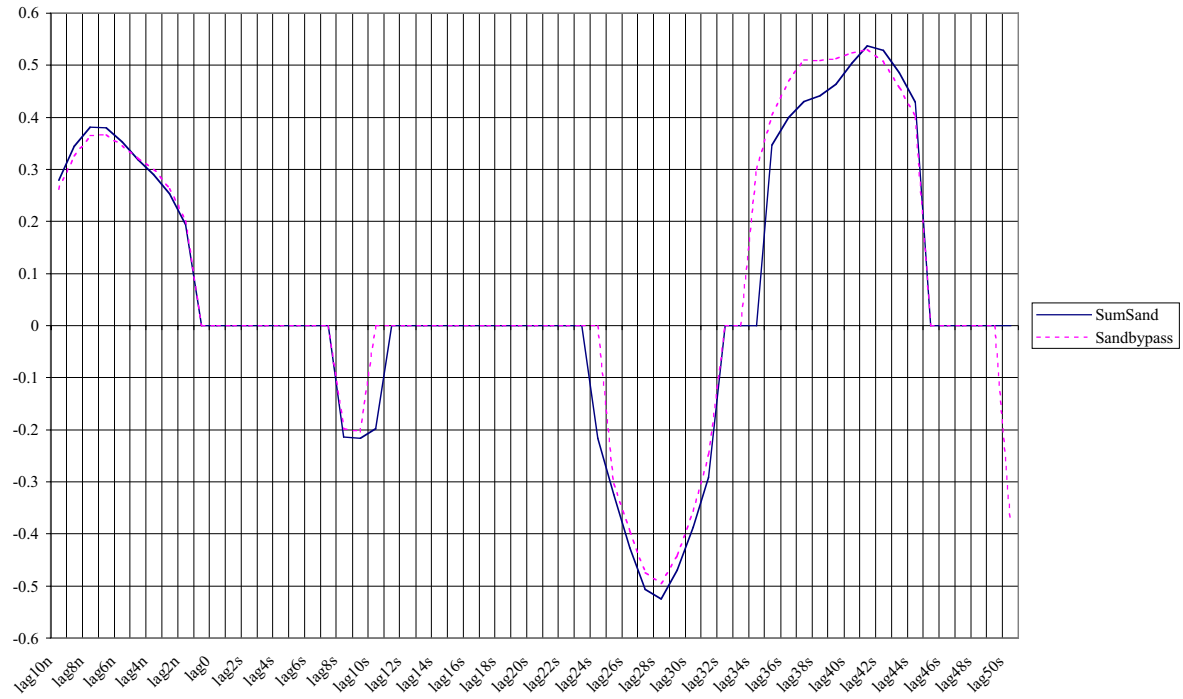

Diagram 7.16. Lagged SumSea correlated with SumSand and Sandbypass.

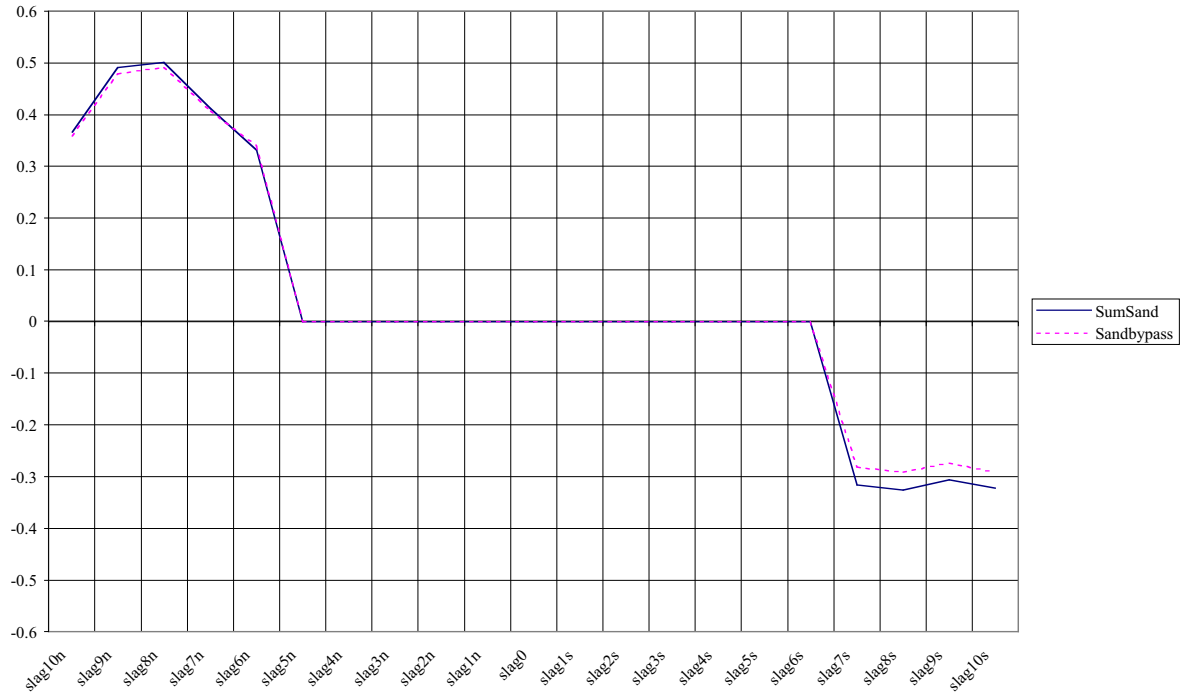

Diagram 7.17. Suspension multiplied with SumSea is here lagged and correlated with SumSand and Sandbypass.

In diagram 7.16, there are two incidents of negative correlation, which would suggest southward transport, but in this case, it is more likely to mean seaward transport. Around 80 km south there is positive correlation, suggesting northward transport on a larger scale. Diagram 7.17 does not support this, but that is simply due to the limitations in grain size samples, which inhibits correlation further than 20 km lag.

7.4.5 Sugarloaf Point to Port Stephens (Boxes 412-433)

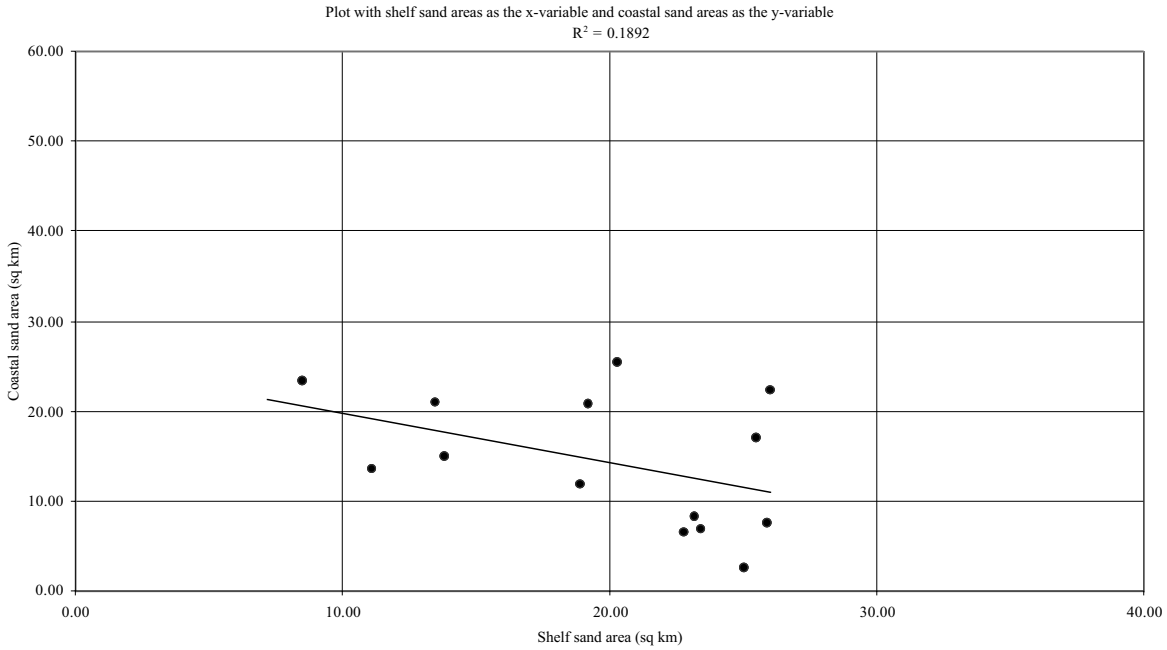

Plot 7.11. Correlation of SumSea and SumSand for Sugarloaf Point to Port Stephens.

This section has no significant correlations simply because there are not enough samples in this zone to make a satisfactory base for a statistical analysis. There is no point in lingering here, and so we move on to the next section.

7.4.6 Port Stephens to Botany Bay (Boxes 429-499)

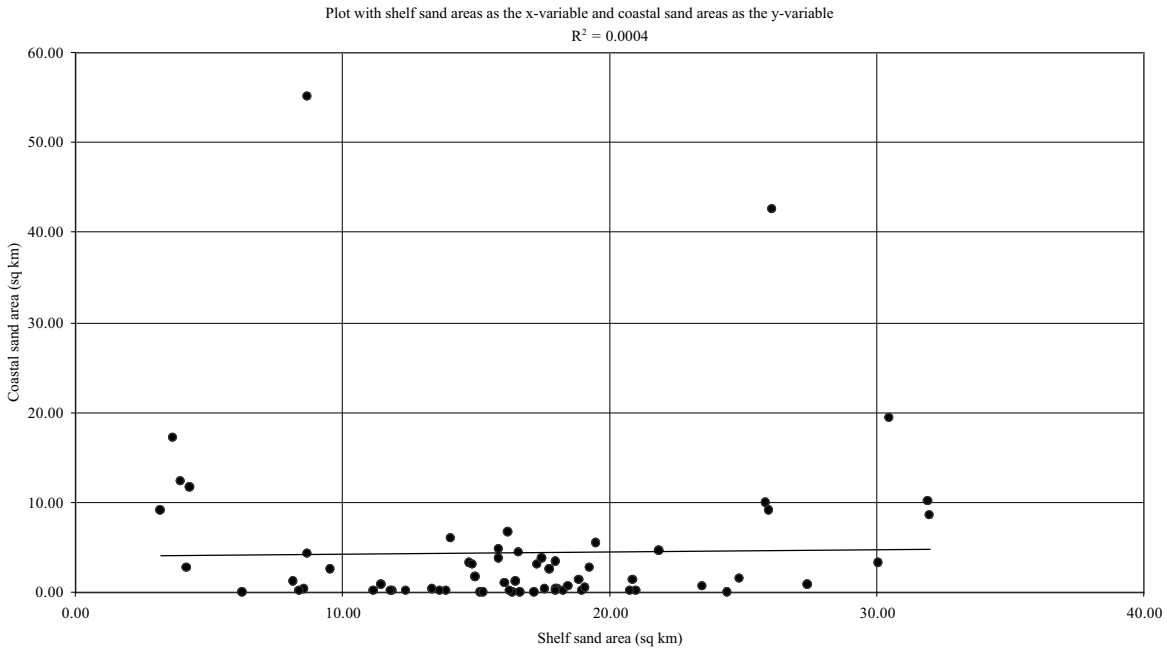

Plot 7.12. Correlation of SumSea and SumSand for Port Stephens to Botany Bay.

Table 7.10. Significant correlations between computed variables.

	SumSand	Sandbypass	Sand4k	Sand6k	Sand8k	Sand10k
SumSea	*	*	*	*	*	-0.52
Sea4k	*	*	*	*	*	*
Sea6k	*	*	*	*	*	*
Sea8k	0.464	0.509	0.427	*	*	*
Sea10k	0.521	0.521	*	*	*	*
Slopeangle	*	*	*	0.372	0.449	0.551
Slope4k	*	*	*	*	*	0.124
Slope6k	*	*	*	*	*	*
Slope8k	*	*	*	*	*	*
Slope10k	*	*	*	*	*	*
Suspension	0.417	0.452	0.334	0.338	*	0.747
slag0	*	*	*	*	*	*
Sus4k	*	*	*	0.568	0.704	0.81
Sus6k	0.553	0.557	0.725	0.463	0.829	0.816
Sus8k	*	*	*	*	*	*
Sus10k	0.863	0.897	0.927	*	*	*

The correlation in the plot is once again not significant. Some significant correlations are found for this zone. Most notable are the correlations with suspension and especially with Sus6k, which is quite high. The highest correlation is for Sand4k/Sus10k.

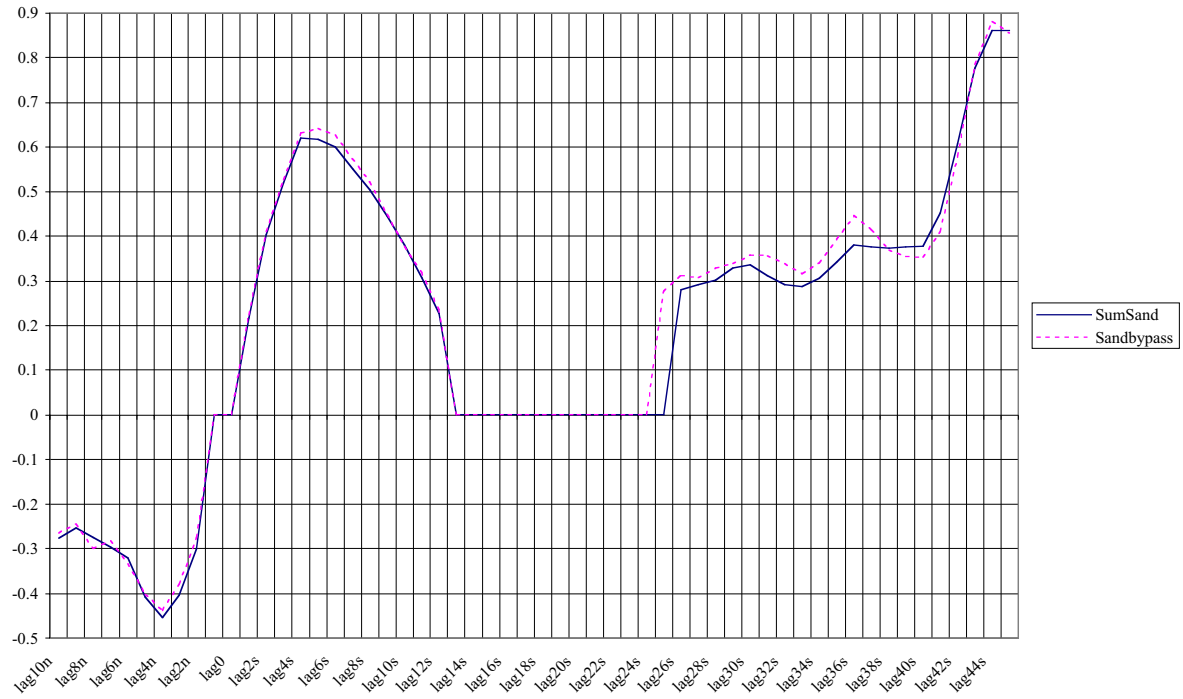

Diagram 7.18. Lagged SumSea correlated with SumSand and Sandbypass.

Diagram 7.19. Suspension multiplied with SumSea is here lagged and correlated with SumSand and Sandbypass.

The correlation in diagram 7.18 clearly shows that a northward transport in this area is very likely on many different scales. The highest correlation is found for 8-12 km south, and at the far right in the diagram, but one must be careful not to rely heavily on those border values.

Diagram 7.19 also supports northward transport.

7.4.7 Botany Bay to Beecroft Head (Boxes 500-558)

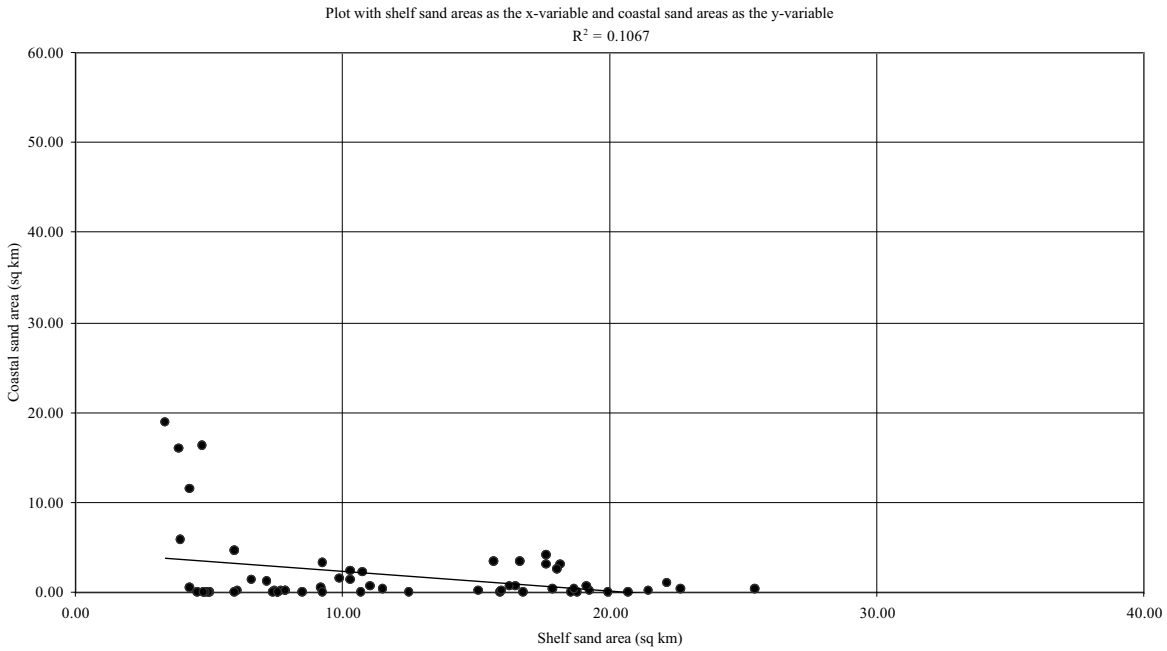

Plot 7.13. Correlation of SumSea and SumSand for Botany Bay to Beecroft Head

Table 7.11. Significant correlations between computed variables.

	SumSand	Sandbypass	Sand4k	Sand6k	Sand8k	Sand10k
SumSea	-0.327	-0.414	-0.344	*	*	*
Sea4k	-0.371	-0.494	-0.345	*	*	*
Sea6k	-0.405	-0.491	*	*	*	*
Sea8k	*	*	*	*	*	*
Sea10k	*	*	*	*	*	*
Slopeangle	0.536	0.633	0.559	0.626	0.59	0.594
Slope4k	0.593	0.713	0.563	0.735	0.605	0.744
Slope6k	0.637	0.72	0.729	0.574	0.783	0.99
Slope8k	0.613	0.726	0.597	0.831	0.584	*
Slope10k	0.638	0.659	0.826	0.986	*	0.634
Suspension	*	*	*	*	*	*
slag0	*	*	*	*	*	*
Sus4k	*	*	*	*	*	*
Sus6k	*	-0.508	*	*	*	*
Sus8k	*	*	*	*	*	*
Sus10k	*	*	-0.912	*	*	*

The negative correlation in this area is due to there being a large amount of sand in the south concentrated in a few major sand barriers. Most other sand barriers in this area are very small. It is doubtful whether any useful information can be wrested from this table.

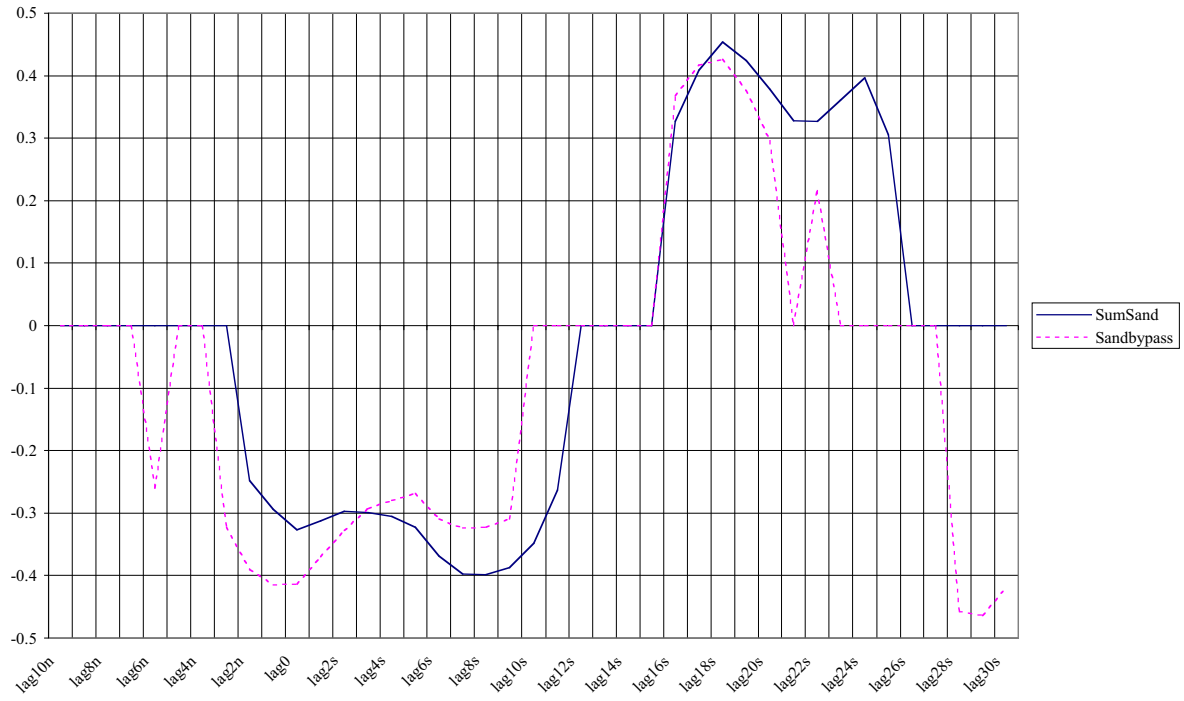

Diagram 7.19. Lagged SumSea correlated with SumSand and Sandbypass.

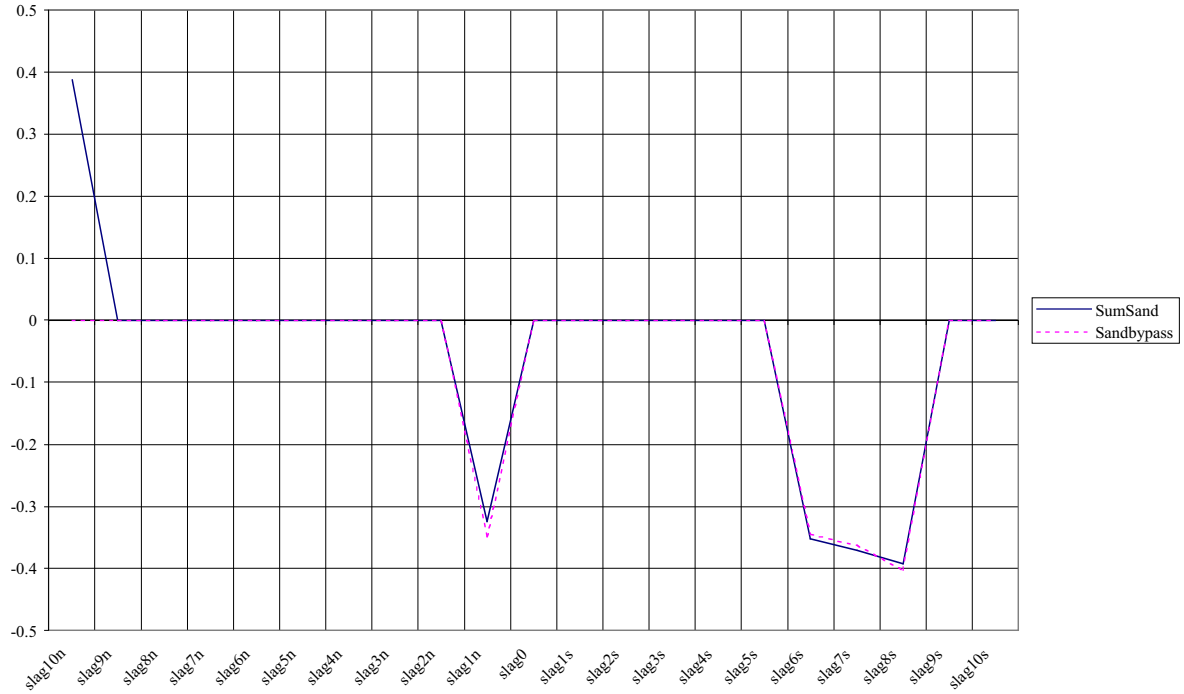

Diagram 7.20. Suspension multiplied with SumSea is here lagged and correlated with SumSand and Sandbypass.

As in table 7.11, the small-scale transport seems to be southward, but this is probably unreliable information. More reliable is the correlation between 32 and 40 km south, which again points toward northward transport on a larger scale. Further south, low significance makes the correlations somewhat unreliable.

Diagram 7.20 does not support the hypothesis.

7.4.8 St. Georges Head to Burrewarra Point (Boxes 566-604)

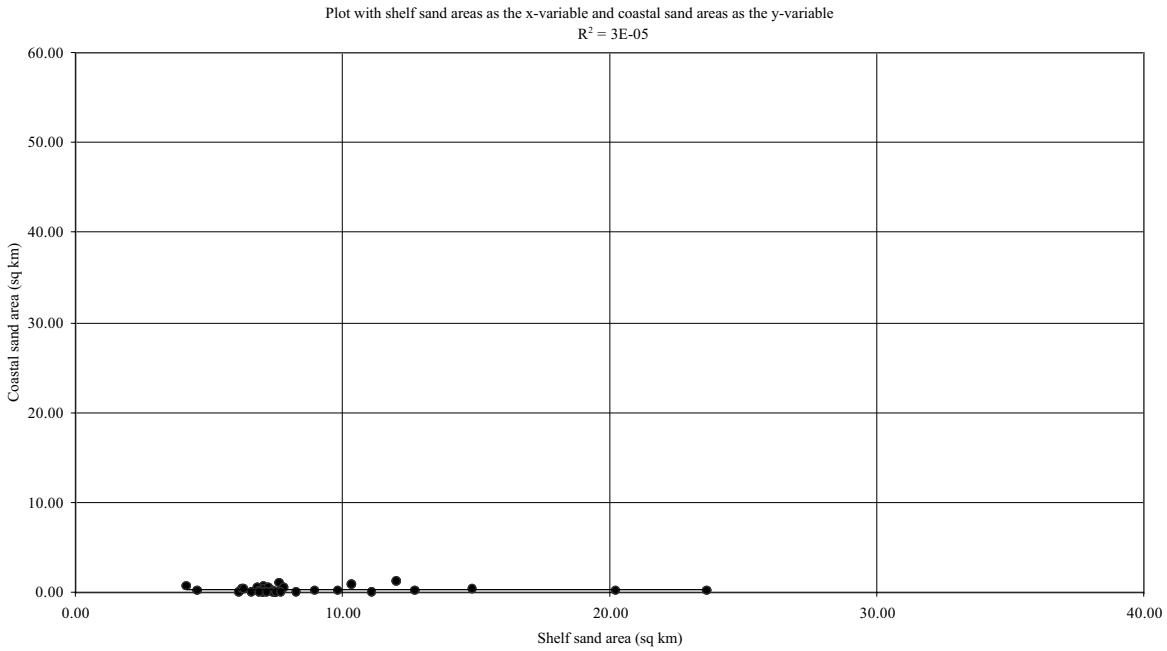

Plot 7.14. Correlation of SumSea and SumSand for St. Georges Head to Burrewarra Point.

This zone makes a rather small sample, but the main problem is the lack of sand in this area. It is impossible to determine any correlation because of this. Again, we will have to turn to the correlation of the lagged variables in order to wrest some information from this zone.

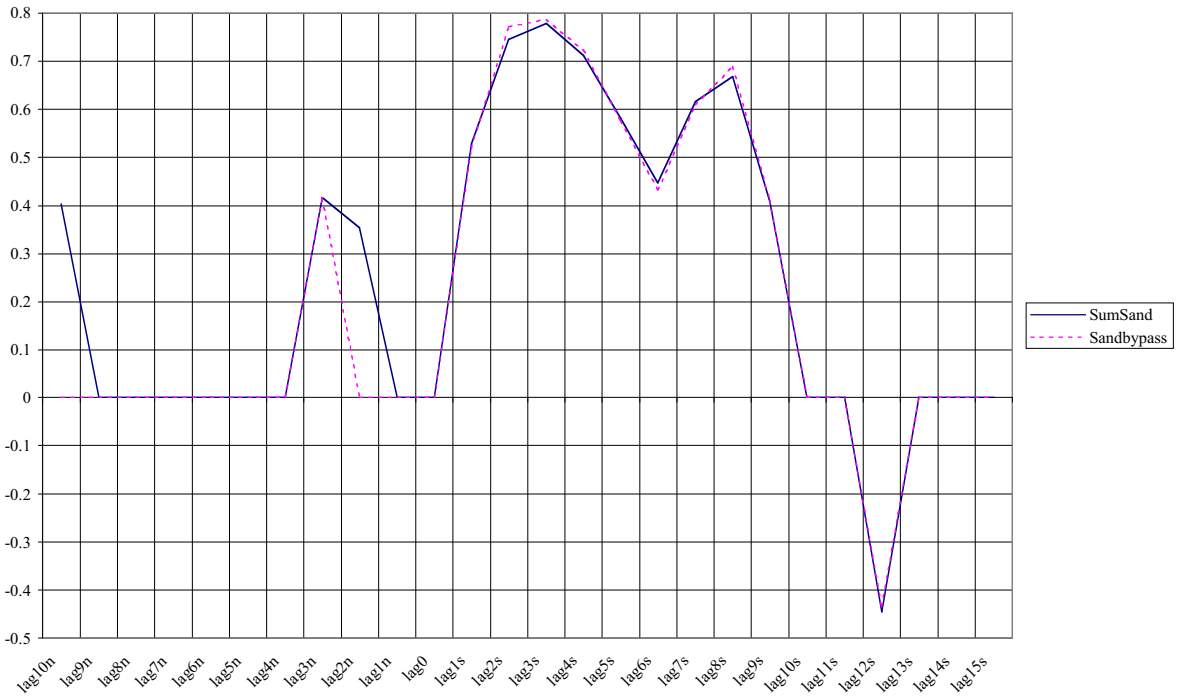

Diagram 7.21. Lagged SumSea correlated with SumSand and Sandbypass.

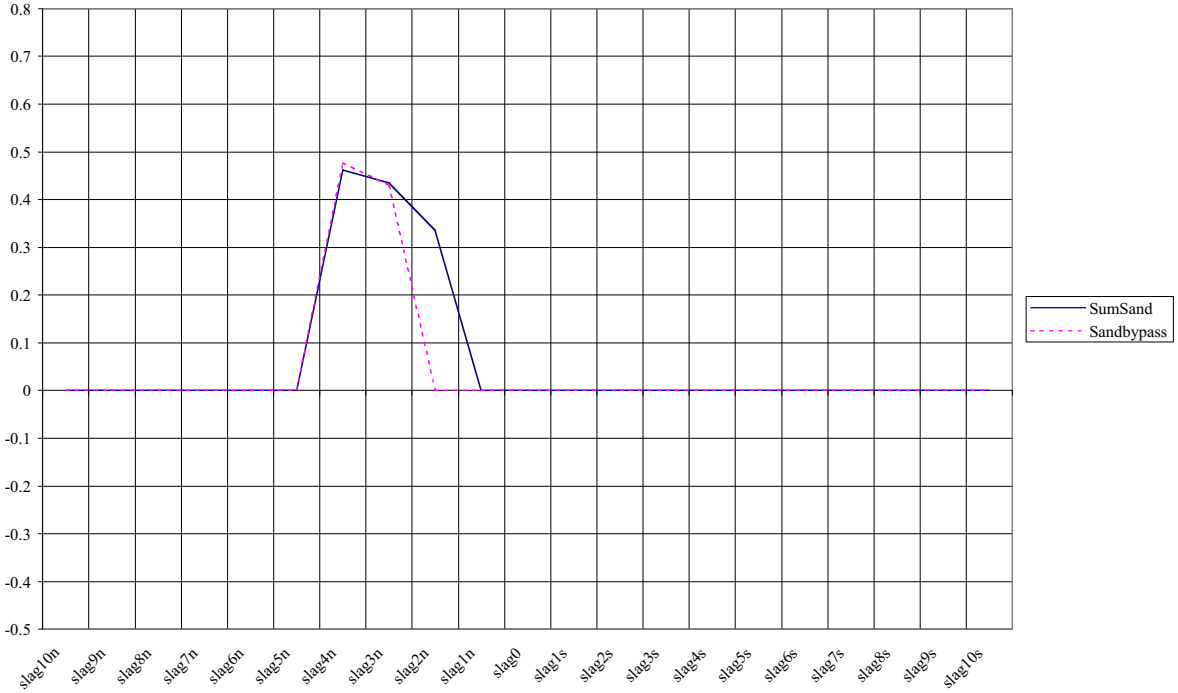

Diagram 7.22. Suspension multiplied with SumSea is here lagged and correlated with SumSand and Sandbypass.

The few samples in this area makes it difficult to make any large scale correlations, but the small scale correlations do show that northward transport is favoured also in this zone.

Diagram 7.22 does not support the hypothesis. An extremely small sample size makes it highly unreliable.

7.4.9 Burrewarra Point to Cape Howe (Boxes 605-698)

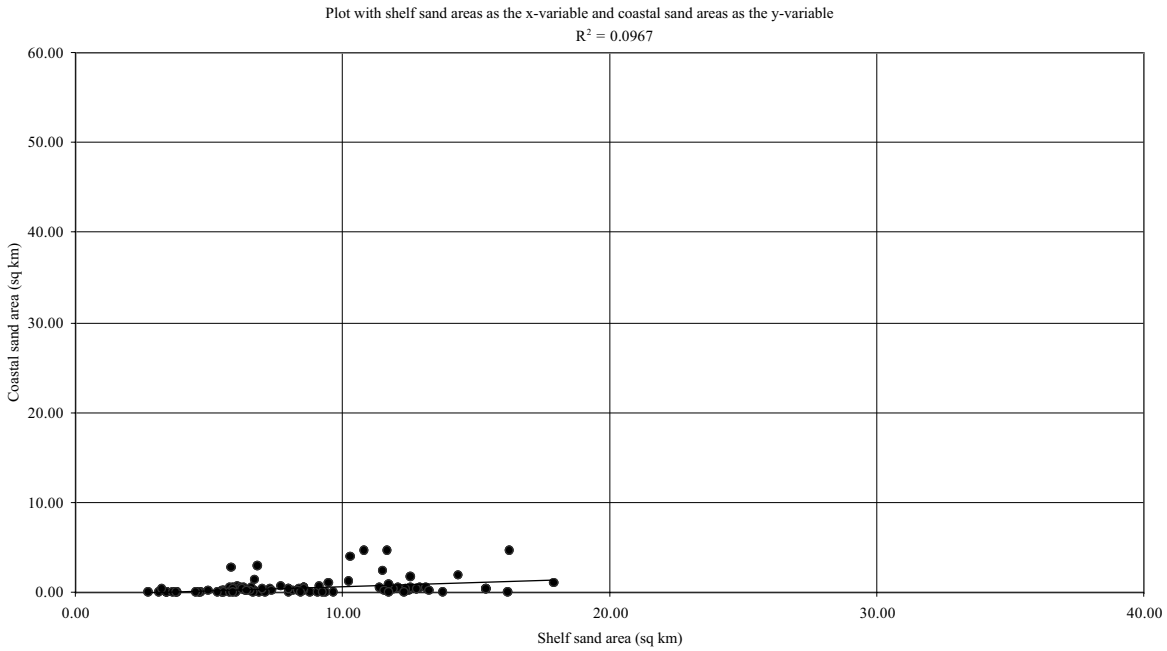

Plot 7.15. Correlation of SumSea and SumSand for Burrewarra Point to Cape Howe.

Table 7.12. Significant correlations between computed variables.

	SumSand	Sandbypass	Sand4k	Sand6k	Sand8k	Sand10k
SumSea	0.31	0.241	0.311	*	*	*
Sea4k	0.46	0.451	0.376	*	*	*
Sea6k	0.338	*	*	*	*	*
Sea8k	0.443	0.442	0.459	*	*	0.328
Sea10k	0.454	0.438	*	*	*	*
Slopeangle	-0.287	-0.237	-0.249	-0.056	*	*
Slope4k	-0.355	-0.391	-0.31	*	*	*
Slope6k	-0.335	*	*	*	*	*
Slope8k	-0.362	*	-0.424	*	*	*
Slope10k	*	*	*	*	*	*
Suspension	*	*	*	0.743	*	*
slag0	0.5	0.504	0.585	*	*	*
Sus4k	*	*	*	*	*	*
Sus6k	0.389	*	*	0.419	*	*
Sus8k	*	*	*	*	*	*
Sus10k	*	*	*	*	*	*

Surprisingly, this area provides quite a few significant results. Correlations generally increase with larger sand shelf area averages, the exception being the highest correlation between SumSand and Sea4k. Even higher correlation is found for Suspension/Sand6k, and for slag0. The latter one is quite unusual. In fact, the only other occasion where there has been found a positive correlation for slag0 is for zone St. George - Cape Howe, which this area is a part of.

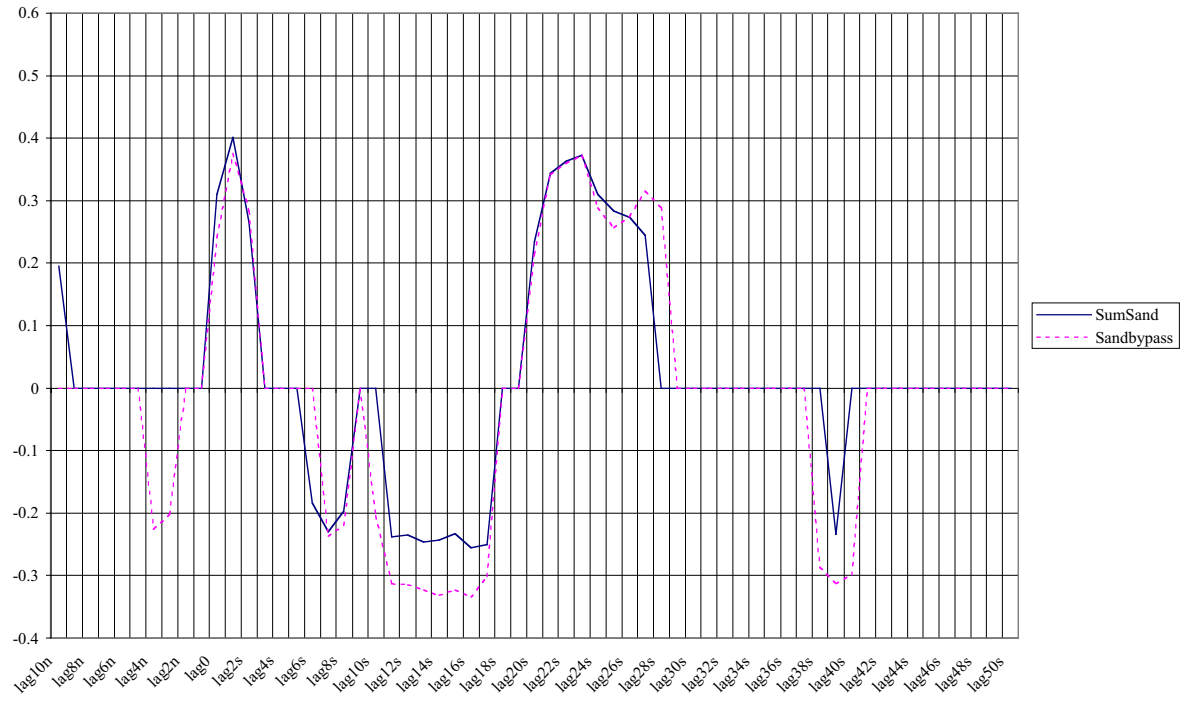

Diagram 7.23. Lagged SumSea correlated with SumSand and Sandbypass.

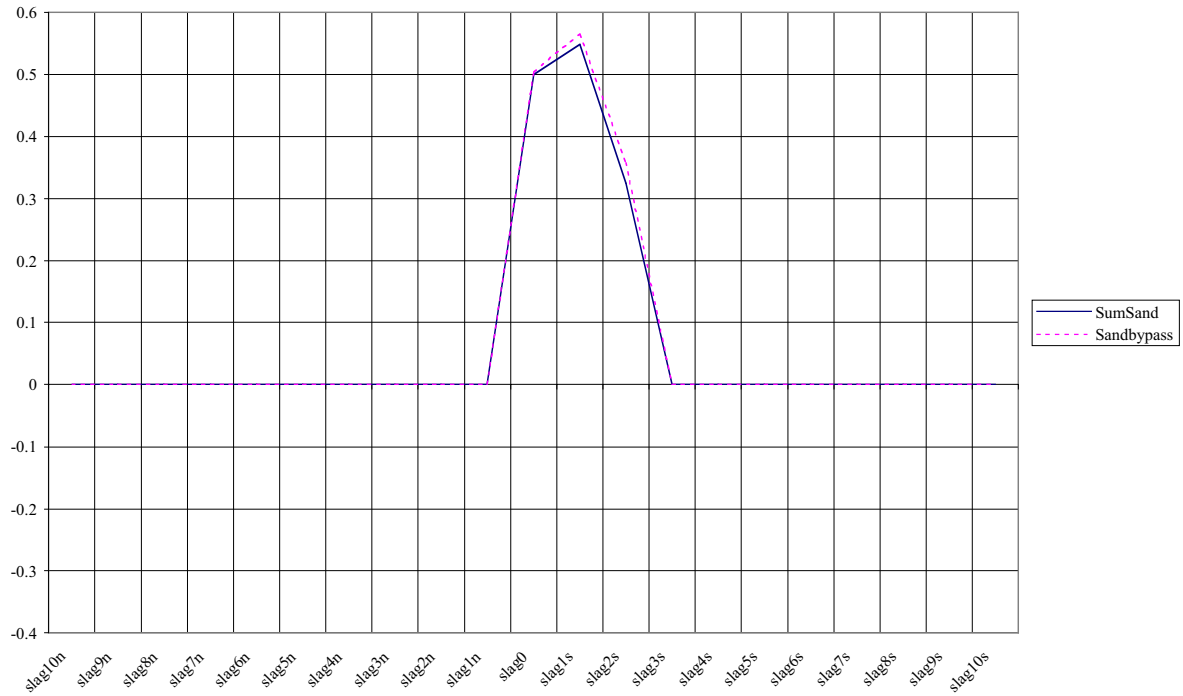

Diagram 7.2. Suspension multiplied with SumSea is here lagged and correlated with SumSand and Sandbypass.

There seems to be evidence for a northward transport at two different scales in this zone. The first is at a small scale: 0-4 km south, which is supported by both diagrams. The second is at a larger scale: 40-54 km south. In between these positive correlations, there is a significant negative correlation, suggesting a southward transport being active between 22 and 34 km south. It is possible that the sand is swept around a bit in this area, as it moves northward.

8 Discussion

Jervis Bay must be included in the analysis of the whole dataset, as most correlations are slightly lower when Jervis Bay is excluded. However, when analysing different zones within the data set it is efficient to exclude areas that may skew the population unnecessarily. Jervis Bay is excluded because of the shape of the bay, which is cut off from the open sea by a major headland. It has no sand barrier, and the areas between twenty and sixty metres of depth are outside the headland.

The division of the data set into four zones and nine zones makes it possible to analyse parts of the data set that are morphologically, geologically, and geographically separated. Although the success of analysis varies from zones to zone, they provide the study with a multitude of results that can be used to test the hypothesis. In addition, the results give rise to questions about scale and method. The division into zones means that the number of samples decreases, and this is a problem for a statistical analysis. A smaller sample size may solve this type of problem, but when the time-scale is decade to millennia, it is questionable whether smaller samples provide a better basis for analysis.

Correlation between areas of sand barriers and areas of seabed between 20 and 60 metres depth is significant for the data set as a whole, but only for six of the thirteen zones. One of these significant correlations is negative. Correlation tends to increase when sand barriers are correlated with averages of larger areas of seabed. Direct correlation between these variables only tells us whether there may be a near-linear relationship. The nature of this relationship is difficult to determine. One could say that the seabed area supplies the sand barrier with sand, but then again, the opposite is also true. It is a dynamic process, shifting the sand between them, and the relationship would then be that of the process itself.

The substrate gradient is an important factor, determining the direction of residual transport across the shelf. The correlation with shelf inclination gives significant results for seven zones. The correlations with substrate inclination are negative because more sand move onshore when the inclination is gentle than when it is steep. Two of these significant correlations are, however, positive. The positive correlations would mean that sand is moving offshore. It is important to remember that the inclination used is not the actual substrate gradient. It is simply calculated from the distance between the isobars of 20 and 60 metres depth. As such, it is a good variable in estimating the residual transport direction over thousands of years.

Correlation of sand barrier areas and lagged seabed areas generally increases with increased lag, which suggests a northward flow of sand. The data set as a whole and all zones, but one (Sugarloaf Point - Port Stephens, boxes 412-433), supports a northward transport of sand. The zone that does not support the hypothesis was excluded from analysis because it had less than thirty samples. This is the most important kind of correlation analysis, testing the hypothesis directly by correlating variables spatially.

Modelling of sand suspension did not give satisfactory results, and hence the correlations with sand suspension are largely insignificant. Still, there are results that are of interest. In some zones significant results are especially scant, and in those cases significant correlations with suspension variables are invaluable. For example, Port Stephens - Beecroft Head shows very high correlation between Sand10k and Sus6k. This kind of correlation may be an indication that the sand sample taken from the beach originates in the sea directly offshore. In addition, when many of the suspension variable produce significant correlations, it gives extra credibility to the correlations with lagged seabed areas multiplied with suspension estimates.

The correlation of sand barrier areas and lagged seabed areas multiplied with suspension estimates tend to increase with increased lag. In most cases, the graphs depicting this kind of

correlation show more complexity than the graphs describing the correlations between sand barrier areas and lagged seabed areas. Some of these graphs are quite similar, while others differ radically, and some contradict each other entirely.

A re-occurring phenomenon in the graphs of correlations with lagged data is a dip, or several dips, which may be interpreted as indicating different orders of scale. Interpreted this way, the whole data set and most of the zones have at least two different orders of scale to be considered. These scales are probably determined by morphology. A region with small embayments will have a small scale transport from bay to bay, but also a larger scale transport, where sand moves not from bay to bay, but for example from major headland to the next major headland. In other cases, negative correlations indicate southward transport on a smaller scale, i.e. locally, while the large scale transport still is northward.

Unfortunately, the correlation of sand barrier areas and lagged seabed areas multiplied with suspension estimates is inhibited by a modest sand grain sample size, which means that the larger scale order can not be confirmed for the nine zones, except in the case of Caloundra Head - Byron Bay. In addition, this kind of correlation was not possible for the area between Fraser Island and Byron Bay, as a result of no, or extremely few, sand grain size samples. This only leaves four zones and the data set as a whole to corroborate that this kind of correlation supports the larger scale transport hypothesis. Interpolation of grain size samples to generate samples for areas with no samples was considered, but rejected for two reasons. Firstly, an interpolation would create sand grain size samples that are false, and for locations that do not even have sand barriers. Secondly, sand grain size samples could not be produced for the whole data set without extrapolation.

The correlation with Sandbypass, where boxes with no sand are excluded, is partly succesful. The direct correlation is usually lower than for SumSand, but for the correlations of lagged data there is, on occasion, a considerable improvement in correlation. In any case, the lagged correlation graph for Sandbypass usually differs from SumSand in some way. On the whole, Sandbypass mostly serves as a control device, showing graphically when there are areas with no sand in the data set.

An interesting part of the graphs with correlations of lagged data is the far right, i.e. high lags. Diagram 7.1 shows the correlation of sand barrier areas and lagged seabed areas. After a slight dip, the curve takes off, and the highest correlation is found at the highest lag. This is by no means impossible, since we are dealing with the whole data set, which is roughly 1,400 km from north to south, and the highest lag suggests a transport scale of 100 km. However, with higher lag the curve may start to display a behaviour that is more a result of the method, than an indication of residual transport direction. As diagram 7.2 shows, it may be that the increase at the far right in diagram 7.1 is indeed not reliable. Attempts to correlate with lags up to 200 km show a high degree of irregularities that cannot be explained any other way. In addition, it is impossible to correlate with higher lags for most zones.

9 Conclusion

A simple linear correlation shows that the size of a barrier is partly controlled by the size of the potential sediment supply directly offshore. Correlation tends to increase when sand barriers are correlated with averages of larger areas of seabed. This correlation only shows that there is a near-linear relationship between the sand barrier areas and the seabed areas. The relationship manifests itself in a dynamic process that is moving the sand around, and which is driven by external forcing and the unattainable state of equilibrium. This dynamic equilibrium is what barrier morphodynamics is all about.

Added lag shows that much more can be explained by littoral transport. The correlation improves when the size of a deposit is explained by the steepness of the substrate south of its location. There are variations in the strength of the correlation that seem to reflect the different sizes of the coastal cells. This can be seen when the correlation is plotted on one axis and the lag on the other. More importantly, each zone has a different "lag correlation pattern", which seems to give insight into the many different scales involved, i.e. we can see that sand is transported from one embayment to the next, that the sand is transported passed the next major headland, and so on.

Correlation of sand barrier areas and lagged seabed areas generally increase with increased lag, which suggests a northward flow of sand. Although, the input for the sand suspension prediction model is not ideal, the output enhanced the analysis, and generated higher correlations for the lagged seabed areas. The correlation of sand barrier areas and lagged seabed areas multiplied with suspension estimates tends to increase with increased lag, but the "lag correlation pattern" is more complex than the one for sand barrier areas correlated with lagged seabed areas.

The statistical analysis cannot disprove the hypothesis. In fact, most results seem to support the hypothesis. The correlations may not be very high, but they are certainly significant (in most cases at a significance level closing on zero). It is my conclusion that the residual large-scale sand transport along the coast between Cape Howe and past Fraser Island is northward. On smaller scales, there seem to be some residual southward sand transport, but most of the small-scale processes are shifting the sand northward as well.

This study attempts to use a top-down GIS model, using geological and geographical data, in conjunction with a bottom-up sand suspension prediction model, using sand grain size samples, wave data, and bathymetry, in an attempt to determine the direction of a process. This process is the transport of sand along the SE Australian coast. Future research in the field of oceanography will hopefully improve our understanding of waves and currents, which will facilitate modelling, and give us a solid theory that will explain these matters from a process point of view. Nevertheless, for now, the top-down approach is the most convenient way of studying barrier morphodynamics.

References

Bowler, J.M. (1983) *Southern Australia hydrologic evidence 7±2 ka*. Proceedings, lst Climanz Conference. Department of Biogeography and Geomorphology, Australian National University, 91 pp.

Chapman, D.M., Geary, M., Roy, P.S. and Thom, B.G. (1982) *Coastal Evolution and Coastal Erosion in New South Wales*. Coastal Council of New South Wales, 341 pp.

Church, J.A., Freeland, H.J. and Smith, R.L. (1986) Coastal-trapped waves on the east Australian continental shelf, Part 1: propagation and modes. *Journal of Physical Goegraphy*, **16**, 1929-1943.

Cowell, P.J. and Nielsen P. (1984) *Prediction of sand movement on the south Sydney inner-continental shelf, south east Australia*. Coastal Studies Unit Technical Report 84/2. Department of Geography, University of Sydney.

Cowell, P.J., Roy, P.S. and Jones, R.A. (1992) Shoreface Translation Model: Computer Simulation of Coastal-Sand Body Response to Sea Level Rise. *Mathematics and Computers in Simulation*, **33**, 603-608.

Cowell, P.J., Roy, P.S. and Jones, R.A. (1995) Simulation of large-scale coastal change using a morphological behaviour model. *Marine Geology, Special Issue on Large Scale Coastal Behaviour*, **126**, 45-61.

de Vriend, H.J., ed. (in review) The Coastal-Tract (Part 1): A conceptual approach to aggregated modelling of low-order coastal change. *Journal of Coastal Research, Special Issue on PACE: Predicting Aggregate-Scale Coastal Evolution*.

Erskine, W.D. and Nanson, G.C. (1988) Geomorphic effects of alternating flood- and drought-dominated regimes of NSW coastal rivers. In *Fluvial Geomorphology in Australia*. Ed. R.G., Warner. Academic Press, 223-244.

Field, M.E. and Roy, P.S. (1984) Offshore transport and sand-body formation: evidence from a steep, high-energy shoreface, southeastem Australia. *Journal of Sedimentary Petrology*, **54**, 1292- 1302.

Godfrey, J.S., Cresswell, G.R, Golding, T.J., Pearce, A.F. and Boyd, R. (1980) The separation of the East Australian Current. *Journal of Physical Geography*, **10**, 430-440.

Griffin, D.A. and Middleton, J.H. (1991) Local and remote wind forcing of New South Wales inner shelf currents and sea level. *Journal of Physical Goegraphy*, **21**, 304-322.

Hesp, P.A. and Short, A.D. (in press) Barrier Morphodynamics. In *Beach and Shoreface Morphodynamics*. Ed. Short, A.D.. John Wiley & Sons.

Langford-Smith, T. and Thom, B.G. (1969) Coastal Morphology of New South Wales. *Journal of the Geological Society of Australia*, **16**, 572-580.

Nielsen, P. (1983) Explicit formulae for practical wave calculations. *Coastal Engineering*, **7**, 233-51.

Pittock, A B. (1975) Climatic change and the patterns of variation in Australian rainfall. *Search*, **6**, 498-508.

Raudkivi, A.J. (1976) *Loose Boundary Layer Hydraulics*. 2nd ed., Pergamon, 397 pp.

Roy, P.S., Thom, B.G. and Wright, L.D. (1980) Holocene sequences on an embayed high-energy coast: an evolutionary model. *Sedimentary Geology*, **26**, 1-19.

Roy, P.S. and Thom, B.G. (1981) Late Quatemary marine deposition in New South Wales and southern Queensland - an evolutionary model. *Journal of Geological Society of Australia*, **28**, 471-489.

Roy, P.S., Cowell, PJ., Ferland, M A. and Thom, B.G. (1995) Chapter 4: Wave Dominated Coasts. In *Coastal Evolution*. Eds. R.W.G., Carter and C.D., Woodroffe. Cambridge University Press, 121-186.

Roy, P. S. (1998) Geology of New South Wales - Synthesis: Cainozoic geology of the coast and shelf. Ed. H. Basden. *Memoir Geology*, **13**(2), Geological Survey of New South Wales, 361-385.

Short, A. D. and Trenaman, N. L. (1992) Wave Climate of the Sydney Region, an Energetic and Highly Variable Ocean Wave Regime. *Australian Journal of Marine and Freshwater Research*, **43**, 148-173.

Swift, D.J.P., Figueiredo, A.G., Freeland, G.L. and Oertel, G.F. (1983) Hummocky cross-stratification and megaripples: a geological double standard?. *Journal of Sedimentary Petrology*, **53**(4), 1295-1317.

Thom, B.G. (1965) The Quaternary coastal morphology of the Port Stephens-Myall Lakes area, NSW. *Journal of the Royal Society of New South Wales*, **98**, 23-36.

Thom, B.G. (1978) Coastal sand deposition in southeast Australia during the Holocene. In *Landform Evolution In Australasia*. Eds. J.L., Davies and M.A.J., Williams. Australian National University Press, 197-214.

Thom, B.G. (1984) Transgressive and regressive stratigraphies of coastal sand barriers in southeastern Australia. *Marine Geology*, **56**, 137-158.

Thom, B.G. and Roy, P.S. (1985) Relative sea levels and coastal sedimentation in southeast Australia in the Holocene. *Journal of Sedimentary Petrology*, **55**, 257-264.

Thom, B.G., Shepherd, MJ., Ly, C.K., Roy, P.S., Bowman, G.M. and Hesp, P.A. (1992) *Coastal Geomorphology and Quaternary Geology of the Port Stephens-Myall Lakes Area*. Monograph No. 6. Department of Biogeography and Geomorphology, Australian National University, 407 pp.

Ward, W.T. (1977) *Sand movements on Fraser Island: a response to changing climates*. Paper. Department of Anthropology, University of Queensland, **8**, 113- 126.

Ward, W.T. (1978) Notes on the origin of Stradbroke Island. In *Handbook of Recent Geological Studies of Moreton Bay, Brisbane River and North Stradbroke Island*. Eds. G.R. Orme and R.W. Day. Paper. Department of Geology University of Queensland, **8**, 97-104.

Warner, R.F. (1991) Floodplain evolution in a New South Wales coastal valley, Australia: spatial process variations, *Geomorphology*, **4**, 447-458.

Warner, R.F. (1994) A theory of channel and floodplain responses to alternating regimes and its application to actual adjustments in the Hawkesbury River. In *Process Models and Theoretical Geomorphology*. Ed. M.J., Kirkby. John Wiley & Sons Ltd., 173-200.

Appendices

Appendix I Digitised Maps

The maps digitised where made available by the Geography Map Library at Sydney University and by Peter Roy, except in a few cases where maps had to be purchased.

Bathymetric Maps

National Bathymetric Map Series
Transverse Mercator Projection: Australian Map Grid 1966 (Zone 56 & 55)
Horizontal datum: AGD 1966
Vertical datum: Mean Sea Level
Scale: 1:250 000
Produced and distributed by the Division of National Mapping, NATMAP, now known as AUSLIG (Australian National Mapping Agency). Published by the authority of the Minister for National Development and Energy 1976-1983. Edition 1 & 2.

Wide Bay SG56-7 1977 (Edition 2)
Caloundra SG56-11 1976
Brisbane SG56-15 1976
Coolangatta SH56 Part 3 & 4 1977
Yamba SH56-7 & Part 8 1976
Nambucca SH 56 Part 10 & 11 1976
Port Macquarie SH56 Part 14 & 15 1976
Port Stephens SI56-2 Part 3 1976
Port Jackson SI56 Part 5 & 6
Port Kembla SI56 Part 9 & 10
Jervis Bay SI56 Part 13 & 14
Montagu Island SJ56-1 Part SJ55-4 (zone 55 in the south-west corner)
Green Cape SJ56-5 1983

Royal Australian Navy Hydrographic Map Series
Projection: Mercator Lat/Long
Scale: 1:150 000
From Royal Australian Navy Surveys 1956-61 and Colonial-Admiralty Surveys 1871-87.
Published by the Hydrographic Service of the Royal Australian Navy.
Depth is shown in fathoms.
1 fathom = 6 feet ≈ 1.82875 metres

Gabo Island to Montague Island AUS. 806 1965

Topographic Maps

National Topographic Map Series
Transverse Mercator Projection: Australian Map Grid 1966 (Zone 56 & 55)
Horizontal datum: AGD 1966
Vertical datum: Australian Height Datum 1971
Scale: 1:100 000

* Accuracy: ± 25 metres in hoizontal position and ± 5 metres in elevation.
Produced by the Division of National Mapping, NATMAP, now known as AUSLIG (Australian National Mapping Agency).
** Accuracy: ± 25 metres in hoizontal position and ± 10 metres in elevation.
Produced by the Division of National Mapping, NATMAP, now known as AUSLIG (Australian National Mapping Agency).
*** Accuracy: ± 50 metres in hoizontal position and ± 10 metres in elevation. Produced by the Royal Australian Survey Corps.
**** Accuracy: ± 25 metres in hoizontal position and ± 5 metres in elevation. Produced by the Royal Australian Survey Corps.
***** Accuracy: ± 25 metres in hoizontal position and ± 5 metres in elevation. Produced by the Department of Mapping and Surveying, Brisbane, Queensland.
******Accuracy: ± 25 metres in hoizontal position and ± 5 metres in elevation.
Produced by the Snowy Mountains Engineering Corporation.

Happy Valley 9547 1981 (Edition 2) *
Wide Bay 9546 1981 (Edition 2) *
Maryborough 9446 1981 (Edition 2) *
Laguna Bay 9545 1982 (Edition 1-AAS) ***
Caloundra 9544 1982 (Edition 1-AAS) ***
Brisbane 9543 1982 (Edition 2) *****
Beenleigh 9542 1976 (Edition 1) *****
Murwillumbah 9541 & Part 9641 1983 (Edition 2-AAS) ***
Lismore 9540 & part 9640 1974 (Edition 1) *
Woodburn 9539 1971 (Edition 1-AAS) ****
Bare Point 9538 1970 (Edition 1-AAS) ****
Coffs Harbour 9537 1975 (Edition 1) **
Nambucca 9536 1974 (Edition 1) **
Macksville 9436 1975 (Edition 1) **
Kempsey 9435 1976 (Edition 1) **
Camden Haven 9434 1976 (Edition 1) **
Buladelah 9333 1983 (Edition 1) *
Newcastle 9232 & Part 9332 1983 (Edition 1) *
Gosford 9131 1979 (Edition 1) *
Lake Macquarie 9231 1976 (Edition 1) *
Sydney 9130 1976 (Edition 1) **
Port Hacking 9129 1976 (Edition 1) *
Wollongong 9029 1976 (Edition 1) *
Kiama 9028 1983 (Edition 1) *
Jervis Bay 9027 1983 (Edition 1) *
Ulladulla 8927 1975 (Edition 1) **
Batemans Bay 8926 1973 (Edition 1) *
Narooma 8925 1972 (Edition 1) ******
Bega 8824 1982 (Edition 1) *
Eden 8823 1973 (Edition 1) **
Green Cape 8923 1972 (Edition 1) *

Appendix II Mapinfo Map

The digitised map from Mapinfo is shown here in its entirity (scale 1:6,250,000 in the north, and approximately 1:6,249,999 in the south). Since this does not reveal much, the map is also shown in nine sections, roughly corresponding to the nine zones that the data set is broken up into for analysis (scale 1:1,200,000 in the north, and approximately 1:1,198,800 in the south). The maps have been printed, scanned, and then compiled, which explains some of the irregularities.

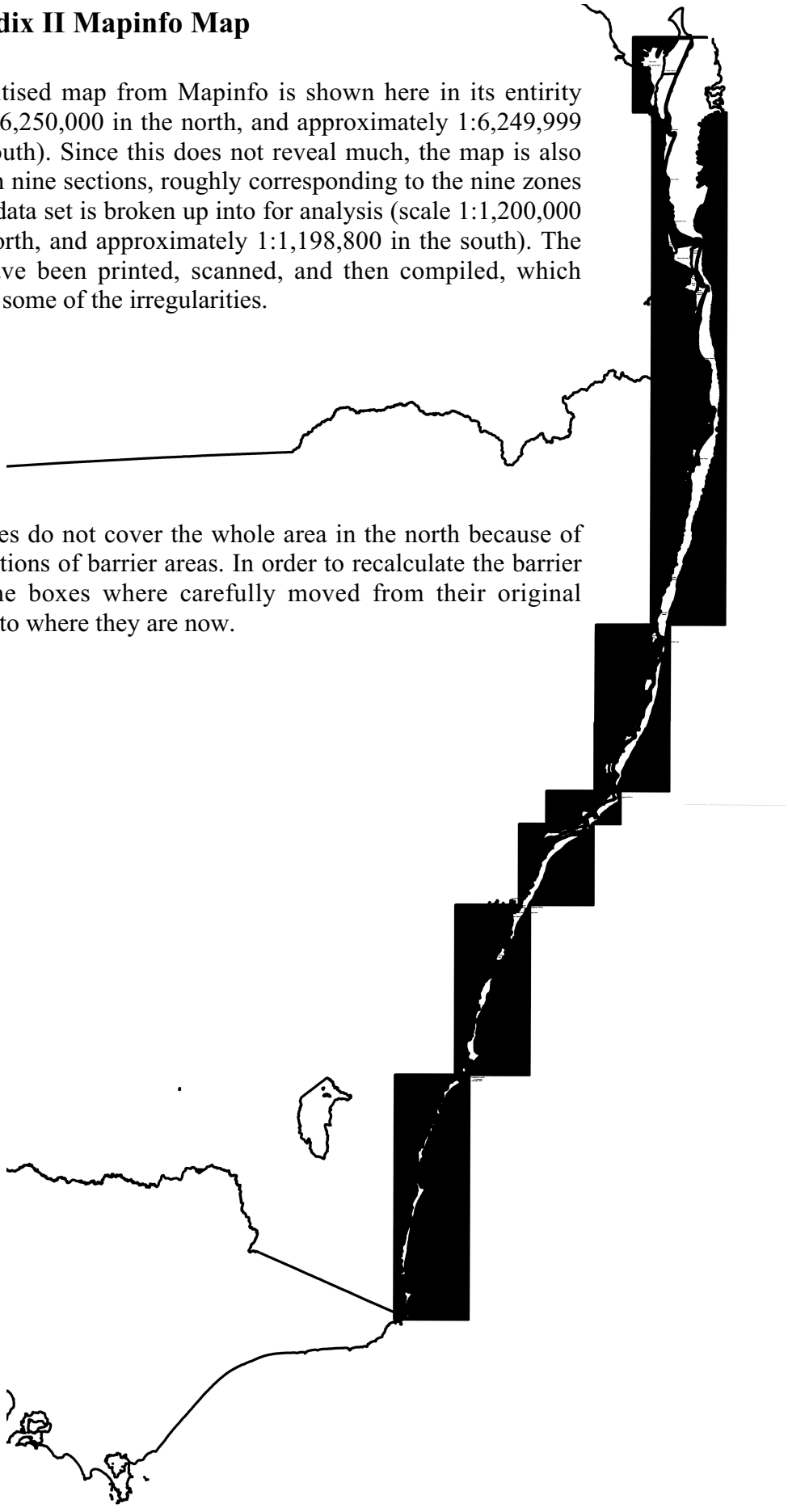

The boxes do not cover the whole area in the north because of late additions of barrier areas. In order to recalculate the barrier areas, the boxes where carefully moved from their original position to where they are now.

Fraser Island to Caloundra Head (Boxes 1-109)

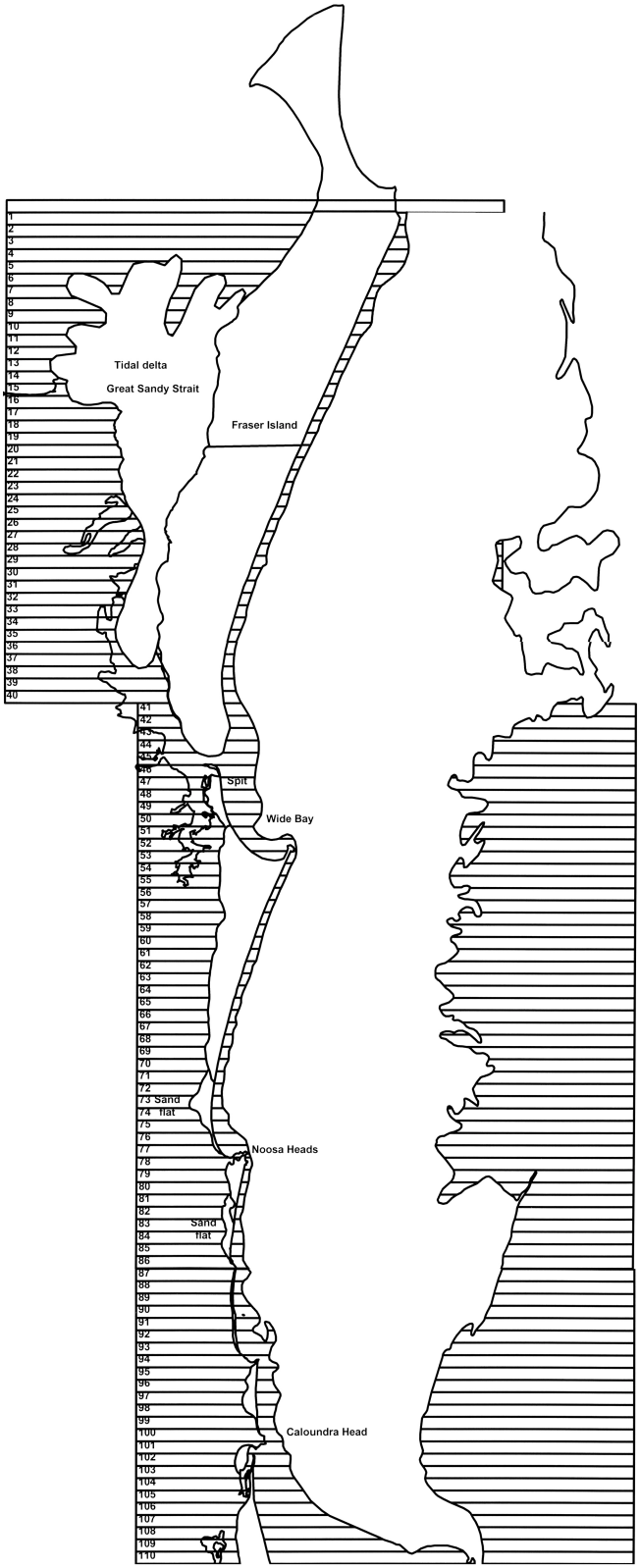

Caloundra Head to Byron Bay (Boxes 101-204)

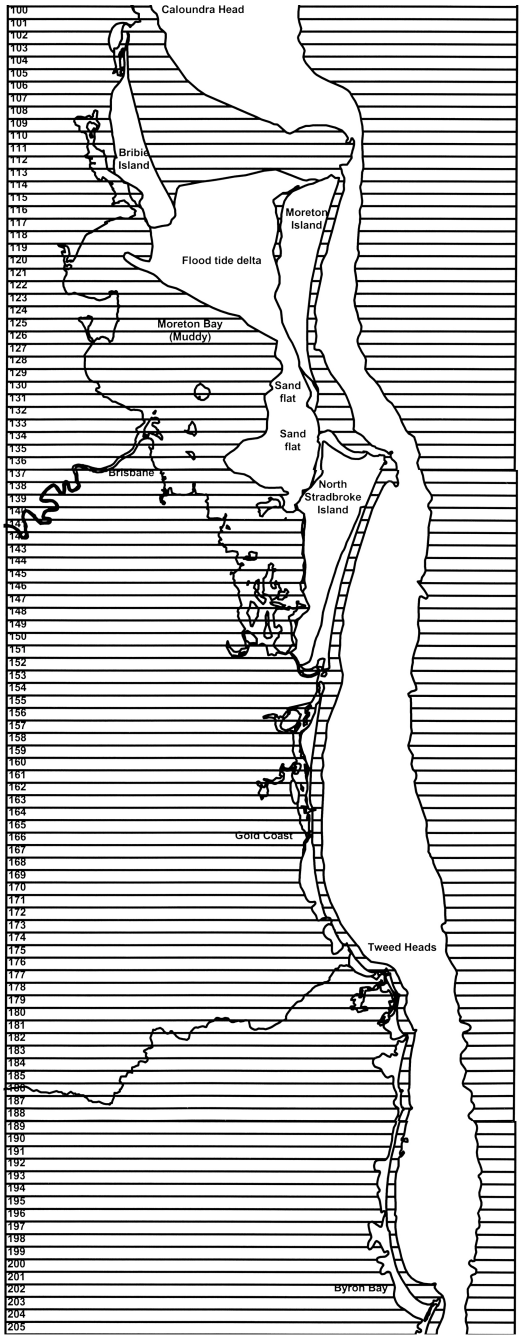

Byron Bay to Smoky Cape (Boxes 202-329)

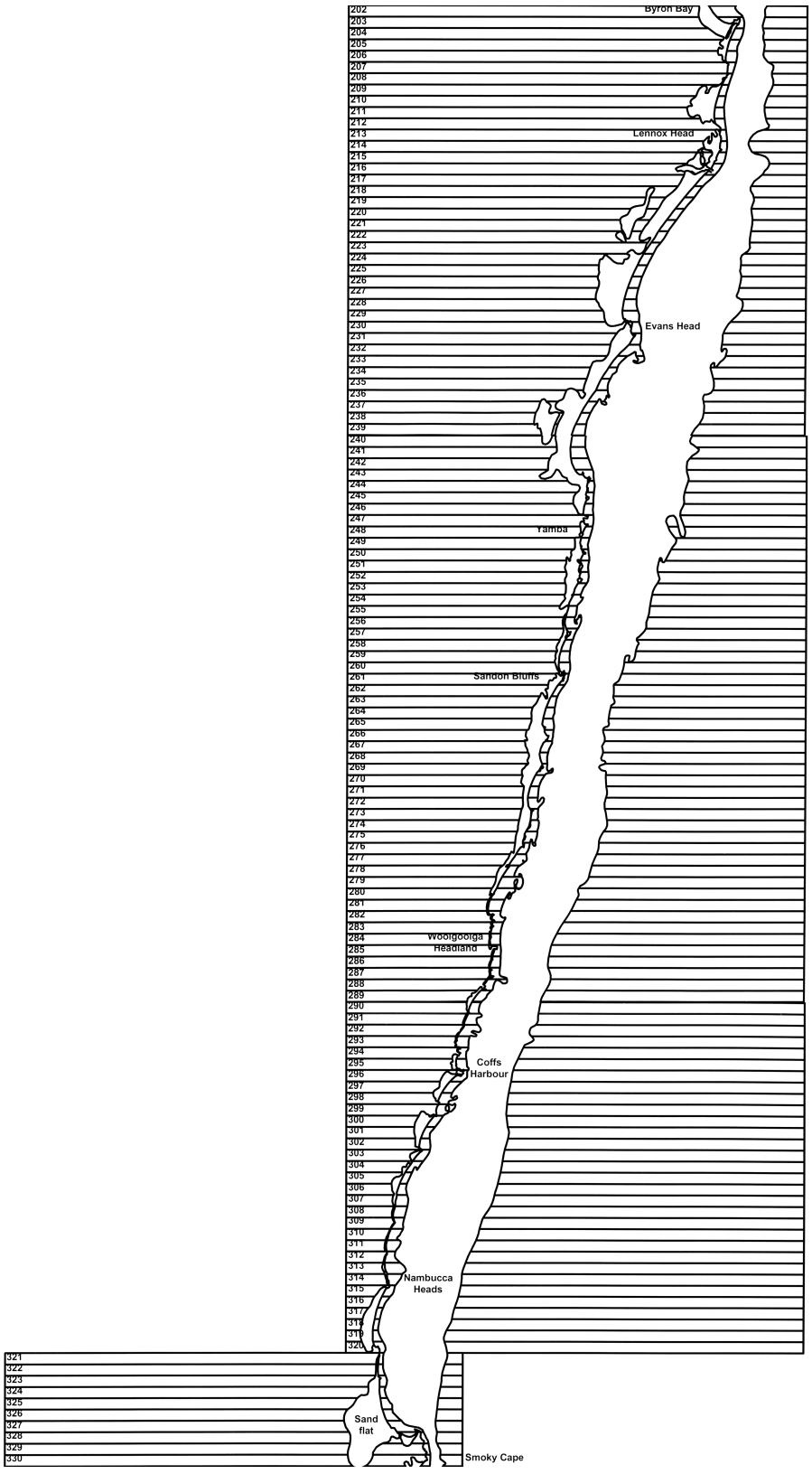

Smoky Cape to Sugarloaf Point (Boxes 330-414)

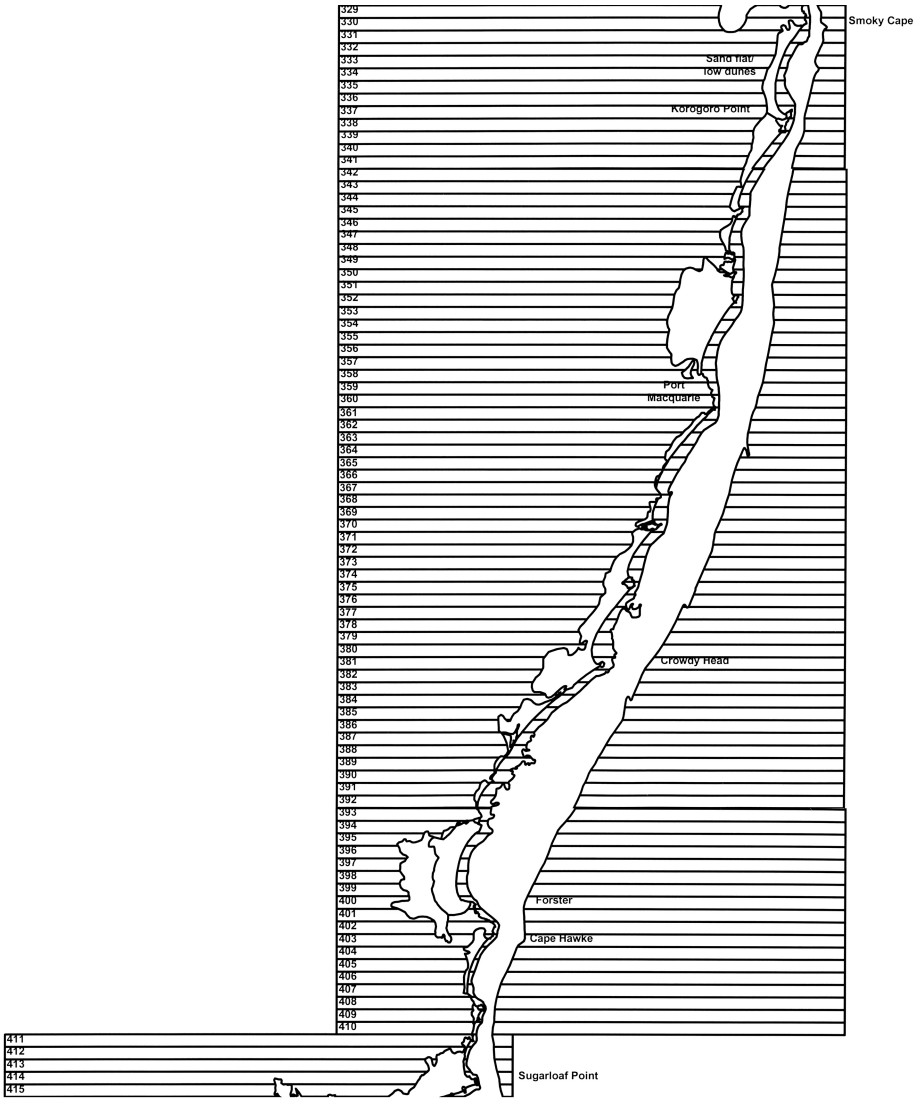

Sugarloaf Point to Port Stephens (Boxes 412-433)

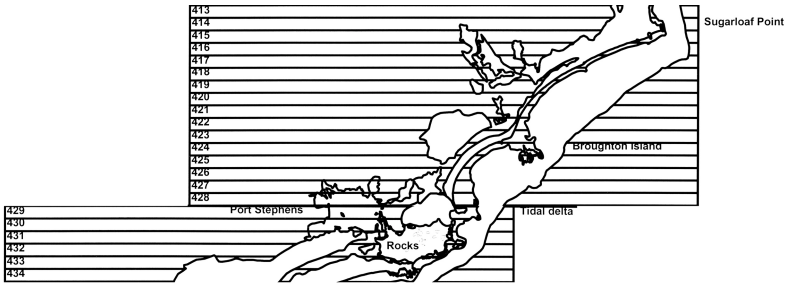

Port Stephens to Botany Bay (Boxes 429-499)

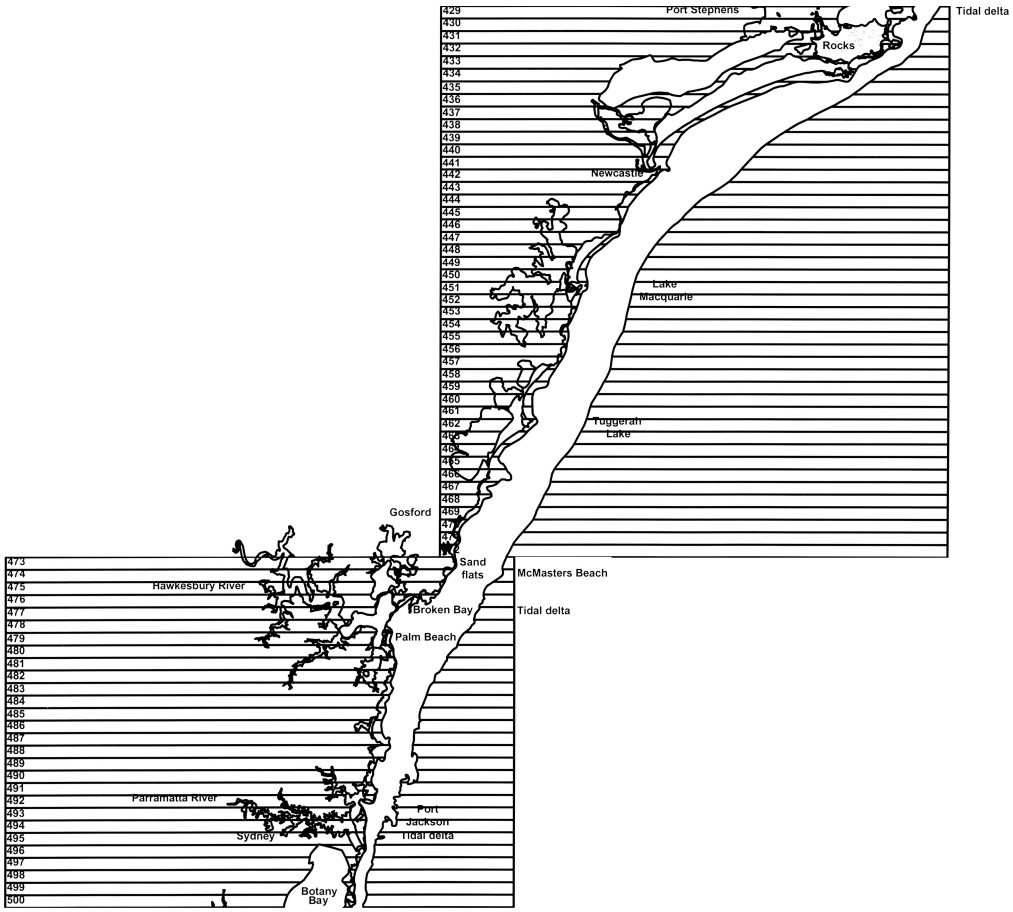

Botany Bay to Beecroft Head (Boxes 500-558)

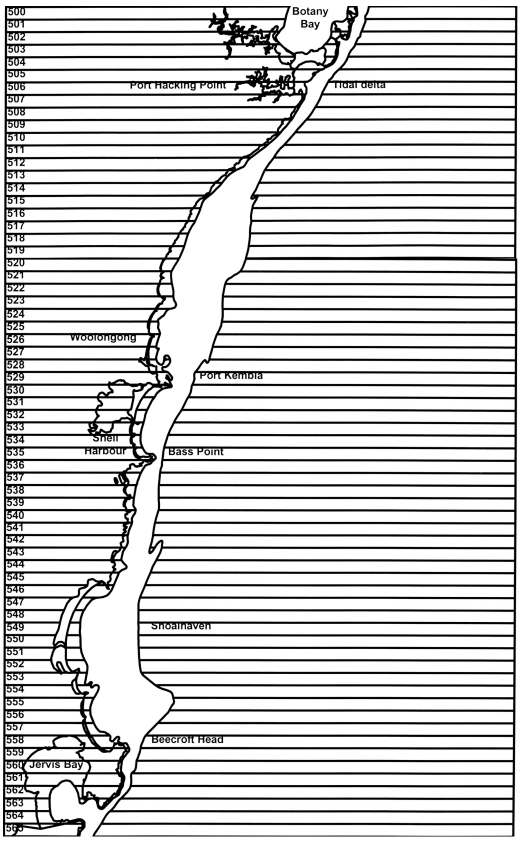

St. Georges Head to Burrewarra Point (Boxes 566-604)

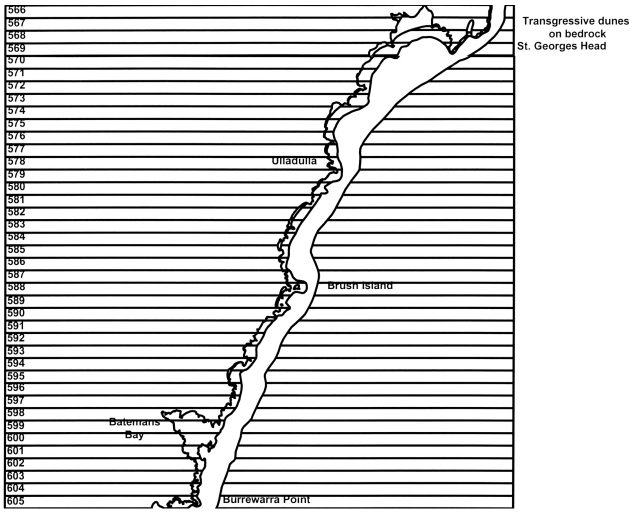

Burrewarra Point to Cape Howe (Boxes 605-698)

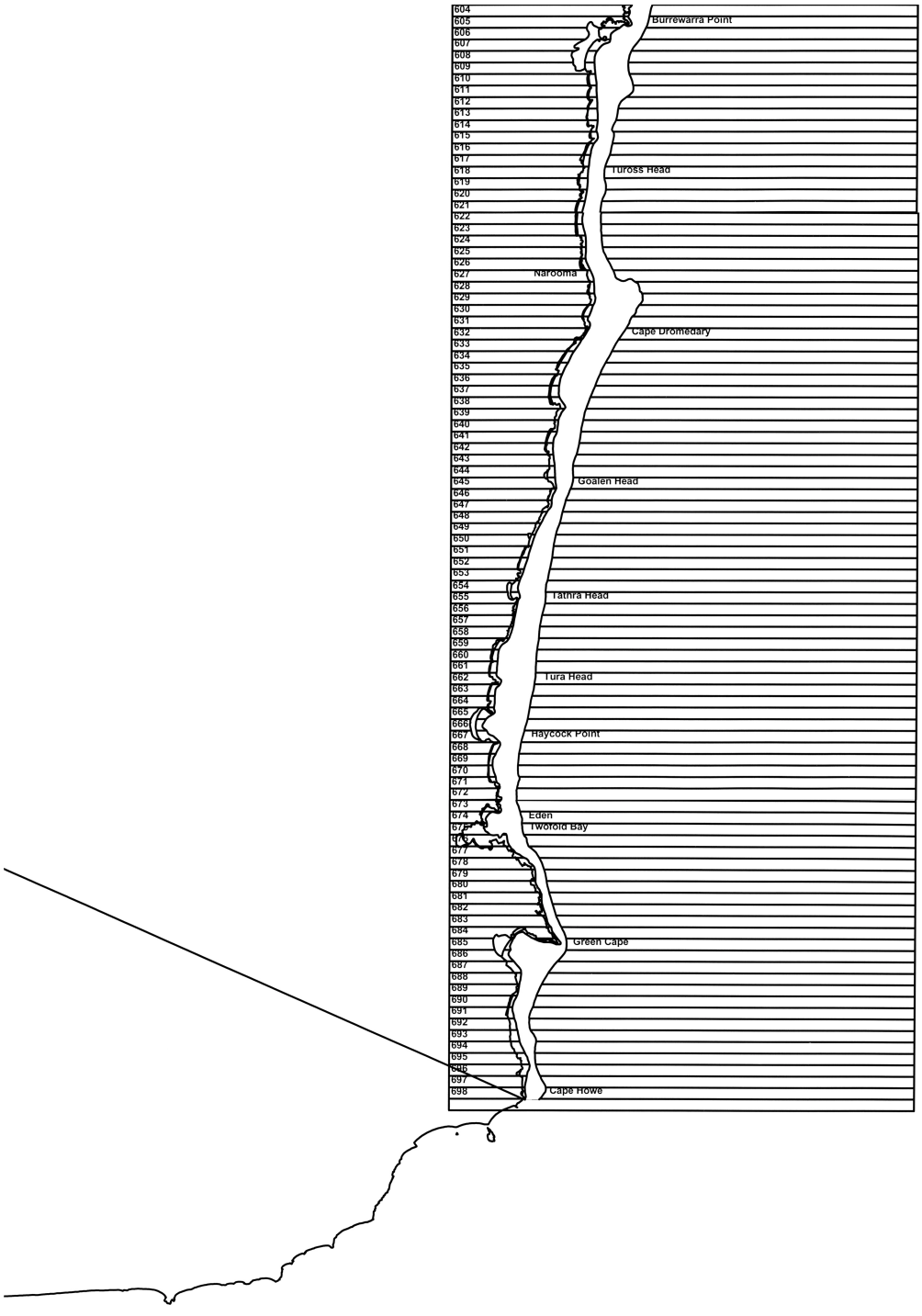

Appendix III Diagrams

Here is a graphical representation of the data extracted from Mapinfo. This page shows the whole data set. The following pages show the same diagram broken up into four parts, roughly corresponding to the four zones the data set is also analysed as. The zones do sometimes have different borders for sand barrier and shelf area, which explains "missing" data at either end of the diagram.

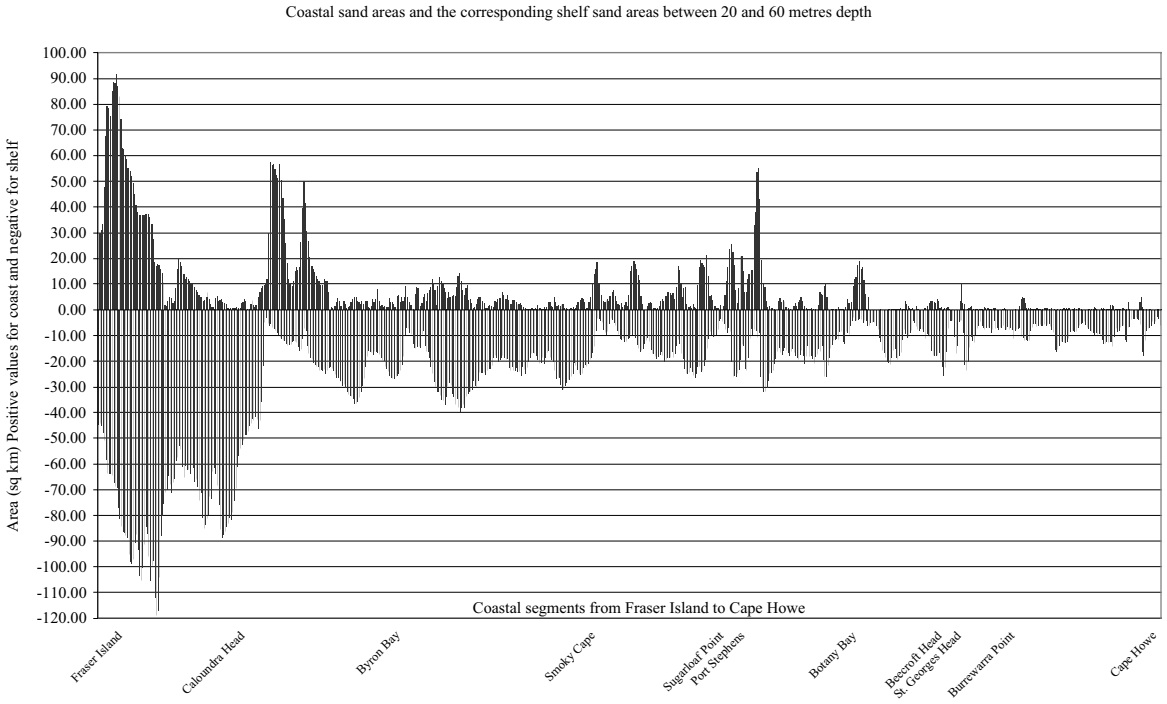

Fraser Island to Byron Bay (Boxes 1-204)

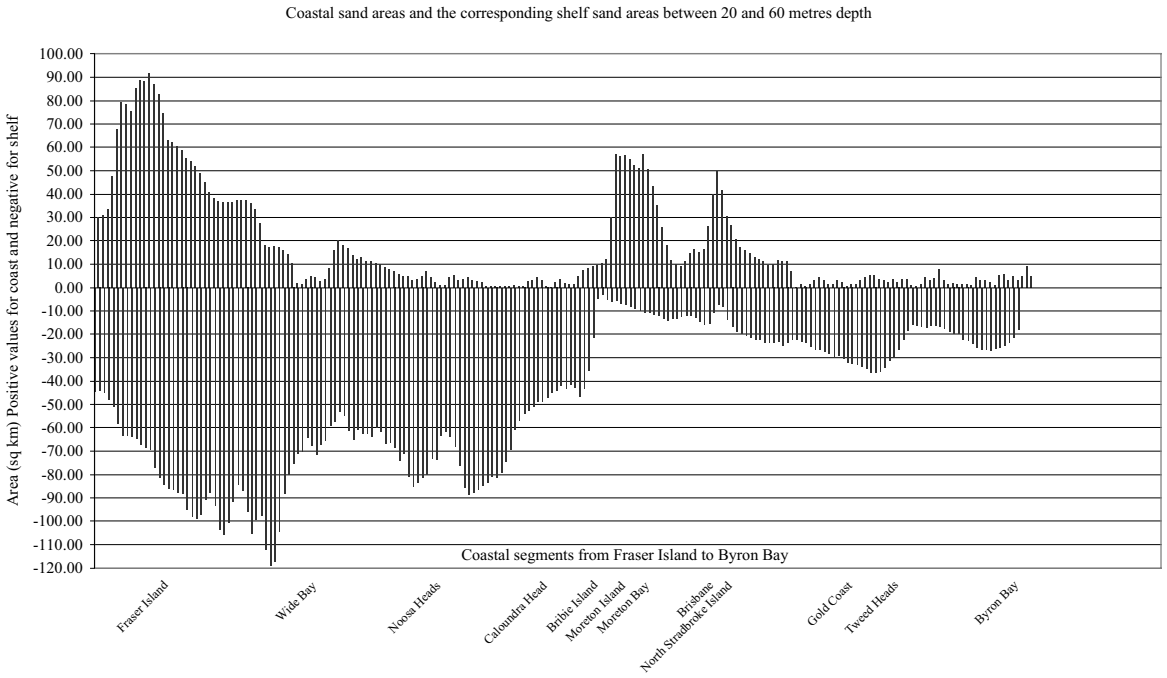

Byron Bay to Port Stephens (Boxes 202-433)

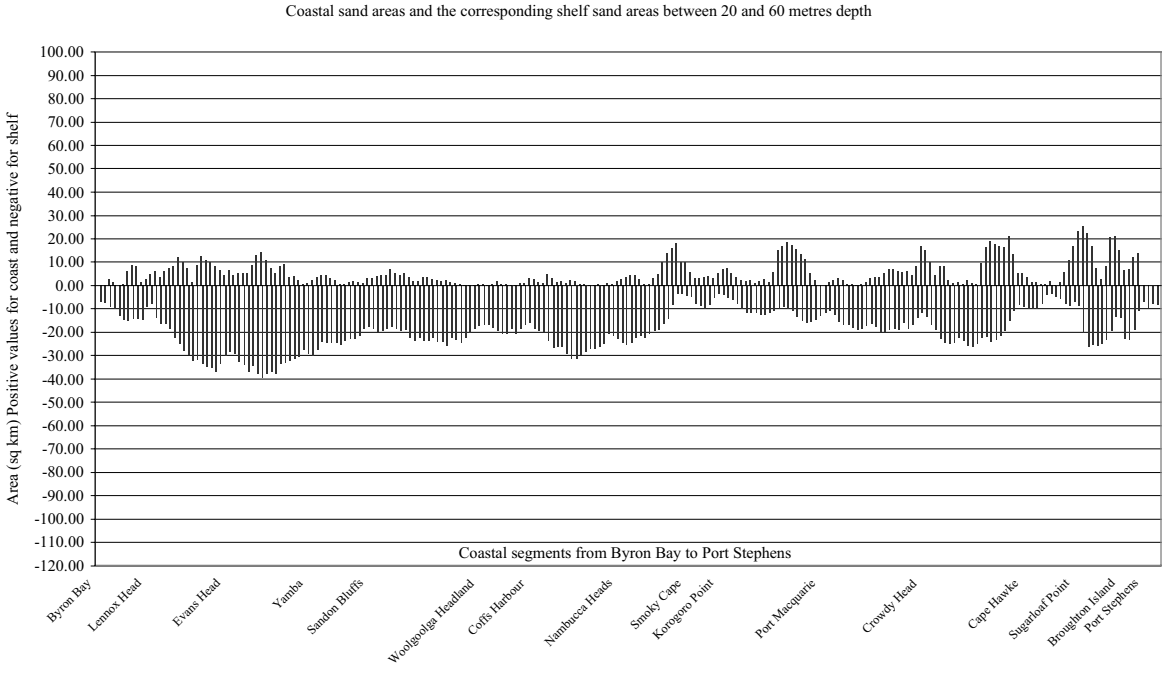

Port Stephens to Beecroft Head (Boxes 429-558)

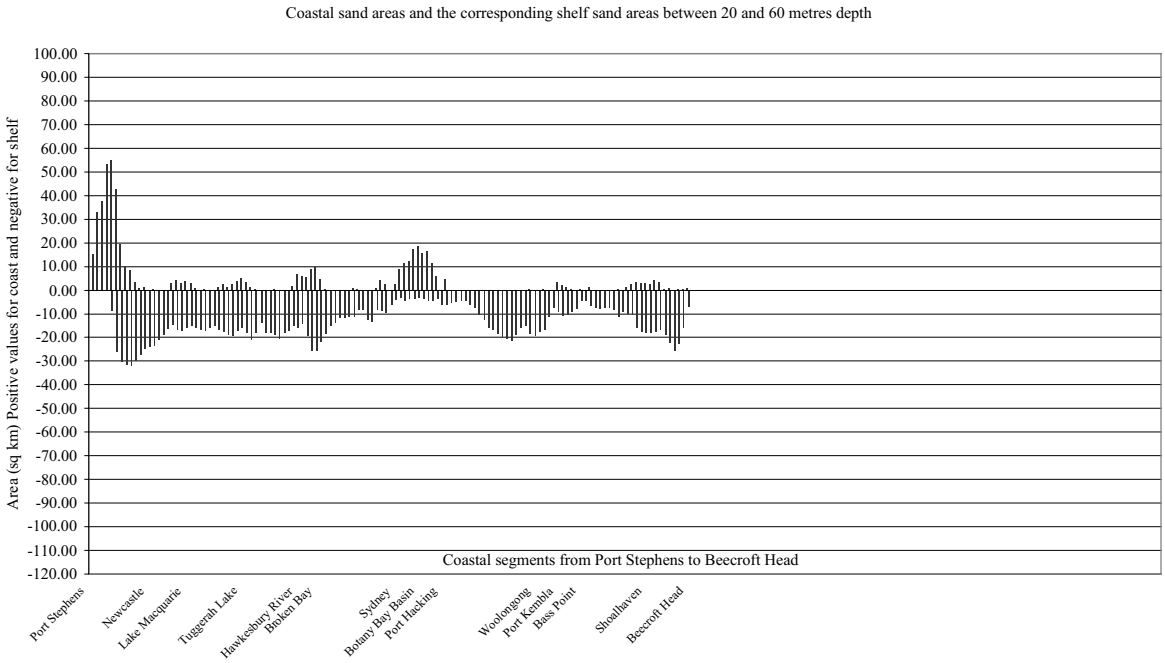

St. Georges Head to Cape Howe (Boxes 566-698)

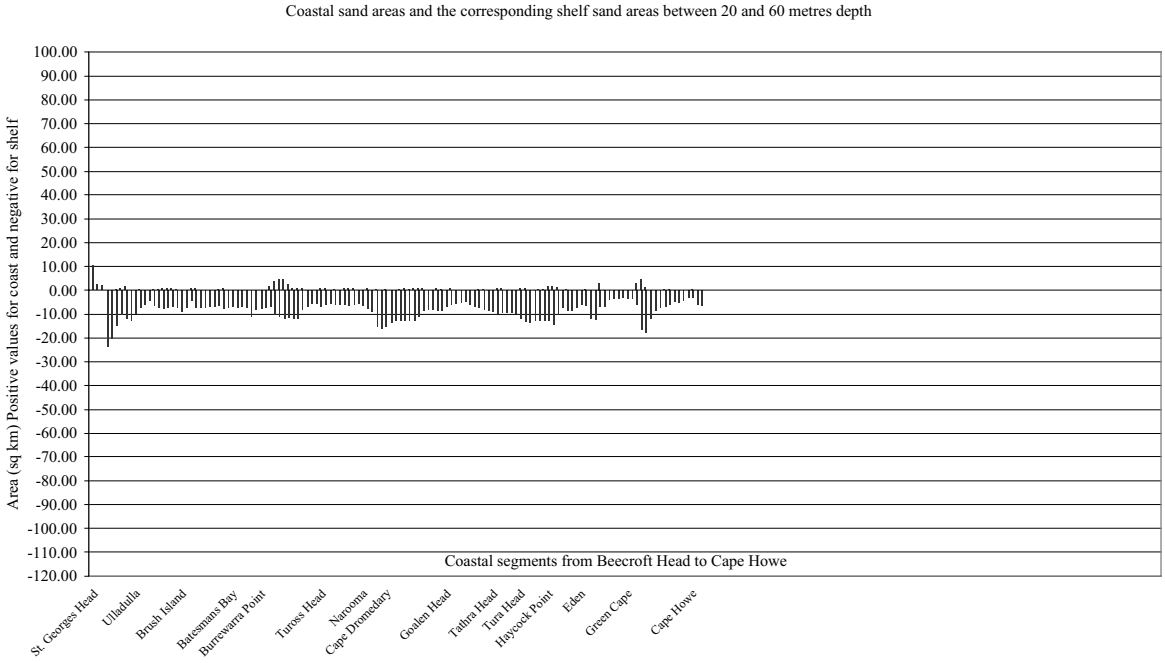

Appendix IV Visual Basic code

The equations for calculating suspended sediment concentration and some other variables are shown below in Visual Basic code. Using this code, one can execute the calculations on data in an Excel spreadsheet by running a macro with appropriate additional code for the spreadsheet in question.

Variables and outputs

wp = wave period in seconds (T)
wh = wave height in meters (H)
wd = water depth in metres (h)
rsd = relative sediment density in kg/m^3 (s)
sd2 = sediment diametre in metres (d)
sd, gs = sediment diametre in millimetre
sfv3 = sediment fall velocity in m/s (w)
sfv, fvel = sediment fall velocity in mm/s
K8 = deepwater wave number (k_o)
K9 = wave number (k)
P, mn = mobility number (ψ)
N1 = ripple height in metres (η)
rh = ripple height in centimetre
L1 = ripple length in metres (λ)
rl = ripple length in centimetre
S1, sp = Shields parameter (θ)
R2 = bed roughness in metres (r)
br = bed roughness in millimetres
F2, ff = friction factor (f_w)
L2 = boundary layer diffusion length in metres (ι_s)
dl = boundary layer diffusion length in millimetres
A3 = water semi excursion in metres (a)
se = water semi excursion in centimetres
A4 = critical semi excursion in metres
cgs = critical grain size in millimetres
scm = suspension concentration in m^3/m^2
sckg = suspension concentraion in kg/m^2
va = velocity amplitude in cm/s
cv = critical velocity cm/s
fr = friction ratio
dtn = Dean-Type number
dsn = Davidson-Stokes number

Visual Basic code for calculating sediment suspension

```
Pi = 3.14159265358979
K9 = 4 * Pi ^ 2 / 9.8 / wp ^ 2
K8 = K9 * wd
If K8 > 1.26 Then
K = K8 * (1 + 2 * Exp(-2 * K8))
Else
K = K8 ^ 0.5 * (1 + K8 / 6 + 11 / 360 * K8 ^ 2)
End If
A = wh / (Exp(K) - Exp(-K))
sd2 = sd / 1000
p = (A * 2 * Pi / wp) ^ 2 / 9.8 / sd2 / (rsd - 1)
sfv2 = sfv / 1000
If sfv = 999 And sd > 1.5 Then
sfv3 = (10 ^ (-3 / 2) * 134.5 * sd2 ^ 0.5)
ElseIf sfv = 999 And sd > 0.15 Then
sfv3 = 109.9 * sd2
ElseIf sfv = 999 And sd <= 0.15 Then
sfv3 = 663 * (sd ^ 2)
Else
sfv3 = sfv2
End If
If p >= 10 Then
N1 = 21 * p ^ (-1.85) * A
Else
N1 = (0.275 - 0.022 * Pi ^ 0.5) * A
End If
L1 = A * Exp((693 - 0.37 * Log(p) ^ 8) / (1000 + 0.75 * Log(p) ^ 7))
R1 = 2.5 * sd2
If R1 / A >= 0.63 Then
F1 = 0.3
Else
F1 = Exp(5.213 * (R1 / A) ^ 0.194 - 5.977)
End If
S1 = F1 * p / 2
If S1 >= 1 Then
R2 = 230 * (S1 - 0.05) ^ 0.5 * (sd2)
ElseIf S1 < 0.05 Then
R2 = 8 * N1 ^ 2 / L1
Else
R2 = 8 * N1 ^ 2 / L1 + 190 * Abs(S1 - 0.05) ^ 0.5 * (sd2)
End If
If R2 / A >= 0.63 Then
F2 = 0.3
Else
F2 = Exp(5.213 * (R2 / A) ^ 0.194 - 5.977)
End If
If sfv <> 999 Then
W2 = A * 2 * Pi / wp / sfv2
```

```
Else
End If
W2 = A * 2 * Pi / wp / sfv3
If S1 >= 1 Then
L2 = 158 * sd2 * (S1 - 0.05) ^ (2 / 3)
ElseIf W2 > 17.4 Then
L2 = N1 * 3.32 * W2 ^ -0.22
Else
L2 = N1 * 0.05 * W2 ^ 1.25
End If
A3 = ((rsd - 1) * 9.8 * sd2 ^ 0.5 * wp ^ 2 / Pi) ^ (2 / 3) / 2
If sd >= 0.55 Then
A4 = A3 * ((0.46 / Pi) ^ (2 / 3))
Else
A4 = A3 * (0.21) ^ (2 / 3)
End If
D3 = (Pi ^ 2) * (A ^ 3) / (((rsd - 1) * 9.8 * (wp ^ 2)) ^ 2)
D4 = D3 * Pi ^ 2 / 0.01
If D4 <= 0.55 Then
cgs = F2 / F1 * D4 * 1000
ElseIf D4 / Pi ^ 2 * 0.01 / 0.03 > 0.55 Then
cgs = F2 / F1 * (D4 / Pi ^ 2 * 0.01 / 0.03 > 0.55) * 1000
Else
cgs = F2 / F1 * (((D4 / Pi ^ 2 * 0.01 / 0.03 > 0.55) + D4) / 2) * 1000
End If
gs = sd
C9 = 0.006 * S1 ^ 2 * L2
scm = C9
sckg = C9 * rsd * 1000
If A <= A4 And S1 < 1 Then
rh = Int(N1 * 100 + 0.5)
Else
rh = 0
End If
If A <= A4 And S1 < 1 Then
rl = Int(L1 * 100 + 0.5)
Else
rl = 0
End If
ff = F2
sp = S1
br = R2 * 1000
dl = L2 * 1000
If sfv <> 999 Then
fvel = Int(sfv + 0.5)
Else
fvel = Int(sfv3 * 1000 + 0.5)
End If
se = Int(A * 100 + 0.5)
va = Int(200 * Pi * A / wp + 0.5)
```

cv = Int(F1 / F2 * A4 * 200 * Pi / wp + 0.5)

fr = F2 / F1

mn = p

dtn = W2

dsn = (A * K) / wd

Lunds Universitets Naturgeografiska institution. Seminarieuppsatser. Uppsatserna finns tillgängliga på Naturgeografiska institutionens bibliotek, Sölvegatan 13, 223 62 LUND.

The reports are available at the Geo-Library, Department of Physical Geography, University of Lund, Sölvegatan 13, S-223 62 Lund, Sweden.

1. Pilesjö, P. (1985): Metoder för morfometrisk analys av kustområden.
2. Ahlström, K. & Bergman, A. (1986): Kartering av erosionskänsliga områden i Ringsjöbygden.
3. Huseid, A. (1986): Stormfällning och dess orsakssamband, Söderåsen, Skåne.
4. Sandstedt, P. & Wällstedt, B. (1986): Krankesjön under ytan - en naturgeografisk beskrivning.
5. Johansson, K. (1986): En lokalklimatisk temperaturstudie på Kungsmarken, öster om Lund.
6. Estgren, C. (1987): Isälvsstråket Djurfälla-Flädermo, norr om Motala.
7. Lindgren, E. & Runnström, M. (1987): En objektiv metod för att bestämma läplanteringars läverkan.
8. Hansson, R. (1987): Studie av frekvensstyrd filtringsmetod för att segmentera satellitbilder, med försök på Landsat TM-data över ett skogsområde i S. Norrland.
9. Matthiesen, N. & Snäll, M. (1988): Temperatur och himmelsexponering i gator: Resultat av mätningar i Malmö.
10A. Nilsson, S. (1988): Veberöd. En beskrivning av samhällets och bygdens utbyggnad och utveckling från början av 1800-talet till vår tid.
10B. Nilson, G., 1988: Isförhållande i södra Öresund.
11. Tunving, E. (1989): Översvämning i Murciaprovinsen, sydöstra Spanien, november 1987.
12. Glave, S. (1989): Termiska studier i Malmö med värmebilder och konventionell mätutrustning.
13. Mjölbo, Y. (1989): Landskapsförändringen - hur skall den övervakas?
14. Finnander, M-L. (1989): Vädrets betydelse för snöavsmältningen i Tarfaladalen.
15. Ardö, J. (1989): Samband mellan Landsat TM-data och skogliga beståndsdata på avdelningsnivå.
16. Mikaelsson, E. (1989): Byskeälvens dalgång inom Västerbottens län. Geomorfologisk karta, beskrivning och naturvärdesbedömning.
17. Nhilen, C. (1990): Bilavgaser i gatumiljö och deras beroende av vädret. Litteraturstudier och mätning med DOAS vid motortrafikled i Umeå.
18. Brasjö, C. (1990): Geometrisk korrektion av NOAA AVHRR-data.
19. Erlandsson, R. (1991): Vägbanetemperaturer i Lund.
20. Arheimer, B. (1991): Näringsläckage från åkermark inom Brååns dräneringsområde. Lokalisering och åtgärdsförslag.
21. Andersson, G. (1991): En studie av transversalmoräner i västra Småland.
22A. Skillius, Å., (1991): Water havesting in Bakul, Senegal.
22B. Persson, P. (1991): Satellitdata för övervakning av höstsådda rapsfält i Skåne.
23. Michelson, D. (1991): Land Use Mapping of theThat Luang _ Salakham Wetland, Lao PDR, Using Landsat TM-Data.
24. Malmberg, U. (1991): En jämförelse mellan SPOT- och Landsatdata för vegetations-klassning i Småland.
25. Mossberg, M. & Pettersson, G. (1991): A Study of Infiltration Capacity in a Semiarid Environment, Mberengwa District, Zimbabwe.

26. Theander, T. (1992): Avfallsupplag i Malmöhus län. Dränering och miljöpåverkan.
27. Osaengius, S. (1992): Stranderosion vid Löderups strandbad.
28. Olsson, K. (1992): Sea Ice Dynamics in Time and Space. Based on upward looking sonar, satellite images and a time series of digital ice charts.
29. Larsson, K. (1993): Gully Erosion from Road Drainage in the Kenyan Highlands. A Study of Aerial Photo Interpreted Factors.
30. Richardson, C. (1993): Nischbildningsprocesser _ en fältstudie vid Passglaciären, Kebnekaise.
31. Martinsson, L. (1994): Detection of Forest Change in Sumava Mountains, Czech Republic Using Remotely Sensed Data.
32. Klintenberg, P. (1995): The Vegetation Distribution in the Kärkevagge Valley.
33. Hese, S. (1995): Forest Damage Assessment in the Black Triangle area using Landsat TM, MSS and Forest Inventory data.
34. Josefsson, T. och Mårtensson, I. (1995). A vegetation map and a Digital Elevation Model over the Kapp Linné area, Svalbard -with analyses of the vertical and horizontal distribution of the vegetation.
35. Brogaard, S och Falkenström, H. (1995). Assessing salinization, sand encroachment and expanding urban areas in the Nile Valley using Landsat MSS data.
36. Krantz, M. (1996): GIS som hjälpmedel vid växtskyddsrådgivning.
37. Lindegård, P. (1996). Vinterklimat och vårbakslag. Lufttemperatur och kådflödessjuka hos gran i södra Sverige.
38. Bremborg, P. (1996). Desertification mapping of Horqin Sandy Land, Inner Mongolia, by means of remote sensing.
39. Hellberg, J. (1996). Förändringsstudie av jordbrukslandskapet på Söderslätt 1938-1985.
40. Achberger, C. (1996): Quality and representability of mobile measurements for local climatological research.
41. Olsson, M. (1996): Extrema lufttryck i Europa och Skandinavien 1881-1995.
42. Sundberg, D. (1997): En GIS-tillämpad studie av vattenerosion i sydsvensk jordbruksmark.
43. Liljeberg, M. (1997): Klassning och statistisk separabilitetsanalys av marktäckningsklasser i Halland, analys av multivariata data Landsat TM och ERS-1 SAR.
44. Roos, E. (1997): Temperature Variations and Landscape Heterogeneity in two Swedish Agricultural Areas. An application of mobile measurements.
45. Arvidsson, P. (1997): Regional fördelning av skogsskador i förhållande till mängd SO_2 under vegetationsperioden i norra Tjeckien.
46. Akselsson, C. (1997): Kritisk belastning av aciditet för skogsmark i norra Tjeckien.
47. Carlsson, G. (1997): Turbulens och supraglacial meandring.
48. Jönsson, C. (1998): Multitemporala vegetationsstudier i nordöstra Kenya med AVHRR NDVI
49. Kolmert, S. (1998): Evaluation of a conceptual semi-distributed hydrological model – A case study of Hörbyån.
50. Persson, A. (1998): Kartering av markanvändning med meteorologisk satellitdata för förbättring av en atmosfärisk spridningsmodell.
51. Andersson, U. och Nilsson, D. (1998): Distributed hydrological modelling in a GIS perspective – an evaluation of the MIKE SHE model.

52. Andersson, K. och Carlstedt, J. (1998): Different GIS and remote sensing techniques for detection of changes in vegetation cover - A study in the Nam Ngum and Nam Lik catchment areas in the Lao PDR.
53. Andersson, J., (1999): Användning av global satllitdata för uppskattning av spannmålsproduktion i västafrikanska Sahel.
54. Flodmark, A.E., (1999): Urban Geographic Information Systems, The City of Berkeley Pilot GIS
55A. Lyborg, Jessic & Thurfell, Lilian (1999): Forest damage, water flow and digital elevation models: a case study of the Krkonose National Park, Czech Republic.
55B. Tagesson, I., och Wramneby, A., (1999): Kväveläckage inom Tolångaåns dräneringsområde – modellering och åtgärdssimulering.
56. Almkvist, E., (1999): Högfrekventa tryckvariationer under de senaste århundradena.
57. Alstorp, P., och Johansson, T., (1999): Översiktlig buller- och luftförorenings-inventering i Burlövs Kommun år 1994 med hjälp av geografiska informations-system – möjligheter och begränsningar.
58. Mattsson, F., (1999): Analys av molnklotter med IRST-data inom det termala infraröda våglängdsområdet
59. Hallgren, L., och Johansson, A., (1999): Analysing land cover changes in the Caprivi Strip, Namibia, using Landsat TM and Spot XS imagery.
60. Granhäll, T., (1999): Aerosolers dygnsvariationer och långväga transporter.
61. Kjellander, C., (1999): Variations in the energy budget above growing wheat and barley, Ilstorp 1998 - a gradient-profile approach
62. Moskvitina, M., (1999): GIS as a Tool for Environmental Impact Assessment - A case study of EIA implementation for the road building project in Strömstad, Sweden
63. Eriksson, H., (1999): Undersökning av sambandet mellan strålningstemperatur och NDVI i Sahel.
64. Elmqvist, B., Lundström, J., (2000): The utility of NOAA AVHRR data for vegetation studies in semi-arid regions.
65. Wickberg, J., (2000): GIS och statistik vid dräneringsområdesvis kväveläckage-beskrivning i Halland.
66. Johansson, M., (2000): Climate conditions required for re-glaciation of cirques in Rassepautasjtjåkka massif, northern Sweden.
67. Asserup, P., Eklöf, M., (2000): Estimation of the soil moisture distribution in the Tamne River Basin, Upper East Region, Ghana.
68. Thern, J., (2000): Markvattenhalt och temperatur i sandig jordbruksmark vid Ilstorp, centrala Skåne: en mätnings- och modelleringsstudie.
69. Andersson, C., Lagerström, M., (2000): Nitrogen leakage from different land use types - a comparison between the watersheds of Graisupis and Vardas, Lithuania.
70. Svensson, M., (2000): Miljökonsekvensbeskrivning med stöd av Geografiska Informationssystem (GIS) – Bullerstudie kring Malmö-Sturup Flygplats.
71. Hyltén, H.A., Uggla, E., (2000): Rule.Based Land Cover Classification and Erosion Risk Assessment of the Krkono_e National Park, Czech Republic.
72. Cronquist, L., Elg, S., (2000): The usefulness of coarse resolution satellite sensor data for identification of biomes in Kenya.
73. Rasmusson, A-K., (2000): En studie av landskapsindex för kvantifiering av rumsliga landskapsmönster.

74. Olofsson, P., Stenström, R., (2000): Estimation of leaf area index in southern Sweden with optimal modelling and Landsat 7 ETM+Scene.
75. Uggla, H., (2000): En analys av nattliga koldioxidflöden i en boreal barrskog avseende spatial och temporal variation.
76. Andersson, E., Andersson, S., (2000): Modellering och uppmätta kväveflöden i energiskog som bevattnas med avloppsvatten.
77. Dawidson, E., Nilsson, C., (2000): Soil Organic Carbon in Upper East Region, Ghana - Measurements and Modelling.
78. Bengtsson, M., (2000): Vattensänkningar - en analys av orsaker och effekter.
79. Ullman, M., (2001): El Niño Southern Oscillation och dess atmosfäriska fjärrpåverkan.
80. Andersson, A., (2001): The wind climate of northwestern Europe in SWECLIM regional climate scenarios.
81. Lalloo, D., (2001): Geografiska informationssystem för studier av polyaromatiska kolväten (PAH) – Undersökning av djupvariation i BO01-området, Västra hamnen, Malmö, samt utveckling av en matematisk formel för beräkning av PAH-koncentrationer från ett kontinuerligt utsläpp.
82. Almqvist, J., Fergéus, J., (2001): GIS-implementation in Sri Lanka.
    Part 1: GIS-applications in Hambantota district Sri Lanka : a case study.
    Part 2: GIS in socio-economic planning : a case study.
83. Berntsson, A., (2001): Modellering av reflektans från ett sockerbetsbestånd med hjälp av en strålningsmodell.
84. Umegård, J., (2001): Arctic aerosol and long-range transport.
85. Rosenberg, R., (2002): Tetratermmodellering och regressionsanalyser mellan topografi, tetraterm och tillväxt hos sitkagran och lärk – en studie i norra Island.
86. Håkansson, J., Kjörling, A., (2002):
87. Arvidsson, H., (2002): Coastal parallel sediment transport on the SE Australian inner shelf – A study of barrier morphodynamics.